Titanium Oxide Hydrates:

Optical Properties and Applications

A thesis submitted to

University of London

for the degree of

Doctor of Philosophy

of

Engineering and Material Sciences

presented by

Manuela Russo

Supervisor

Natalie Stingelin

October 2009

Summary

TiO_2 has been extensively studied in the last decades due to its interesting optical and electronic properties, which, combined with low fabrication costs, renders this material very attractive for applications in photovoltaic and photo-catalysis. However, the performances of titania in specific device applications were found to be strongly dependent on the synthetic methods selected for its production. The majority of such synthetic procedures rely on the hydrolysis of suitable precursors and often produce an amorphous solid, generally referred as the "amorphous" titanium oxide beside the crystalline titania.

In this thesis, we thus set out to investigate amorphous materials produced by the hydrolysis of titanium tetrachlorides and tetraisopropoxide. We show that these amorphous products consists of titanium oxide hydrates, which are relatively stable at room temperature and fully convert into crystalline titania only after extended temperature treatments. We also find that titanium oxide hydrates may display highly desirable characteristic such as a strong photochromic response – especially when placed in a suitable chemical environment. In the following chapter, we then show

that hybrid systems can be readily prepared of titanium oxide hydrates with, for instance, macromolecular materials such as poly(vinylalcohol). The amorphous nature of the titanium oxide hydrates allows to introduce more than 90 vol.% of the inorganic species into such systems – compared to 15 vol.% or less when producing hybrids comprising, e.g., *crystalline* nanoparticles of TiO_2. Therefore, materials can be realized that display a refractive index n of at least 2.1, without compromising transparency of the resulting structures. Remarkably, n can not only be adjusted by varying the content of the inorganic species, but also through suitable heat treatments and/or irradiation with UV-light. Potential applications for such new, versatile and tunable optical systems are also discussed in this thesis.

Content

Chapter 2: **Pronounced photochromism of titaniumoxide hydrates (hydrous TiO_2)**

Chapter 1

Introduction

1.1. Background

Titania, alias titanium dioxide, is an extremely versatile material which is widely used in paints, plastics and ceramics as a pigment, in healthcare products as antimicrobial coatings or in photo-catalysis and photovoltaic applications [1]. This broad variety of options is due to its highly desirable set of optical and electronic properties which are combined with good chemical and thermal stability.

TiO_2 exhibitis several crystalline forms [1], among which the most important in terms of applications, anatase and rutile, occur in nature. These two polymorphs, besides sharing the same chemistry, crystallize both in the tetragonal crystal system and possess in many cases comparable (however not identical) physical properties such as refractive index and density (see table 1.1). However, despite these similarities, the applications they are used for differ distinctly.

In the following, we will give an overview on the optoelectronic properties of titanium dioxide with respect to the characteristic crystalline arrangement and electronic band structure of anatase and rutile. Also, the methods to manipulate

opto-electronic characteristics of these two polymorphs and the relevant photo-induced charge separation phenomena will be described. Furthermore, in view of the fact that the performance of TiO_2 in various applications are often enhanced when the particle dimensions are reduced to the nanoscale, we will attempt to summarize existing synthetic routes employed to produce titanium dioxide nano-particles. We will, thereby, mainly focus on those methods that are based on the hydrolysis of suitable titania precursor. These routes generally produce at first a material of low crystallinity, most often accounted as "amorphous" TiO_2, however, as we will show, can comprise significant content of titanium oxide hydrates. The chemical nature of this intermediate material, including its opto-electronic properties, is summarized at the end of this introduction before a brief scope of this thesis is given.

1.2. TiO_2 crystalline structure

Titania is found in various crystal forms, the most relevant in terms of industrial applications are, as mentioned above, rutile and anatase. In this introduction we will therefore focus on these two polymorphs.

Rutile and anatase crystallize in a tetragonal crystal system of, respectively, the space groups P42/mnm and I41/mmm (Fig.1.1). The nature of the bonds in TiO_2 is predominantly ionic (70%), as a consequence, the ligand oxygen atoms are arranged around a central Ti atom to form slightly distorted octahedra of TiO_6. In such structures, the inter-atomic distances in the apical Ti-O bonds are larger than those found for the four equatorial bonds (Table1.1) due to the repulsion between the apical and equatorial oxygen atoms [1-3].

The different extent of distortion and the specific spatial arrangement of the TiO_6 octahedra are responsible for the main differences in the properties of the two

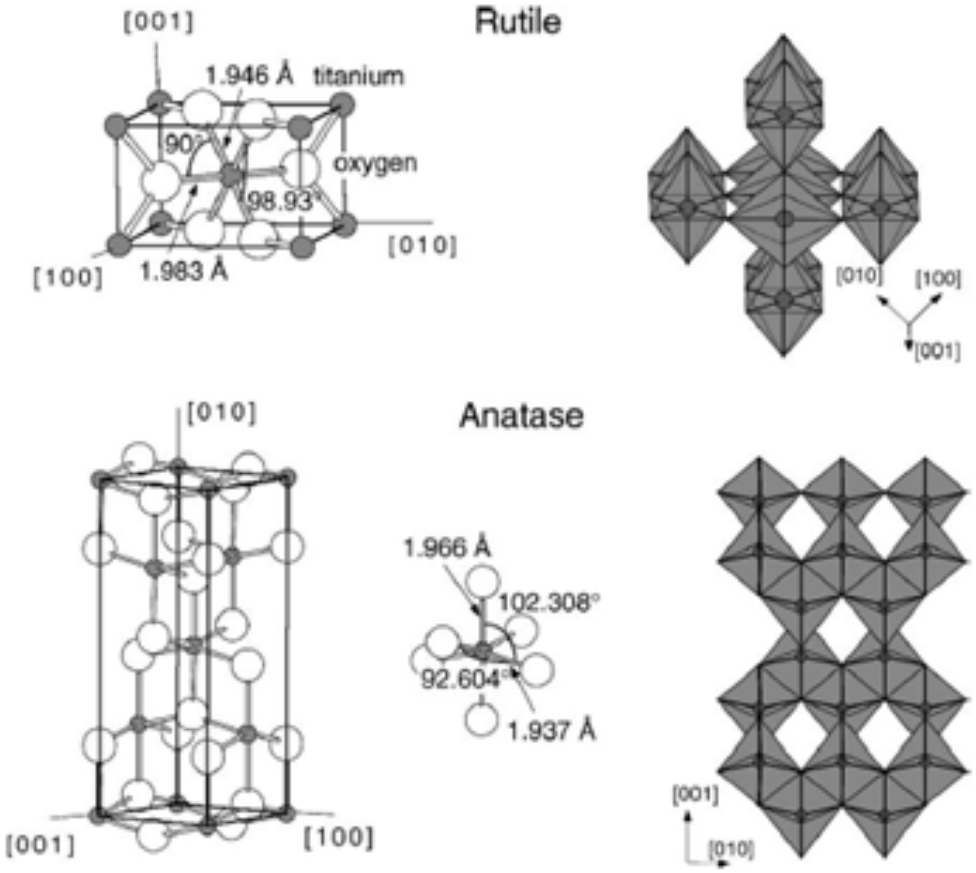

Figure 1.1: Schematic of the cystalline structures of the two main TiO_2 forms – rutile and anatase – and the respective spatial arrangements of the TiO_6 octahedra in these titania polymorphs (after[1]). The octahedra share two edges in rutile and four edges in anatase. As a consequence, the rutile structure is the denser form.

polymorphs. In fact, in rutile each octahedron shares two edges with the next octahedra forming chains –[-O-Ti-O-O-Ti-O-]–, which are perpendicularly interconnected with the neighbouring chains through an oxygen atom. This results in a very dense structure [4]. In anatase, instead, each octahedron shares four edges with the neighbouring octahedra producing a structure which is about 8.5 % less dense when compared to rutile. The crystallographic parameters and physical properties of the rutile and anatase are summarized in Table 1.1.

	Rutile	Anatase
Crystal system	Tetragonal	Tetragonal
Space group	*4/mmm*	*4/mmm*
Point group	*P42/mnm*	*I41/mmm*
N of formula units /unit cell	2	4
Unit cell parameters (Å)		
a=b	4.5937	3.7845
c	2.9587	9.5143
Ti-O ap	1.983	1.966
Ti-O eq	1.946	1.937
Band gap (eV)	3.0	3.2
Molar volume(m3/mol)	18.69	20.156
Density (g/cm3)	4.27	3.895
Refractive index	2.70	2.55

Table 1.1: Selected properties and crystallographic data of rutile and anatase (as extracted from Ref. [1])

Among the different polymorphs of TiO_2 only rutile is thermodynamically stable; anatase as well all the other polymorphs can be converted into rutile by suitable heat treatments – a transition that is irreversible. However, the temperature at which the phase transition occurs (usually around 700-900 ^{o}C) and the time necessary for the conversion to complete, strongly depends on the synthetic pathway selected for the production of the oxide [5, 6].

1.3. Optical and electronic properties of TiO_2

The optical and electronic properties of titanium dioxide have been widely studied [1, 4, 7-15] which provided the necessary insight for the broad range of

applications of this material. In fact, as already mentioned above, the – although little differences – in optical and electronic properties of rutile and anatase [13-16] open distinctive application areas for the two TiO_2 forms. For instance, anatase was found to be better performing in photo-driven applications and, thus, attracts considerable interests for use in photovoltaics and photocatalysis [17-21], whereas rutile is the preferred polymorph for pigment production. However, other useful properties such as refractive index, semiconductivity and photoactivity of this metal oxide still stimulate intense research efforts in the scientific community which are discussed in the next chapter.

1.3.1. Refractive index of TiO_2

Because of the tetragonal symmetry of their crystal structure, both rutile and anatase are optically anisotropic *i.e.* the refractive index in the direction parallel to the crystal *c*-axis, $n_{\parallel}$, differs from the one in the perpendicular direction, $n_{\perp}$, with $n_{\parallel} > n_{\perp}$ for both the polymorphs [8, 9] (Fig. 1.2). However, a significantly different temperature dependence is observed between the two structures. Indeed whilst the natural birefringence of the two polymorphs increases with the temperature, anatase displays a stronger dichroism than rutile [14].

As a consequence of the high refractive indices of rutile and anatase (*n* is 2.70 and 2.55 respectively) (Table 1) titania powders of both micro- and nano-metric dimensions, can scatter light very effectively, appearing therefore opaque bright white whereas the bulk dioxide crystals are of a transparent colorless or pale yellowish appearance. For this reason, even small amounts of titania pigment can provide a strong opacity and enhanced hiding power, when compared to other commonly used pigments, such as zinc oxide [22]. TiO_2 powders, especially those

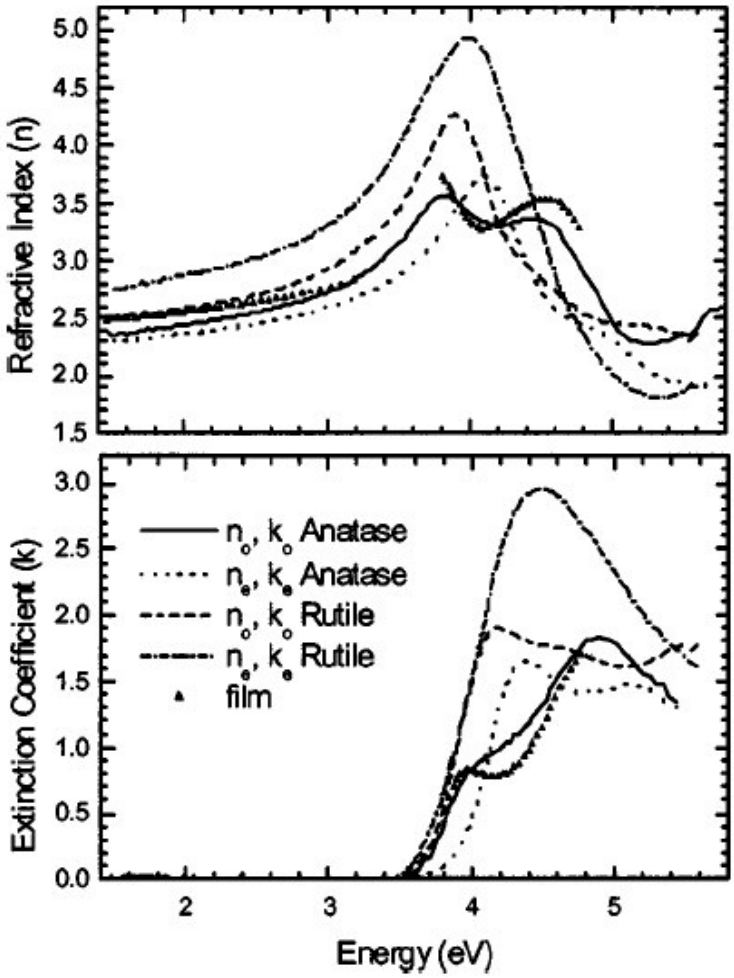

Figure 1.2: Refractive index and the extinction coefficient for anatase and rutile; n_0 and k_0 refer to the direction along the *c* axis, while ne and k_e to the direction perpendicular to the *c* axis. After [9]

comprised of the rutile polymorph, are, therefore, much-sought-after ingredients for the manufacture of pigments. More recently, they have begun to attract attention also in various other fields; for instance, in the area of "photonic crystals" and other photonic band-gap applications [23, 24].

1.3.2. Chromism in TiO_2

Contrary to various other common transition metal salts and oxides, which display characteristic colours, rutile and anatase are, in general, colourless solids with negligible absorption in the visible light. This is due to the fact that in these two

polymorphs, titanium is present as Ti^{IV}, which is a d^0-center and the lower shell electrons cannot be readily excited by the visible light. In fact the absorption edge in both titania crystals is found around 400 nm corresponding at band gap energy around 3 eV. Commercial rutile (Aldrich) and anatase (P25-Degussa), for instance, exhibit a band gap of 3.1 eV and 3.02 eV, respectively; see Figure 1.3.

Both rutile and anatase have been described to reversibly turn to blue by partial reduction of titanium, from Ti^{IV} to Ti^{III}. This can occur if external stimuli provide enough energy to promote electronic transitions or if charge transfer involving ligand compounds take place leading to the reduction of the Ti^{IV} to Ti^{III}. As an example blue rutile single crystals were observed after heating at high temperature in high vacuum or in H_2 atmosphere, or through electron bombarding [1, 25]. In such cases the high strength of the respective treatment induced the abstraction of oxygen atoms from the structure of the crystal, each one leaving behind two electrons that can be trapped in *d* orbitals of the Ti atoms which, in turn, are reduced to Ti^{III}.

Interestingly, the appearance of a blue colour was also observed in titania powders irradiated with UV light in presence of some chemical compounds. Such photochromism was first observed in synthetic titania by Renz in 1921 [26] who reported that some titanium dioxides exposed to sun light turned blue if dispersed in certain hydrocarbons or alcohols; and various nanocrystalline and colloidal titania were found to display a distinct blue colour after irradiation with UV-light in presence of organic solvents or polyhydroxylated compounds [27-29]. Furthermore a blue colouration also developed in compressed crystalline nanopowders of the commercial anatase-based pigment P25 (Degussa) immersed in dimethyl formamide (DMF) when a voltage was applied; the same material turned blue upon refluxing in DMF or in presence of metallic zinc and hydrochloric acid [28]. In all cases, it was

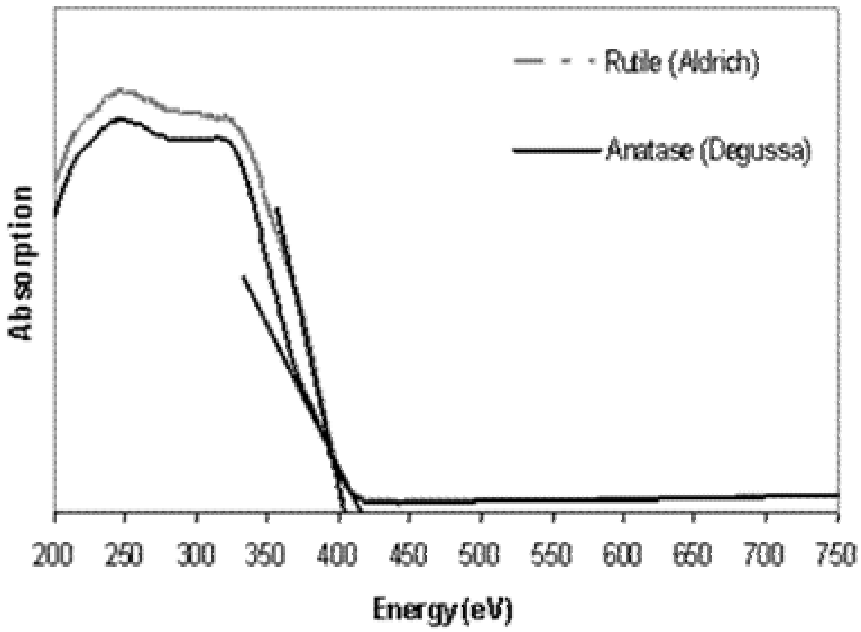

Figure 1.3: UV-Vis absorption spectra for commercial rutile (Aldrich) and anatase (P25-Degussa) nanopowders. The absorption edge for the two polymorphs is, respectively, at 400 nm (band gap of 3.1 eV) and 410 nm (band gap of 3.02 eV).

found that the blue colouration could be reversed by exposure to oxidizing agents or chemical reducing species.

Electronic paramagnetic resonance (EPR) studies by various groups support the notion that the characteristic and pronounced colour change to blue in titanium dioxide as consequence of such procedures is indeed caused by the formation of Ti^{III} sites that behave as chromic centres [30, 31]. In fact, blue samples displayed pronounced signals at $g \approx 2$ characteristic of Ti^{III} species. These features were completely absent in the same samples before exposition to UV light or after the bleaching of the UV-induced colouration via exposure to oxygen.

However, while the mechanism that results in the formation of Ti^{III} defects is well investigated in case of titania subjected to high energy treatments, very little is known about the mechanism that promotes the reduction of titania at less energetic

conditions. Muller *et al.* [28] carried out a systematic study to understand the conditions for the appearance of the blue colouration in titania upon UV irradiation in presence of different organic compounds and water. They found that the presence of oxygen, as well as other oxidizing substances, is detrimental to the stabilization of such sites. In fact removing oxygen via thorough degassing of the solvent allowed obtaining a coloration persistent over years. In some cases, however, even in degassed systems the colour faded over time following a first order kinetic.

The above described photoreduction of titania has been analysed in presence of a large number of organics compounds from saturated and unsaturated hydrocarbons to alcohols, acids, amides etc. However, despite all these investigations the process is still not completely clear. A very popular hypothesis exists that involves a separation of charges which are stabilised by chemicals in the surrounding of titania particles [32]. There are also uncertainties on how the UV irradiation can actually affect the stoichiometry of the oxide. Shultz *et al.* [33], for instance, believed that the low energy light they used for irradiation of titania samples (4.7 eV) could not be of sufficiently high energy to lead to the removal of surface oxygen atoms, and even less, of bridging oxygen atoms. This would imply that either the surface oxygen atoms were weakly bound to the surface, such that they could be removed even from low energy photons, or the species involved in this reduction/oxidation cycle are external to the oxide structure itself. Molecular oxygen could fit in the latter proposed mechanism by binding to Ti^{III} and producing Ti^{IV}: O_2^- surface complex.

1.3.3. Electronic properties

Despite the fact that the distance between the metal atoms is larger than in elemental semiconductors like silicon or germanium (due to the presence of oxygen

atoms) the metal-metal interaction in TiO_2 crystals is sufficiently strong to result in a broadening and overlapping of orbitals [4], and, thus, in distinct opto-electronic characteristics of this class of materials.

As a matter of fact, and as mentioned before, titanium dioxide is characterised by a wide band gap of about 3.1 eV for rutile and 3.02 eV for anatase. However, a very interesting characteristic of all TiO_2 is that they can easily be reduced to non-stoichiometric compounds with the generic formula TiO_{2-x} that exhibit a higher conductivity. Mostly, such non-stoichiometric titania is obtained by exposing the dioxide to a reducing environment, such as high temperature (> 600 ^{o}C) treatment in vacuum [34] or hydrogen atmosphere, and upon bombardment with electrons [35, 36] or argon ions [34, 37]. All these procedures have in common that they "extract" oxygen atoms (bridging or exposed ones) from the surface of the respective architecture and each atom removed produces two "free" electrons that are believed to behave as n-type impurities [1, 11-13, 38], while at the same time other oxygen atoms diffuse from the bulk to the surface. The abstraction of these surface oxygen atoms contribute to create a donor band which (initially) lies at 0.8 eV below the conduction band, however may broaden and partially overlap with the conduction band at higher defect concentrations [22]. Indeed anatase is reported to undergo metallic transition when the density of carriers exceedes a certain threshold while for rutile an activation energy seems to be always required for conduction to occur, even at very high density of carriers [14, 15].

It is also worthwhile to note that an increased conductivity (when compared to TiO_2) is found in reduced titania comprising Ti^{III}, for which often a distinc blue colouration has been observed. The higher conductivity is attributed to the presence of electrons in the conduction band [25]. By subsequent oxidation of such titania

derivatives, the stoichiometry is restored (as deduced from EPR), with a contemporaneous increase in resistivity [16].

1.4. Photoinduced generation of charge carriers

In semiconductors, an electron from the valence band can be excited to the conduction band by irradiation with light of larger energy than the band gap of a material [32]. This results in a carrier of opposite charge, a hole, in the valence band. In case of TiO_2 the mechanism can be expressed by Equation 1.1

$$TiO_2 + \varphi \rightarrow TiO_2 + e^- + h^+ \qquad \text{Eq. 1.1}$$

where φ is a photon, and e^- and h^+ are the excited electron and hole in the conduction and valence band, respectively. These photo-generated electron/hole pairs may recombine in absence of a reacting species and involve in charge transfer processes with chemical matter in the surroundings, or be "trapped" by defects, impurities, etc. The interplay between these processes determines the performance of opto-electronic materials in photodriven activities, such as in photocatalysis and photovoltaics. Of course, it is highly desirable to have the capability to enhance charge-carrier separation and inhibit recombination processes in the semiconductor [32] in order to improve the performances of such materials in these specific applications.

In photovoltaic cells, charge carrier separation can be achieved by the application of an external electric field that drives the electrons and holes created on illumination in opposite directions, thus preventing their recombination. A similar effect is due to the electrostatic field at the interface of the dioxide and its chemical environment.

The recombination of the charge carriers in normal conditions (i.e. in absence of a surface carrier depletion layer which neutralise the hole or the electron) is very fast (few tens ps). However, studies on the second harmonic generation (SHG) [33] in high vacuum at low temperature showed that UV irradiation of bulk rutile can actually create stable Ti^{III} sites that, as expected, are very quickly re-oxidized by exposing to air. The oxidation, induced by oxygen, occurs quickly because the reduction potential of oxygen (+0.8 V) is higher than the reduction potential of Ti^{III} (+0.1 V).

1.5. EPR analysis of photoproduced charge carriers

From the above it seems that the formation of Ti^{III}-sites is responsible not only for the photochromic characteristics of titania, but is also responsible of relevant charge-transport phenomena observed in this material. As described in section 1.3.2, EPR spectroscopy provides a powerful tool to obtain information about the presence of such Ti^{III} species. In this section, we, therefore, summarize some of the key issues on the reduction and oxidation processes of Ti^{IV} as observed with EPR spectroscopy.

Various EPR studies [29, 30, 39] reported the presence of Ti^{III}-sites in titania irradiated with UV light carried out on nanometric titania in form of nanopowders or colloidal dispersions at temperatures below 100 K. Before UV irradiation, no distinct signal originating from paramagnetic species could be discerned. In contrast, after exposure to UV light, distinct signals at $g \approx 2$ were recorded which were attributed to the paramagnetic species Ti^{III}. We like to point out that these characteristic features due the presence of Ti^{III} sites decreased with increasing temperatures and were no more discernable above T = 140 K.

Paramagnetic species, other than Ti^{III}, were also found at 77 K in degassed colloidal dispersion of titania irradiated with UV light. These systems revealed features at $g > 2$ that were assigned to species such as $OH^{\cdot}$ and Ti-$O^{\cdot}$-Ti – both potential hole trapping sites – which might result from the homolitic cleavage of Ti-OH group covering the surface of the particles [39].

In some of these studies, most notably regarding colloidal titania dispersions [29, 39], it is reported that the EPR signals resulting from the paramagnetic Ti^{III} species were sensitive to the pH value of the surrounding environment. As a consequence, the intensity of the EPR signal was found to decrease at very basic pH values. However, when varying the pH values of the system, the line-shape of the signals appeared to be almost unaffected. This was attributed to the surface localization of such reduced sites which are likely to be more sensitive to a change in the environment

1.6. TiO_2 nanoparticles

Considering that the processes critical in catalysis or energy harvesting applications take place at the catalyst or semiconductor particle interface, an increase in the surface to volume ratio in such materials is expected to improve their performances as a consequence of a larger number of active sites per unit volume available for reactions. This seems especially relevant when the particle size approaches the nanometer range, as illustrated by the enhanced activity of functional materials such as TiO_2 when using nanoparticles instead than bulk material [31, 32]

However, the reduction of particle size to the nanometer scale may also result in electronic modifications as a consequence of the changes in physico-chemical properties in such low-dimensional solids. These modifications can be extremely

relevant in charge transfer, trapping and recombination processes that determine the photo-activity of a material, and thus, the use of such low-dimensional solids in photocatalysis and photovoltaics. For instance, it has been found that the recombination of charge carriers produced by photo-excitation is strongly reduced when the surface area of the active species increases (i.e. particle size decreases) [40]. This was attributed to the increase in the number of surface imperfections, which are known to result in charge-carrier trapping.

The reduction of particles size may also modify the dimensions of the crystal lattice of the respective species, and in turn, directly affect the electronic band structure of these materials. In rutile, for example, a linear expansion of the crystal lattice is observed when the particles dimension become smaller than 50 nm, while a nonlinear compression was reported for anatase [41] .

In addition, one should note that when some of the critical dimensions approach the Bohr's radius of delocalization of electrons, quantization size effects can occur originating in electronic modifications. Anpo *et al.* [31] attributed, for instance, the enhanced photocatalytic activity and better semiconducting properties of TiO_2 nanoparticles with diameter smaller than 100 Å to such quantum size effects. Indeed, they suggest that the change in electronic structure due to these phenomena is responsible for the higher stability of trapped electron-hole couples.

In very low-dimensional particles (≤ 6 nm) other phenomena may have to be considered. Hagfeldt and Grätzel, for instance, proposed that bending of the valence and conduction band becomes negligible [32]. As a consequence, charge separation would occur predominantly via diffusion processes, which in such small particles can be shorter (3 ps and less) than the recombination time [21, 32].

Considering the interesting characteristics that lower-dimensional solids may offer, it is, thus, not surprising that a wide variety of synthetic routes for the synthesis of nano-sized titania have been proposed which often permit controlling both dimensions and crystal form. A summary of some of the most important routes is given in section 1.7.

1.7. Production of nanometric TiO_2

TiO_2-nanoparticles are most frequently synthesized through low-temperature (0 - 5 ^oC) hydrolysis of suitable precursors (*i.e.* titanium tetrachloride and titanium tetra-alkoxides), in acid or basic environment, which can be described by the following very simplified reaction path (Eq 1.2):

$$TiX_4 + 2H_2O \rightarrow TiO_2 + 4HX \qquad \text{Eq. 1.2}$$

where X=Cl, OR.

Depending on the additives used, and the pH value of the reaction media and post-hydrolysis steps such as thermal annealing procedures, the resulting nature of the polymorphs and the particles dimensions are determined [6, 31, 42-45]. A summary of selected synthetic methods, available in literature, reporting the hydrolysis conditions and the characteristics of the resulting products is given in the schematic in Fig. 1.4. In addition, we will give below a few examples of this broad range of accessible synthetic pathways towards TiO_2 nano-particles; and opportunities and challenges these may offer are briefly discussed.

Colloidal TiO_2, for instance, can be produced following a hydrolysis in acidic conditions (pH = 0.5) with subsequent dialysis to a pH = 3 of the solution produced.

This route does not require any thermal treatment, nor of the solution nor of the particles produced. The low pH value aids in stabilizing the TiO_2 nanoparticles, yet, for pH higher than 3, suitable additives such as poly-hydroxylated compounds (e.g. poly(vinyl alcohol)) need to be employed to prevent aggregation of the particles [17-19, 46].

Particle dimensions and crystal form of titania nano-particles are, however, more often controlled by the hydrolysis conditions selected or by post-hydrolysis steps. Pure rutile of high crystallinity, for example, can be obtained following a low-pH hydrolysis step, using a wide variety of additives and appropriate heat treatments. Anatase nano-particles frequently are produced at higher pH values than those used in the synthesis of rutile particles, or in the presence of additives that can be strongly absorbed or bear large groups.

The dimensions of particles can be controlled by various methods. Some authors [47], for instance, advanced a method to conduct the hydrolysis in micelles (e.g. formed by hydrochloric acid, HCl, in cyclohexane). Each micelle can be regarded as a "micro-reactor" whose dimensions control those of the titanium dioxide particles. Alternatively, the hydrolysis solutions can be aged at room temperature or allowed to precipitate without the need for further thermal treatments [48-50]. Mesoporous anatase with a high BET (Brunauer, Emmet and Teller) surface area can be synthesized following a sol-gel process where the gels obtained in a hydrolysis of the alkoxide precursor in acidic conditions are first aged by heating under pressure (5 MPa), with subsequent calcination at 300 ^{o}C [51]. One should note, though, that in several synthetic pathways, a mixture of the two TiO_2 polymorphs (rutile and anatase) is often obtained which, not infrequently, comprises also a significant fraction of "amorphous" titania.

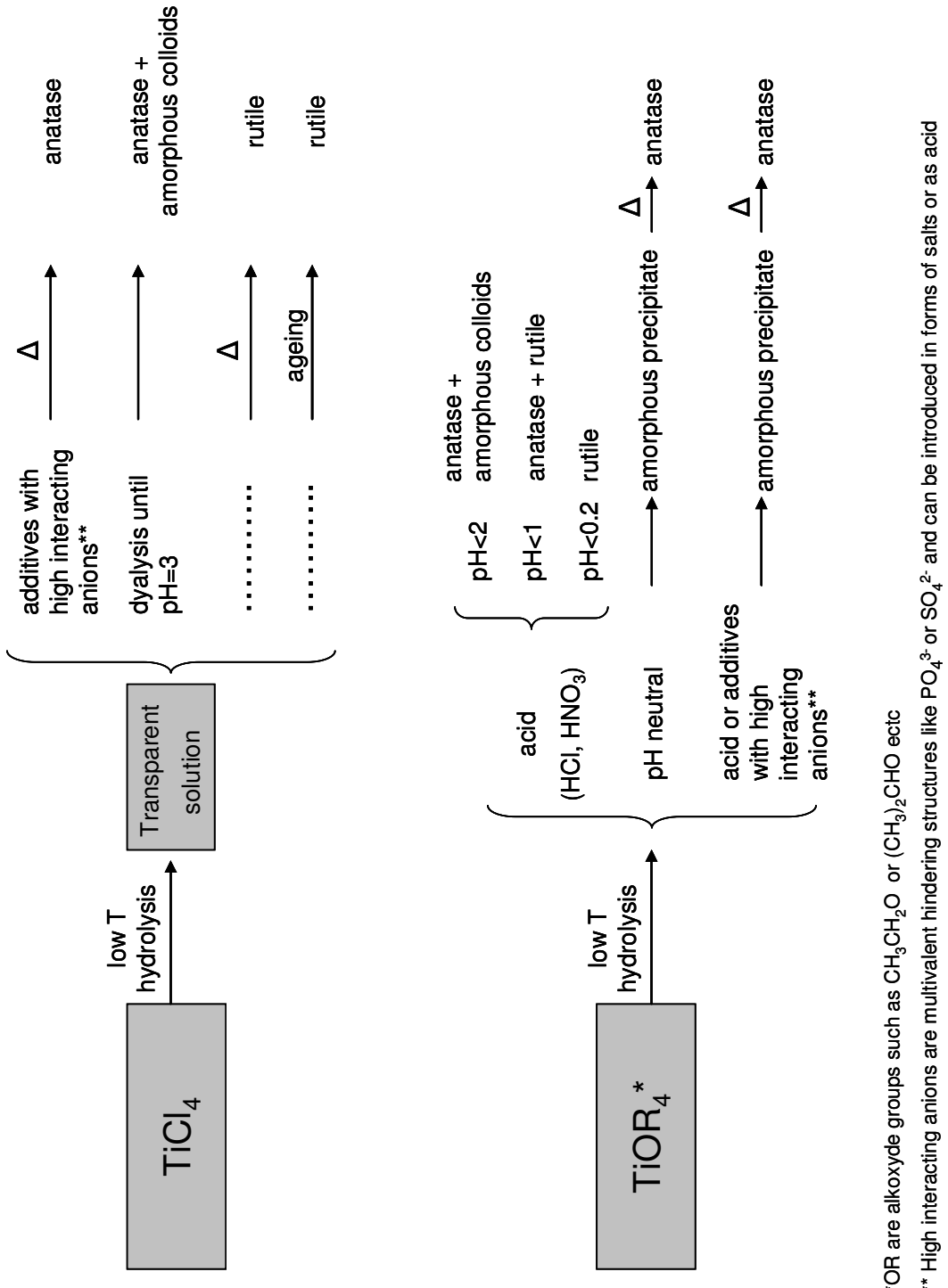

Figure 1.4: Schematic of the common routes for the production of titania nanoparticles that use $TiCl_4$ and alkoxy-titanates, $TiOR_4$, as precursor compounds and the effect of pH and temperature on the resulting titania crystalline structure.

1.7.1. Control of crystal structure, morphology and dimensions

Reaction conditions strongly influence also the characteristics of the final particles of titanium dioxide, including crystal phase, dimensions and microstructure of the final architectures. Among a number of relevant reaction parameters that can be adjusted, it seems most interesting to analyse the effect of temperature, pH value and use of additives.

1.7.2. Effect of the temperature

The temperature used for the thermal treatment significantly affects the crystalline form induced as well as the dimensions of the resulting particles. In addition, heat treatment procedures may aid removing by-products and traces of excess precursor material.

The calcination temperature can therefore be used to control the crystal phase. In fact, higher temperatures in such post-hydrolysis steps is known to enhance the crystallinity content of the final product and generally favour the formation of rutile. However, the temperature of the phase transition as well as the duration of the complete transformation of anatase fractions into the more stable rutile strongly depend on the condition by which the dioxide has been synthesized – thus on the nature the additives and the pH value used for the hydrolysis – and can vary from 500 to 900 °C. The dimension of the particles is also affected from annealing procedures. Calcination leads, for instance, to an increased particle growth and, thus, particle size, mostly by coalescence.

1.7.3. Effect of pH value

The resulting crystalline structure and in many cases also the morphology and dimension of TiO_2 particles is strongly influenced by the pH value of the solution

where the hydrolysis of the precursor occurs. Polymorphs, in pure forms or as a mixture, can be obtained simply by varying the acidity of the hydrolysis solution. More specifically, Zhang *et al.* [47] observed that when titanium alkoxides were used as precursor for titania production, the formation of pure, shuttle like, rutile phase particles could be synthesised using 2.5 M hydrochloric acid solutions. Lower concentration of acid, below 2 M, produced a mixture of the two crystalline forms or "amorphous" dioxide, while much higher concentrations, *i.e.* 4 M, lead to unstructured material. In other investigations in which titanium tetrachloride was used [31, 45, 52], lower concentration of acid were sufficient to obtain analogous results. Of course, also the temperature should be considered as it could have had an effect in assisting the formation of structured material. However, in general the correlation between the pH value and the resulting crystal structure seems evident: higher pH values lead to the formation of anatase or mixture of the two crystal modifications, while lower pH values allowed obtaining pure rutile. Very high or very low pH values, instead, prevent any ordered aggregation and produce "amorphous" titanium dioxide. This dependence can be explained considering that the kinetics of the hydrolysis and condensation reactions can be slowed down or accelerated when adjusting the pH values of the reaction medium. The number of crystal seeds as well as the time given for the formation of the resulting structure is thereby affected.

1.7.4. Effect of additives

The presence of additives can have a strong influence on the aggregation of the TiO_2 and can be fundamental for the formation of rutile rather than anatase or amorphous titanium dioxide. In this context chemical species in the reaction process

other than titanium dioxide precursor and water can be considered as additives. Therefore, at some extent, also the acid used to control the rate of hydrolysis and condensation is an additive as the counterion provided from the acid might interfere with the aggregation of the forming TiO_2.

Zhang *et al*" found, for instance, that when using different acids it was possible both to obtain a different TiO_2 morphology and to modify the dimensions of the particles. In fact, when HCl and HNO_3 were used, where the Cl^- and the NO_3^- ions are poorly interacting with TiO_2, shuttle-like morphologies were obtained comprised of particles presenting a very narrow size distribution. In contrast, when the acid used to control the pH provided more interacting counterions, then, significantly different morphologies were obtained. In case of SO_4^{2-} and PO_4^{3-}, for example, that strongly interact with the titanium ions, an ordered arrangement of TiO_2 molecules was prevented leading to "amorphous" phases.

Tolchev *et al.* [6] analysed the effect of different chemical compounds on the transformation of "hydrated" or "amorphous" TiO_2 obtained from the thermal hydrolysis of titanyl sulphate. The effect of such compounds was investigated on both phase transition temperature from anatase to rutile and particle dimensions. It was found that large and multivalent ions such as phosphates retarded the formation of anatase and shifted of the anatase-rutile phase transition to higher temperatures. Possibly this was due to the fact that such ions are able to establish bonds with different titanium ions belonging to different forming titanates chains, preventing in this way the formation of an ordered crystalline structure. In contrast, $MgCl_2$ and $ZnCl_2$ decreased the phase transition temperature while increasing the dimensions of the resulting crystalline particles.

1.8. Titanium oxide hydrates

It is evident, from the schematic shown in Figure 1.4, that the majority of synthetic routes used to produce TiO_2 are based on the hydrolysis of suitable precursors. As a consequence, the first product is most frequently an amorphous material generally termed "amorphous titania" or "hydrous titania". This unstructured compound is known to consist of titanium oxide hydrates which are an interesting class of hydrates that were investigated in particular during a period that lasted more than 100 years and ended about 60 years ago. Since that time, however, essential studies on these materials – and therewith their attractive and useful properties and potential applications – have been widely forgotten. Indeed, titanium oxide hydrates are used nowadays mainly as precursors for the preparation of TiO_2 [53], for which, at closer look, full knowledge of their chemical composition is not a key requirement.

Formally being of the composition $Ti_xO_y(H_2O)_z$, titanium oxide hydrates generally are referred to as a category of titanium compounds which contain a fraction of Ti-OH groups and, thus, convert to TiO_2 by aging under release of water [54, 55]. This process may be supported by evolution of water molecules which were previously bound to titanium oxide hydrates by coordination to titanium atoms, or H-bonds to OH-groups. An additional characteristic property of these species is their amorphous nature in the solid state [54, 55]. As a consequence, also the denotation "amorphous titania" is applied for them. We like in addition to emphasise that titanium oxide hydrates can be present as either mononuclear ($x = 1$) or polynuclear species ($x \geq 2$). The latter can be considered to be of polymeric nature if x is well above 2. These *polymeric* titanium oxide hydrates are of variable composition

represented by the more detailed general formula $Ti_xO_y(OH)_z(H_2O)_v(H_3O)_w$, as it has been suggested that also hydronium ions can be part of titanium oxide hydrates [56].

In several synthetic routes for the preparation of crystalline titania this unstructured material is subjected to specific treatments in order to induce the formation of the desired polymorphs. In many cases, however the treatments adopted do not entirely convert such amorphous into crystalline TiO_2; and strikingly authors completely neglect, usually, the possibility that residues of this material may influence the overall properties of the semicrystalline powders produced – a topic of this thesis.

1.9. Scope of the thesis

In this thesis, we intend to revisit this forgotten class of titanium compounds- *i.e*. titanium oxide hydrates. To this aim in Chapter 2 we present an investigation on photochromic response of titanium oxide hydrates upon exposition to UV light in different chemical environment. The evolution of the photochromic activity in samples with increasing crystalline content is studied in order to deduce the effect of the degree of conversion of titanium oxide hydrates into TiO_2 on the photo-response of such material. We expect that this analysis might provide an insight for other photoinduced properties such as the photocatalytic and the photovoltaic behaviour usually addressed to titania.

In the Chapter 3, the manufacture of such hybrid materials comprising titanium oxide hydrates and poly(vinyl alcohol) is described. Their mechanical properties and eventual photochromic behaviour are investigated, and examples of possible uses and prototypes of applications are given.

A further investigation of the optical properties of such PVAl / titanium oxide hydrates is presented in Chapter 4. We thereby focus on the refractive index *n* of such hybrid materials and describe how *n* can be modulated by selecting the composition of the material, by applying suitable thermal treatment procedures or through irradiation with UV light. Use of this hybrid material for the fabrication of dielectric distributed Bragg reflectors (DBR) is also described.

Some example of possible further work involving titanium oxide hydrates is given in Chapter 5. These can be expected to range from the widening of the photochromic colour spectrum to the evaluation of the potential of titanium oxide hydrates in photocatalytic and photovoltaic applications. We also envision the hybrid PVAl / titanium oxide hydrates hybrid systems for optical applications such as dichroic films and photonic crystals.

1.10. References

1. U. Diebold, *The surface science of TiO_2.* Surf. Sci. Reports., 2003. **48**: p. 53.
2. A. Fahmi, C. Minot, B. Silvi, and M. Causa`, *Theoretical analysis of the structures of titaniumdioxide crystals.* Phys. Rev. B. 1993. **47** (18): p. 11717.
3. C. J. Howard, T. M. Sabine, and F. Dickson, *Structural and thermal parameters for rutile and anatase.* Acta Crystallogr. A, 1991. **B47**: p. 462.
4. F. A. Grant, *Properties of rutile (titanium dioxide).* Rev. Modern Phys. 1959. **31** (3): p. 646.
5. J. Ovenstone and K. Yanagisawa, *Effect of hydrothermal treatment of amorphous titania on the phase change from anatase to rutile during calcination.* Chem. Mater., 1999. **11**: p. 2770.
6. A. V. Tolchev, V. Y. Pervushin, and D. G. Kleshchev, *Thermal tranformations of hydrated titanium dioxide with a globular structure of aggregates.* Russ. J. Appl. Chem., 2001. **75** (5): p. 696.
7. R. Asahi, Y. Taga, T. Mannstadt, and A. J. Freeman, *Electronic and optical properties of anatase TiO_2.* Phys. Rev. B, 2000. **61**: p. 7459.
8. D. C. Cronemeyer, *Electrical and optical properties of rutile single crystals.* Phys. Rev., 1952. **85** (5): 876.
9. G. E. Jellison, L. A. Boatner, J. D. Budai, B.-S. Jeong, and D. P. Norton, *Spectroscopic ellipsometry of thin film and bulk anatase TiO_2.* J. Appl. Phys., 2003. **93** (12): p. 9537.
10. B.-S. Jeong, D. P. Norton, and J. D. Budai, *Conductivity in transparent anatase TiO_2 films epitaxially grown by reactive sputtering deposition.* Solid State Electron., 2003. **47**: p. 2275.

11. N. Yu and J. W. Halley, *Electronic structure of point defects in rutile TiO_2.* Phys. Rev. B, 1995. **51**: p. 4768

12. P. Reinhardt and B. A. Hess, *Electronic and geometrical structure of rutile surfaces.* Phys. Rev. B, 1994. **50**: p. 12015

13. R. Sanjinès, H. Tang, H. Berger, F. Gozzo, G. Margaritondo, and F. Lévy, *Electronic structure of anatase TiO_2 oxide.* J. Appl. Phys., 1994. **75** (6): p. 2945.

14. H. Tang, F. Lévy, H. Berger, and P. E. Schmid, *Urbach tail of anatase TiO_2.* Phys. Rev. B, 1995. **52**: p. 7771.

15. H. Tang, K. Prasad, R. Sanjinès, P. E. Schmid, and F. Lévy, *Electrical and optical properties of TiO_2 anatase thin films.* J. Appl. Phys., 1994. **75** (4): p. 2042.

16. L. Forro, O. Chauvet, D. Emin, L. Zuppiroli, H. Berger, and F. Lévy, *High mobility n-type charge carriers in large single crystals of anatase (TiO_2).* J. Appl. Phys., 1994. **75** (1): p. 633.

17. D. Duonghong, E. Borgarello, and M. Grätzel, *Dynamic of light-induced water cleavage in colloidal systems.* J. Am. Chem. Soc., 1981. **103**: p. 4685.

18. D. Duonghong, J. Ramsden, and M. Grätzel, *Dynamics of interfacial electron tranfer processes in colloidal systems* J. Am. Chem. Soc., 1982. **104**: p. 2977.

19. J. Moser and M. Grätzel, *Photoelectrochemistry with colloidal semiconductors; Laser studies of halides oxidation in colloidal dispersions of TiO_2 and α-Fe_2O_3.* Helv. Chim. Acta, 1982. **65** (5): p. 1436.

20. J. Moser and M. Grätzel, *Light-induced electron transfer in colloidal semiconductor dispersions: single vs. dielectronic reduction of acceptors by conduction band electrons.* J. Am. Chem. Soc., 1983. **105** (65): p. 6547.

21. I. A. Shkrob, M. C. S. Jr, and D. Gostzola, *Efficient, rapid photoxidation of chemisorbed polyhydroxyl alcohols and carbohydrates by TiO_2 nanoparticles in aqueous solution.* J. Phys. Chem. B, 2004. **108**: p. 12512.

22. Z. W. Wicks, F. N. Jones, S. P. Pappas, and D. A. Wicks, eds. *Organic coating science ad technology*. 3rd ed. 2007, John Wiley &Sons, Inc.: Hoboken, New Jersey.

23. X. Wang, M. Fujimaki, and K. Awazu, *Photonic crystal structures in titanium dioxide (TiO_2) and their optimal design.* Opt. Express, 2005. **13** (5): p. 1486.

24. S. Shimada, K. Miyazawa, and M. Kuwabara, *An easy method for fabricating TiO_2 gel photonic crystals using molds and highly concentrated alkoxide solutions.* Jpn. J. Appl. Phys, 2002. **41** (3): p. 291.

25. V. M. Komenko, K. Langer, H. Rager, and A. Fett, *Electronic absorption by Ti^{3+} ions and elecron delocalization in synthetic blue rutile.* Phys. Chem. Miner., 1998. **25**: p. 338.

26. C. Renz, *Lichtreaktionen der Oxide der Titans, Cers und der Erdasäuren.* Helv. Chim. Acta, 1921. **4**: p. 961.

27. C. Naccache, P. Meriaudeau, and M. Che, *Identification of oxygen species adsorbed on reduced titanium dioxide.* Trans. Faraday Soc., 1971. **67**: p. 506.

28. R. P. Müller, J. Steinle, and H. B. Boehm, *Characterization of photochemically or electrochemically reduced blue titanium dioxide.* Z. Naturforsch., 1990. **45b**: p. 864.

29. R. F. Howe and M. Grätzel, *EPR observation of trapped electrons in colloidal TiO_2.* J. Phys. Chem., 1985. **89**: p. 4495.

30. T. Berger, M. Sterrer, O. Diwald, E. Knozinger, D. Panayotov, T. L. Thompson, and J. T. Yates. jr, *Light-induced charge separation in anatase TiO_2 particles.* J. Phys. Chem. B, 2005. **109**: p. 6061.

31. M. Anpo, T. Shima, S. Kodama, and Y. Kubokawa, *Photocatalytic hydrogenation of CH_3CCH with H_2O on small-particle TiO_2: size quantization effects and reaction intermediates.* J. Phys. Chem., 1987. **91**: p. 4305.

32. A. Hagfeldtt and M. Grätzel, *Light-induced redox reactions in nanocrystalline systems.* Chem. Rev., 1995. **95**: p. 49.

33. A. N. Shultz, W. Jang, W. M. Hetherington. III, D. R. Baer, L.-Q. Wang, and M. H. Engelhard, *Comparative second harmonic generation and X-ray photoelectron spectroscopy studies of the UV creation and O_2 healing of Ti^{3+} defects of (110) rutile TiO_2 surfaces.* Surf. Sci., 1995. **339**: p. 114.

34. W. Göpel, J. A. Anderson, D. Frankel, M. Jaehnig, K. Phillips, J. A. Schäfer, and G. Rocker, *Surface defects of TiO_2(110): A combined XPS, XAES and ELS study.* Surf. Sci., 1984. **139**: p. 333.

35. M. L. Knotek and P. J. Feibelman, *Ion desorption by core-hole auger decay.* Phys. Rev. Lett., 1978. **40**: p. 964.

36. L.-Q. Wang, D. R. Baer, and M. H. Engelhard, *Creation of variable concentrations of defects on TiO_2 (110) using low-density electron beams.* Surf. Sci., 1994. **320** (3): p. 295.

37. V. E. Henrich, G. Dresselhaus, and H. J. Zeiger, *Observation of two-dimensional phases associated with defect states on the surface of TiO_2.* Phys. Rev. Lett., 1976. **36** (22): p. 1335.

38. P. J. D. Lindan, N. M. Harrison, M. J. Gillan, and J. A. White, *First-principles spin-polarized calculations on the reduced and reconstructed TiO_2 (110) surface.* Phys. Rev. B, 1997. **55**: p. 15919

39. O. I. Micić, Y. Zhang, K. R. Cromack, A. D. Trifunac, and M. C. Thurnauer, *Trapped Holes on TiO_2 colloids studied by electron paramagnetic resonance.* J. Phys. Chem., 1993. **97**: p. 7277.

40. Y. Wang and N. Herron, *Nanometer-sized semiconductor clusters: materials synthesis, quantum size effects and photophysical properties.* J. Phys. Chem., 1991. **95**: p. 525.

41. G. Li, J. Boerio-Goates, B. F. Woodfield, and L. Li, *Evidence of nonlinear lattice expansion and covalency enhancement in rutile TiO_2 nanocrystals.* Appl. Phys. Lett., 2004. **85** (11): p. 2059.

42. R. R. Bacsa and M. Grätzel, *Rutile formation in hydrothermally crystallized nanosized titania.* J. Am. Ceram. Soc., 1996. **79** (8): p. 2185.

43. K. Yanagisawa, K. Ioku, and N. Yamasaki, *Formation of anatase porous ceramics by hydrothermal hot-pressing of amorphous titania spheres.* J. Am. Ceram. Soc., 1997. **80** (5): p. 1303.

44. K. M. Reddy, D. Guin, S. V. Manorama, and A. R. Reddy, *Selective synthesis of nanosized TiO_2 by hydrothermal route: characterization, structure property relation and photochemical application.* J. Mater. Res., 2004. **19** (9): p. 2567.

45. J. Y. Rhene Chu, S. Lian, Y. Wang, F. Yan, D. Chen, *Shape controlled synthesis of nanocrystalline titania at low temperature.* Solid State Comm. 2004. **130**: p. 789.

46. R. J. Nussbaumer, P. Smith, and W. Caseri, *Transparent, anatase-free TiO_2 nanoparticle dispersions.* J. Nanosci. Nanotechnol., 2007. **7**: p. 2422.

47. D. Zhang, L. Qi, J. Ma, and H. Cheng, *Formation of crystalline nanosized titania in reverse micelles at room temperature.* J. Mater. Chem., 2002. **12**: p. 3677.

48. P. H. Borse, L. S. Kankate, F. Dassenoy, W. Vogel, J. Urban, and S. K. Kulkarni, *Synthesis and investigations of rutile phase nanoparticles of TiO_2.* J. Mater. Sci.-Mater. El., 2002. **13**: p. 553.

49. N.-G. Park and A. J. F. J. van de Langemaat, *Comparison of dye-sensitized rutile and anatase-based TiO_2 solar cells.* J. Phys. Chem. B, 2000. **104**: p. 8989.

50. E. A. Barringer and H. K. Bowen, *High-purity, monodisperse TiO_2 powders by hydrolysis of titanium tetraethoxide. 1. Synthesis and physical properties.* Langmuir, 1985. **1** (4): p. 414.

51. M. Schneider and A. Baiker, *High-surface-area titania aerogels: preparation and structural properties.* J. Mater. Chem., 1992. **2** (6): p. 587.

52. M. Wu, J. Long, A. Huang, Y. Luo, S. Feng, and R. Xu, *Microemulsion-mediated hydrothermal synthesis and characterization of nanosize rutile and anatase particles.* Langmuir, 1999. **15** (26): p. 8822.

53. U. Gesenhues, *Calcination of metatitanic acid to titanium dioxide white pigments.* Chem. Eng. Technol., 2001. **24** (7): p. 685.

54. R. Fricke, *Röntgenoskopie (und Elektronoskopie) anorganischer Gele, insbesondere von Hydroxyden und Oxyden.* Kolloid Z., 1934. **69**: p. 312

55. R. Fricke, *Über Hydroxydgele und Oxydhydratgele sowie ihre amphoteren Eigenschaften.* Kolloid Z., 1935. **73**: p. 300

56. O. M. Rozental, T. A. Denisova, R. N. Pletnev, and A. A. Ivakin, *Relation between the proton structure and stoichiometry of titanium dioxide.* J. Appl. Chem.-USSR (Zh. Prikl. Khim. 53, 13 (1980)), 1980. **53**: p. 10.

Chapter 2

Pronounced photochromism of titanium oxide hydrates (hydrous TiO_2)

2.1. Introduction

Titanium oxide hydrates, formally described by the formula $Ti_xOy(H_2O)$ are a class of materials that attracted strong scientific interest at the beginning of the last century, but nowadays find use virtually only as pre-cursors for the preparation of crystalline TiO_2 usually through thermal dehydroxilation. In fact, such titanium compounds contain a fraction of -Ti-OH groups, which can condense leading to the formation of -Ti-O-Ti- bonds and water and thus to the conversion to crystalline titanium dioxide.

Being usually prepared by hydrolysis of titanium tetrachloride, titanyl sulfate (the reported compositions of which are contradictory [1]) or titanium tetraalkoxides (tetra-alkyl orthotitanates) titanium oxide hydrates form through a complex process, and their exact composition depends crucially on a variety of parameters [2]. Dialysis experiments revealed, for instance, that upon hydrolysis of $TiCl_4$ the formation of

(possibly chlorinated) polymeric titanium oxide hydrates proceeds relatively fast at room temperature [3]. Similarly, chlorinated polymeric titanium oxide hydrates may arise when they are prepared in HCl solutions [2].

Solid titanium oxide hydrates can be precipitated, for instance, by addition of bases or suitable heat treatments [4-8]. Initially, such solids can be re-dissolved in, *e.g.* hydrochloric acid [4, 6, 7, 9], whereat the dissolved and precipitated materials can differ in their composition. However, their solubility decreases upon aging [4], which proceeds slowly at room temperature, but more rapidly at elevated temperatures [8]. In this process, the slow release of water, which proceeds over months at room temperature, is irreversible but the material remains completely amorphous as determined by wide-angle X-ray diffraction [10]. As a consequence of this, a number of misleading formulae and designations have historically evolved – and are still in use [11-13], such as $TiO_2 \cdot nH_2O$ [1], $TiO(OH)_2$ or H_2TiO_3, frequently termed as metatitanic acid and corresponding formally to $TiO_2(H_2O)$, [14, 15], or $Ti(OH)_4$ (*i.e.* orthotitanic acid) [16] which corresponds formally to $TiO_2(H_2O)_2$ (the designation titanic acid itself was originally applied to TiO_2 due to its weak acid behaviour [4, 6]). Such formulae assigned to isolated solids, however, have been recognized not to be exact and to cause confusion [17-19]. For instance, the stoichiometry of technically available products with the name metatitanic acid markedly deviates from $TiO_2(H_2O)$ [20].

2.2. Chromic characteristics of titanium oxide hydrates

An interesting but widely forgotten property of titanium oxide hydrates is their colour change in HCl solutions when exposed to either zinc or hydrogen at room temperature [4, 21-23]. The initially colourless systems were reported to turn blue or

blue-violet as a result of reduction processes of Ti^{IV} to Ti^{III} species. In agreement with these observations, titanium oxide hydrates produced from $TiCl_3$ solutions by prolonged standing or, more rapidly, upon heating in the open atmosphere, were found to display such a chromic behaviour [18]. This implies that both Ti^{III} and Ti^{IV} ions (the latter expected having been formed by partial oxidation of Ti^{III}) must be present to result in the observed red/blue colouration (which faded within a few days). As a consequence, it appears likely that an intervalence charge transfer in polynuclear species containing both Ti^{III} and Ti^{IV} might have occurred [24]. Here, we revisited titanium oxide hydrates and reveal that they display also a pronounced *photo*-chromism, particularly in a suitable environment.

2.3. Results and discussion

2.3.1. *Mono*-nuclear titanium species from $TiCl_4$

In order to investigate the full potential of titanium oxide hydrates, especially their interesting chromic characteristics, $TiCl_4$ was hydrolysed at low temperatures [16], in a highly acidic environment (pH < 0.5; due to the release of HCl upon hydrolysis). Under these conditions, we expected the titanium compounds to be predominantly of *mono*-nuclear nature (hydroxides or chlorides) – as long as the temperature was not risen [2]. We tested this hypothesis by treating the initial hydrolysis solutions, which were fully transparent and colourless with metallic zinc which is a well known reducing agent in presence of acids. In such conditions, in fact, the Zn would oxidise to Zn^{2+} and at the same time the titanium is reduced to Ti^{III}. Through this procedure, already after 5 - 10 minutes, the liquids turned to a pink / pale violet colouration that strongly resembled the one reported for systems comprising (mononuclear) $[Ti(H_2O)_6]^{3+}$-ions [25] rather than the blue colour that was

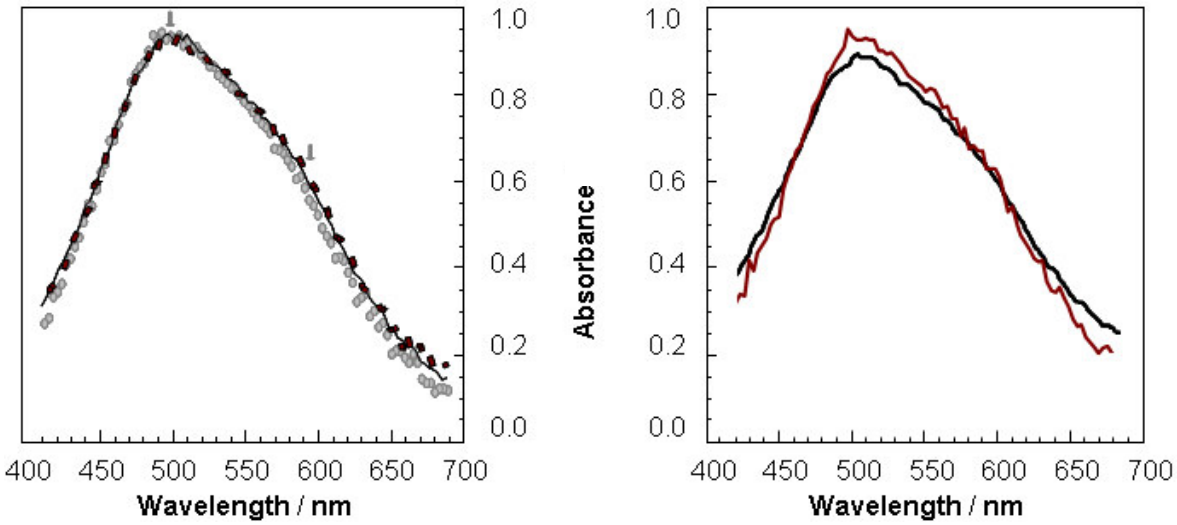

Figure 2.1: Room temperature UV-vis spectra of systems comprising predominantly mono-nuclear Ti-species, that were reduced with metallic Zn. ***Left Panel***: freshly prepared $TiCl_4$ hydrolysis solution (black, thin line); $TiCl_4$ hydrolysis solution comprising glycerol (390 mmol glycerol/mmol Ti) (black symbols); and $TiCl_4$ hydrolysis solution comprising glycerol (390 mmol glycerol/mmol Ti) that first had been neutralized with KOH, then re-acidified with HCl before being reduced with Zn (grey symbols). ***Right panel***: UV-vis spectra of $TiCl_4$ hydrolysis solutions, freshly prepared (black) and stored for > 6 months, then reduced with Zn (red).

observed for *poly*-nuclear Ti^{III}-containing titanium oxide hydrates [4, 19, 21, 22]. In addition, UV-vis spectroscopy (Fig. 2.1, left panel) revealed a maximum peak absorption around 498 nm and a shoulder around 600 nm in agreement with the spectrum of the Ti^{III}-aqua ion [25, 26]. Hydrolysis solutions comprising 0.35 mol Ti/dm^3 remained clear even after storage for more than six months, when kept at 0 °C. Treatment with zinc (at 20 °C) of such solutions led to a colouration and UV-vis absorption that were virtually the same as those obtained for freshly prepared hydrolysis solutions (Fig. 2.1, right panel). It seems therefore that the mononuclear nature of the inorganic species was not altered markedly during storage; *i.e.* the usual ageing that leads to condensation reactions [4, 14] and results in the formation of *poly*-nuclear titanium oxide hydrates (and thus, often, precipitation) was inhibited by the low-temperature environment [2].

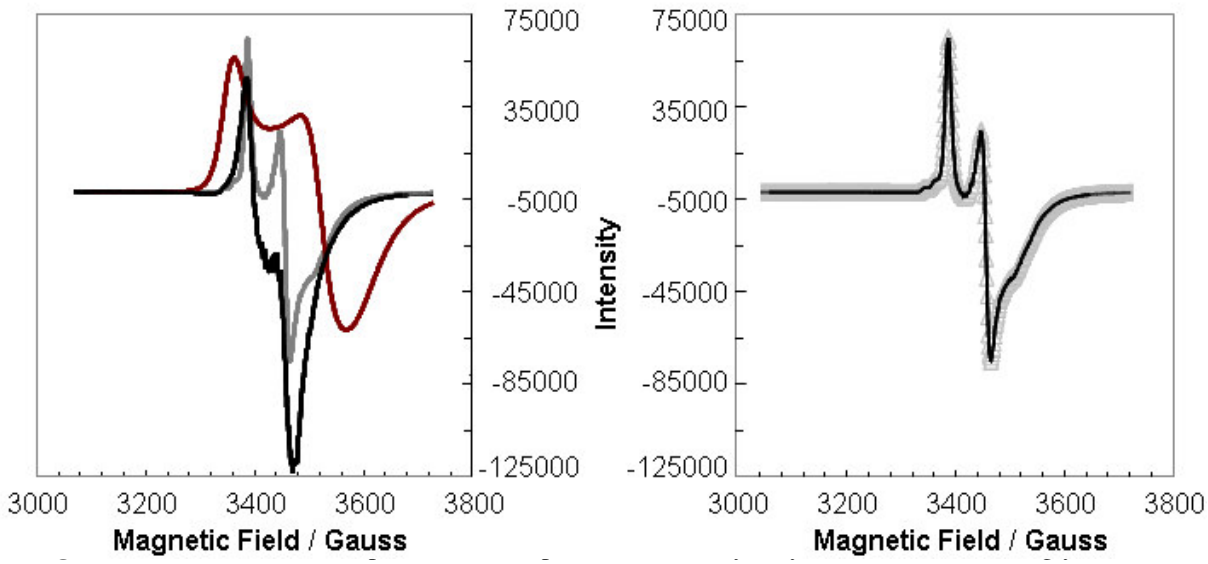

after reduction. ***Left Panel***: Freshly prepared $TiCl_4$ hydrolysis solution without glycerol (red line) and with glycerol (390 mmol glycerol / mmol Ti - grey line) reduced with metallic Zn. In addition, the spectrum of a polynuclear system containing glycerol (390 mmol glycerol / mmol Ti) and reduced via UV-irradiation for 15 min with a 200 W Hg lamp (see for details sec. 2.5.9), is also shown (black line). ***Right panel***: EPR spectra of $TiCl_4$ hydrolysis mixture comprising glycerol freshly prepared (the same as reported in the left panel) (grey) and after being neutralized with KOH and then re-acidified with HCl (black).

2.3.2. Glycerol environment

Addition of glycerol further stabilised the hydrolysis solutions at room temperature when formation of titanium oxide hydrates would be expected to proceed faster. This not only allowed preparation of transparent systems of an unusually high content of the inorganic species, but also permitted their storage at 20 °C. As a matter of fact, we found that an amount of glycerol as little as 1 mmol glycerol / mmol Ti allowed stabilising titanium species at room temperature for about 10 days, and mixtures with a larger molar ratio such as 10 mmol glycerol / mmol Ti remained clear and free of visually perceptible particle for months. The glycerol did not affect the chromic behaviour of the supposed mononuclear titanium compounds when treated with Zn. In fact, a colour change from transparent to pink/pale violet was observed also for the glycerol-containing systems, with essentially identical UV-vis spectra obtained

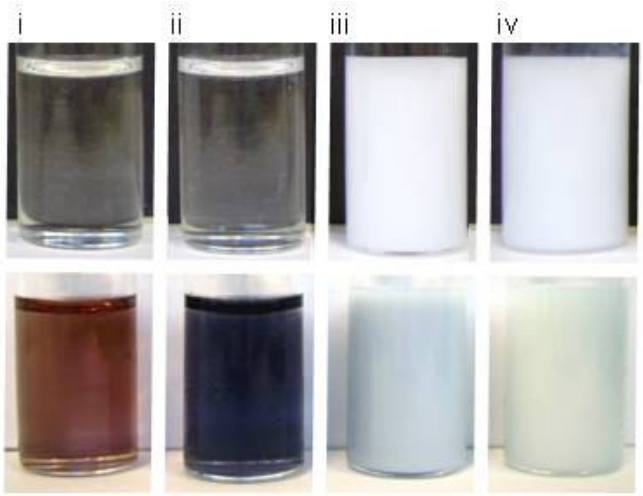

Figure 2.3: Photochromic behaviour of (***i***) hydrolysis solution of $TiCl_4$, (***ii***) systems comprising titanium oxide hydrates (***ii***), and (***iii*** and ***iv***) for comparison, dispersions of commercially available TiO_2 nanopowders ((***iii***): P25 (Degussa), (***iv***): Adrich nanopowders). All systems are mixed with glycerol and are shown before and after illumination with UV-light performed with a 200 W Hg lamp for 10 min (top and bottom panels, respectively). Concentrations are respectively ≈ 50 mmol glycerol / mmol Ti for (***i***) and (***ii***), and 5 ml glycerol / 0.1 mg TiO_2 or 55.44 mol glycerol / mol Ti for (***iii***) and (***iv***).

as for the solutions not comprising any glycerol (Fig. 2.1, left panel). This suggests that glycerol did not strongly coordinate to Ti^{III}, as otherwise, a distinct shift of the absorption maximum toward higher wavelengths in the UV-vis spectrum would have been expected. Of course, coordination to mononuclear Ti^{IV} species cannot be excluded [26] (some difference between systems with and without glycerol are indeed observed in X-band electron-spin resonance (EPR) spectroscopy, carried out at 22 K, which probe the unpaired electrons; *cf.* Fig. 2.2, left panel).

2.3.3. Photochromism of *mono*-nuclear species

Unexpectedly, the addition of glycerol to hydrolysis solutions supposed to comprise predominantly mono-nuclear titanium species rendered them sensitive to

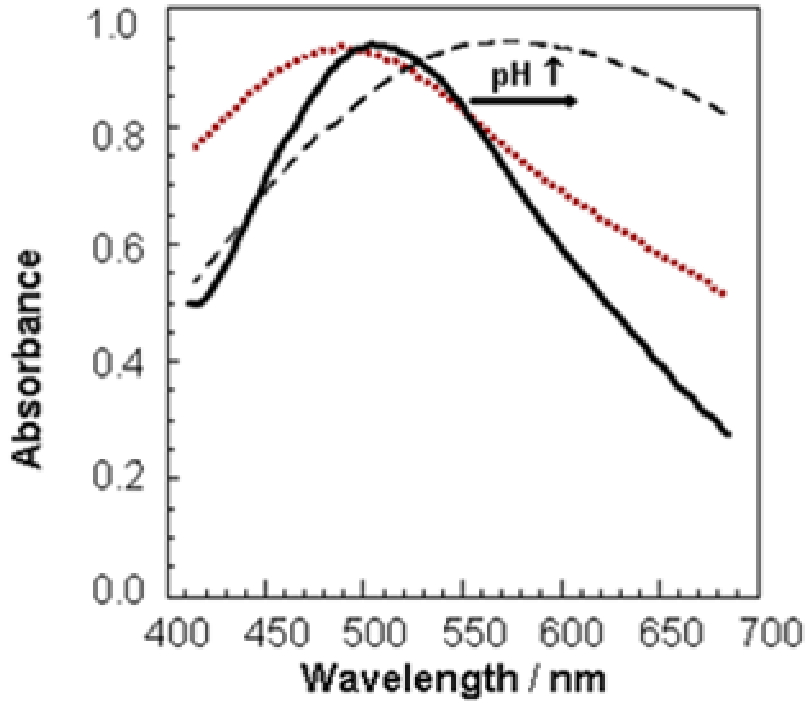

Figure 2.4: UV-vis spectra of $TiCl_4$ hydrolysis solutions comprising glycerol irradiated for 5 min with UV-light using a 200 W Hg lamp. Comparison between two hybrid systems (100 mmol glycerol / mmol Ti) one at pH < 0.5 (black solid line) and the other at pH ≈ 5 (gray dotted line) which shows a visible red shift and widening of the absorption band at higher pH values. In addition, (red dotted line) the spectra of a glycerol mixture made with freshly prepared titanium oxide hydrate solid (obtained by vacuum assisted desiccation of the $TiCl_4$ hydrolysis solution) previously dissolved in water, after exposure to UV-radiation, is displayed. Also this system, similarly to the hybrid mixture at pH < 0,5 produces a spectrum centred at around 500 nm however wider, possibly as a consequence of intermetallic charge transfer effect resulting from a partial condensation of the titanium species during the desiccation.

UV-irradiation. The *photo*-chromic characteristics were found to be very similar to systems reduced with zinc. For instance, systems containing relatively large amounts of the stabilising glycerol (~50 – 390 mmol glycerol / mmol titanium, pH < 0.5) exhibited a pronounced colour change to pink/violet (Fig. 2.3, bottom panel / first picture on the left) already after 3 to 5 minutes of exposure to UV-light (200 W Hg lamp - see sect. 2.5.9 for details) — a colouration that increase with exposition to the

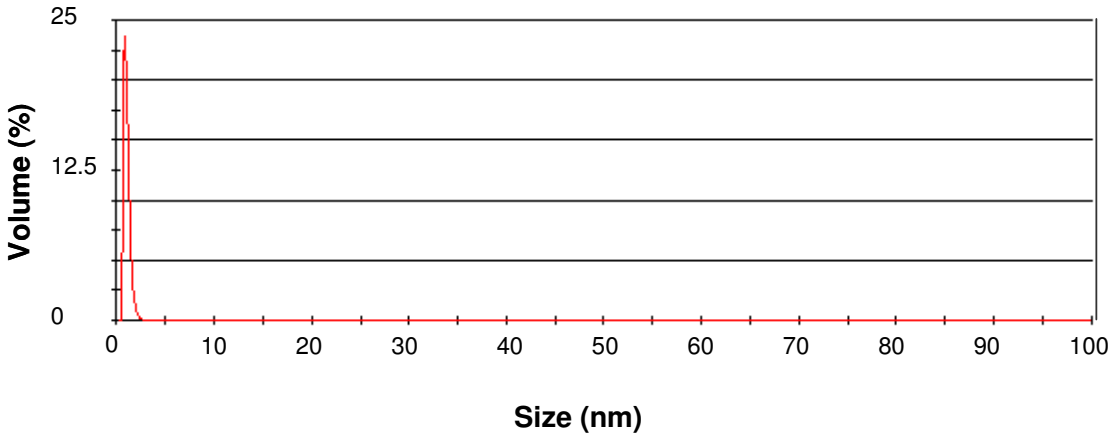

Figure 2.5: Z-sizer scan retrieved for a mixture of glycerol and hydrolysed $TiCl_4$ with concentration of 390 mmol glycerol / mmol Ti, neutralised with KOH and analysed soon after its preparation. The only visible peak is around 1 nm. However peaks below 3 nm cannot be considered reliable.

radiation and was stable in a closed vial at room temperature over weeks. The corresponding UV-vis spectrum (Fig. 2.4) strongly resembled that of the Ti^{3+} aqua ion (maximum peak absorption around 498 nm), although the shoulder in the 600 nm wavelength range was less evident than that observed for the hydrolysis solutions reduced with Zn. By stark contrast, solutions that contained no glycerol stayed colourless when exposed to UV-irradiation, suggesting that glycerol acted as a medium for the photoreduction of Ti^{IV} to Ti^{III}, or at least for the stabilization of the reduced species, which is accompanied by a colour change.

2.3.4. *Poly*-nuclear titanium species from $TiCl_4$ (titanium oxide hydrates)

For the preparation of systems comprising *poly*-nuclear titanium oxide hydrates, we used fresh, cold (0 °C) hydrolysis solutions of $TiCl_4$ pure or added to glycerol upon stirring, and increased their pH- value above 3 using KOH (see sec. 2.5.3) – conditions particularly suited for their formation [22, 27, 28].

Beneficially, the presence of the glycerol already at concentrations of ~ 50 mmol

glycerol / mmol Ti stabilised the formation of titanium oxide hydrates over a broad pH-range (pH = 0.5 – 12) without visible agglomeration or precipitation of the Ti-species. (Fig. 2.3, top panel / second left picture). In fact, no particles were detected in freshly neutralised systems containing glycerol according to light scattering experiments performed using a Malvern Zetasizer (see Fig. 2.5). Reassuringly, mixtures of high glycerol content (390 mmol glycerol / mmol Ti) remained transparent even after 6 months storage at room temperature. On the other hand systems comprising glycerol in an amount lower than ~ 50 mmol glycerol / mmol Ti even if they remained transparent during the neutralization often became opaque within 10 to 15 min if left at room temperature while when stored at 0 °C, all glycerol dispersions with pH > 3 stayed transparent for more than six months. This is in strong contrast to hydrolysis solutions free of glycerol, in which precipitates were already observed to occur instantaneously when the pH was increases above 3.

2.3.5. Photochromism of *poly*-nuclear titanium oxide hydrates

Upon illumination with UV light using a 200 Hg lamp (of such polynuclear titanium oxide hydrate /glycerol samples of pH-value between 3 to 6, a deep *blue* colouration developed (Fig. 2.3, bottom panel/second left picture and Fig 2.6 top panel), which became more intense at longer exposure times (Fig. 2.6, bottom panel) or at higher concentrations of the Ti species. At pH-values around 7 to 8, however, the intensity of the colouration decreased drastically, while at pH > 9 dispersions did not display any photochromic response (Fig. 2.6, top panel). Clearly, the photochromic response of the titanium oxide hydrates is strongly affected by the pH of the system, and/or by the concentration of OH^- in the surrounding.

The *blue* colour developing upon exposure to UV-light seems to be caused by

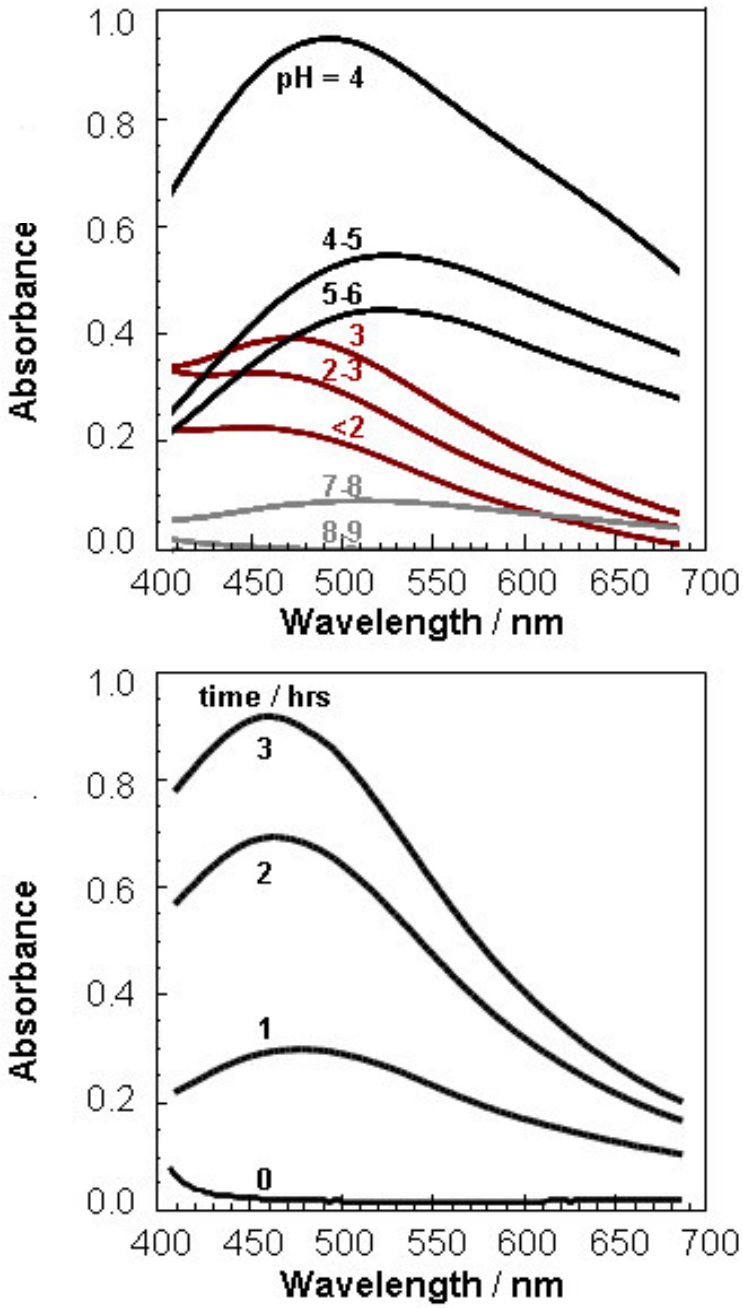

Figure 2.6: ***Top panel:*** UV-vis spectra of $TiCl_4$ hydrolysis solutions containing glycerol (200 mmol glycerol / mmol Ti) at various pH values adjusted with KOH, irradiated with UV-light each for 15 min with a 200 W Hg lamp. The intensity of the photochromic response of the systems increased from pH < 2 to pH ≈ 4, and then decreased for higher pH values. Alkaline systems did not develop any colouration upon of exposition to the UV light. ***Bottom panel:*** In all cases, colouration increased with time of irradiation. As an example, here, the UV absorption spectra collected at increasing time of illumination with a 100 W Hg lamp, is reported for a system at pH = 5-6.

titanium oxide hydrates comprising Ti^{III} atoms, as deduced from the EPR data presented in Figure 2.2, left panel. This is supported by UV-vis spectroscopy in which a distinct red-shift and a broadening of the absorption maximum, compared to the spectra of the acidic solutions containing Ti^{III}-aqua ions, is observed (Fig. 2.4). Essentially, several processes can explain the red shift like the reduction of the coordination number of the Ti^{III} atoms from 6 in the Ti^{III}-aqua ions to 4 in the titanium oxide hydrates, as well as the replacement of coordinated water molecules by hydroxide or oxide ions. Both phenomena result in a weaker crystal field splitting, the latter according to the spectrochemical series [29], originating in a red-shift of the absorption maximum. Furthermore, the blue colour is in agreement with an intervalence charge transfer (IVCT) which frequently causes asymmetric-shaped absorption peaks of high intensity [30], whereat *d-d* bands of Ti^{III} ions might be superimposed [24]. Indeed, the extreme broadness of the absorption seems to indicate a class-II system [30] according to the classification scheme of Robin and Day [24], supporting the notion of having a polynuclear mixed valence compound present with weakly coupled Ti^{III}-Ti^{IV} centres where the electrons are "localized" at Ti^{III} ions.

Summarising the above, whilst the initial acidic systems of hydrolysed $TiCl_4$ and glycerol comprised mononuclear titanium species, upon addition of KOH more complex species, *i.e.* polynuclear titanium oxide hydrates formed. Further, it has to be considered that both, the initial mononuclear species as well as the polynuclear titanium oxide hydrates may be chlorinated, which schematically can be represented with the formulae:

$$\left[Ti(OH)_z(H_2O)_yCl_n\right]^{(4-n-z)+} \xrightarrow{OH^-} \left[Ti_aO_b(OH)_c(H_2O)_d(H_3O)_eCl_f\right]^{(4c-2b-f+e)+} \quad \text{Eq. 2.1}$$

The formation of polynuclear titanium oxide hydrates can be reversible. This is

deduced from observations made on mixtures containing glycerol, which were (*i*) first neutralized to pH 6, (*ii*) re-acidified with HCl to pH < 1 within a short period of time following neutralization, and then (*iii*) either reduced with Zn or irradiated with UV-light. These re-acidified systems developed the same pink/pale violet colouration as Ti^{III} aqua ions; and the UV and EPR spectra (Fig. 2.1, left panel; Fig. 2.2, right panel) were found to be essentially identical to those of the mononuclear titanium species found in freshly prepared solutions of hydrolysed $TiCl_4$ by irradiation in presence of glycerol.

2.3.6. Titanium oxide hydrates from titanium tetraisopropoxide (TTIP)

In order to elucidate if the photochromism observed in glycerol surrounding is restricted to titanium oxide hydrates prepared from $TiCl_4$ (for instance due to the presence of chloride ions), we also investigated dispersions made from titanium tetraisopropoxide (TTIP), another precursor for titanium oxide hydrates [31]. To this end, TTIP was dissolved in a mixture of isopropanol, water and acetic acid, resulting in significantly milder pH conditions for the hydrolysis (pH ≈ 4) compared to $TiCl_4$-based systems. As a consequence, the TTIP mixtures were less stable than the hydrolysis products of $TiCl_4$ when no glycerol was added, with white solids precipitating already after 0.5 – 1 hour during storage at room temperature. Addition of glycerol stabilised also the systems made from TTIP resulting in mixtures that remained transparent also after 4 – 5 days storage at room temperature – or upon increasing the pH-value to 6. Differently from the previous glycerol dispersions containing titanium species from the hydrolysis of $TiCl_4$, less than 3 mmol glycerol / mmol Ti were required to stabilise the dispersions at pH > 3.

A blue coloration developed in TTIP systems upon UV-light exposure (Fig 2.7). Interestingly, also the precipitates from those hydrolysis solutions turned grey-bluish

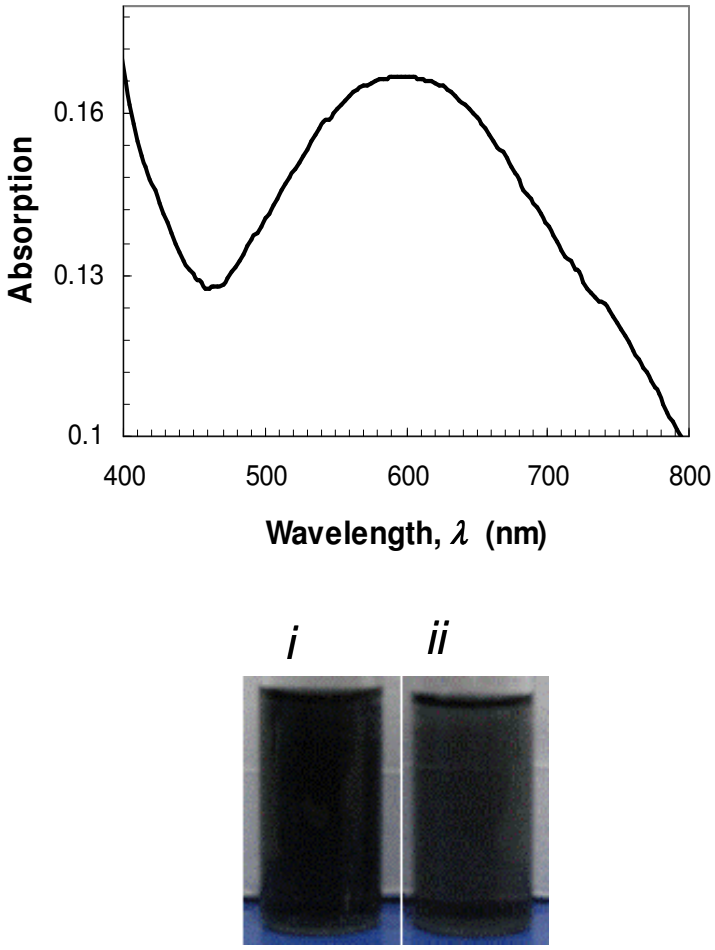

Figure 2.7: ***Top panel:*** UV-vis spectrum of a mixture of hydrolysed TTIP in glycerol with a concentration of $1.60 \cdot 10^2$ mmol glycerol / mmol Ti irradiated for 5 min with UV light from a 200 W Hg lamp (see for details sect. 2.5.9). ***Bottom panel:*** Photograph of *i)* a mixture of hydrolysed TTIP mixed with glycerol ($1.60 \cdot 10^2$ mmol glycerol / mmol Ti) and *ii)* sample of the hydrolysis solution of TTIP, UV-irradiated for 10 min with a 200 W Hg lamp.

(Fig 2.7- bottom panel - *ii*) upon irradiation with UV-light even in absence of glycerol, indicating that also other compounds than glycerol – such as the isopropanol or the acetic acid, being present in excess in the TTIP systems – can induce a photochromic response. In addition, the above observations show that the photochromic behaviour of titanium oxide hydrates is not restricted to materials produced with chlorine-containing species.

2.3.7. Solid titanium oxide hydrates by desiccation

Solid titanium oxide hydrates were produced by desiccation of a hydrolysis solution of $TiCl_4$ in vacuum at 35 – 40 °C. Translucent solids were obtained, which were fully amorphous as deduced from wide-angle X-ray diffraction (Fig. 2.8). These compounds contained a high chlorine content (Table 2.1), in agreement with the literature [7, 32]. As expected for titanium oxide hydrates, such freshly prepared solids were found to be almost fully soluble in water resulting in rather transparent liquids of high acidity (pH < 1). However, mixtures of the solid previously dissolved in water (~10 mg solid / 3 ml water) and glycerol upon irradiation with UV-light developed a violet/bluish colour, rather than the pink / pale violet observed in fresh hydrolysis solutions (Fig 2.9 – bottom panel, first picture on the left). The UV-vis absorption spectrum reported in Figure 2.4 (red dotted curve) indeed, show a broader peak with respect to the freshly prepared hydrolysis solution which may account of the slight colour difference and may point to the formation of a more condensed, polynuclear species. This would be in agreement with our observation that over time when kept at room temperature such solids became insoluble, as expected for titanium oxide hydrates. Therefore, the photochromism is not restricted to *in-situ*-prepared titanium oxide hydrates.

2.3.8. Heat treatments

When solid titanium oxide hydrates were annealed, respectively, for 2.5 hours at 100 °C or 200 °C, 12 hours at 850 °C, or 24 hours at 850 °C, the initially completely amorphous materials became increasingly crystalline with anatase developing during heat treatment procedures above 200 °C and rutile during prolonged annealing at 850 °C (Fig. 2.8) in agreement with the literature on titanium

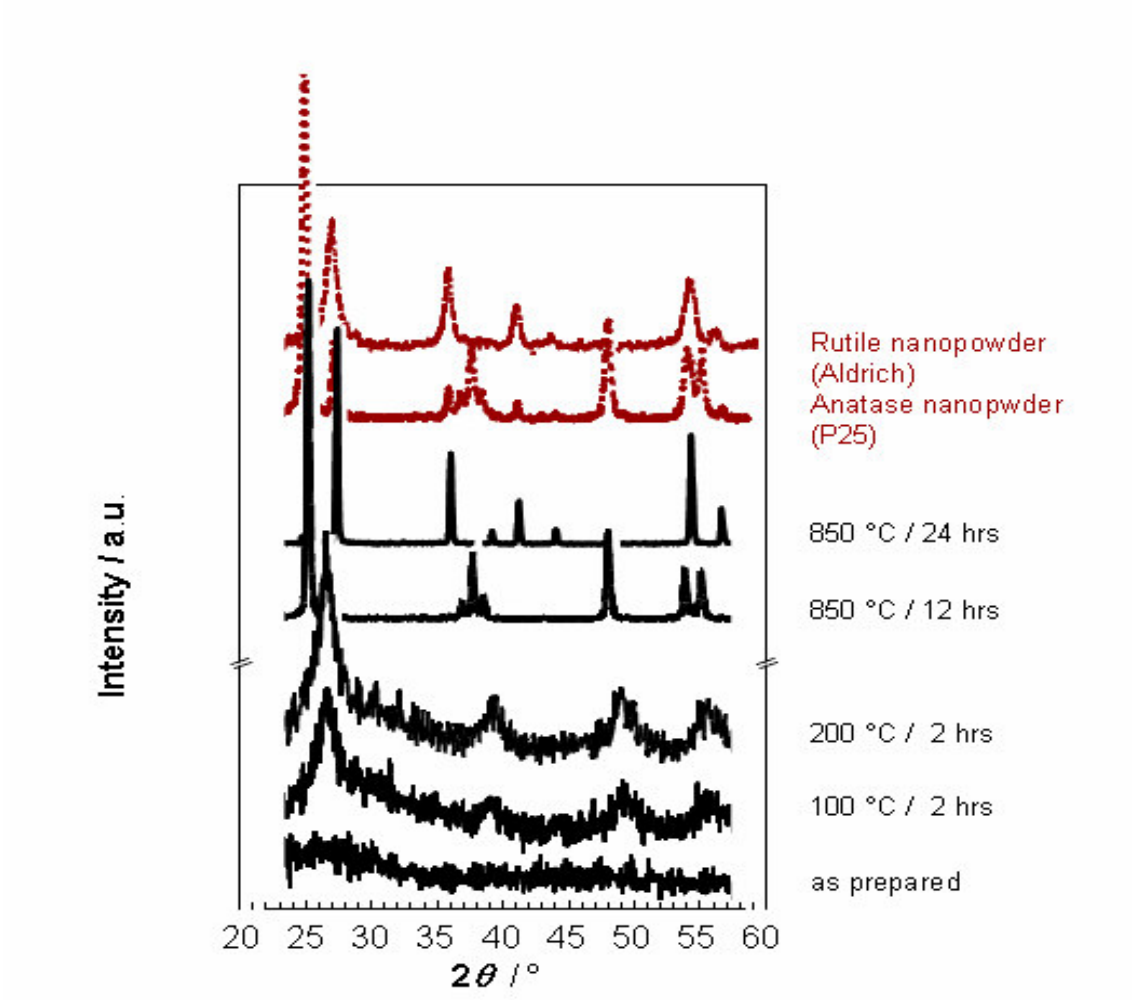

Figure 2.8: Wide-angle X-ray scattering analysis of solid titanium oxide hydrates, freshly prepared and after specific thermal heat treatment. The diffractograms of commercial TiO_2 nanopowders (in red) are here shown for comparison.

Table 2.1: Ti and Cl content in titanium oxide hydrate solids, as prepared and after specific heat treatments.

	Ti		Cl	
	%	**10^{-3} mol**	**%**	**10^{-3} mol**
100 °C / 2.5 hrs	32	7	17	5
200 °C / 2.5 hrs	49	10	6	1.5
850 °C / 24 hrs	57	12	0.15	0.05

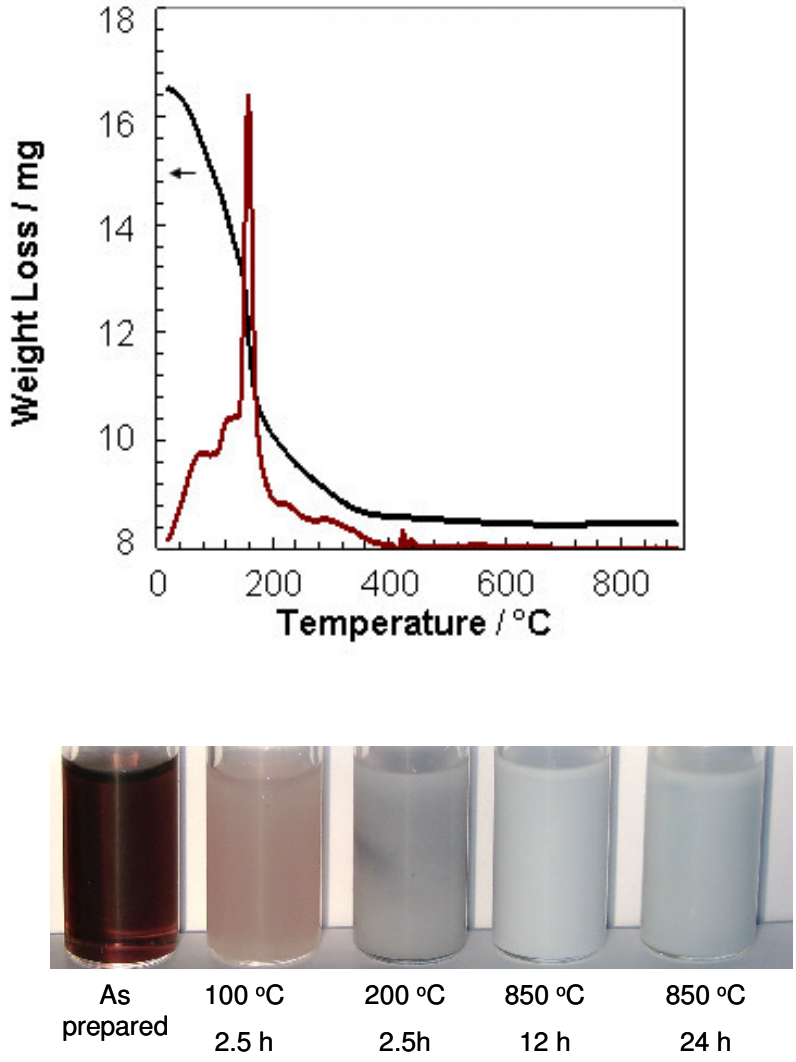

Figure 2.9: ***Top panel:*** Thermogravimetric scan performed on a sample of the solid obtained from the vacuum assisted desiccation of $TiCl_4$ hydrolysis solution (black line). First derivative in the temperature (red line). A significant weight loss of about 45 % is measured between 100 ^oC and 400 ^oC circa, which could be consistent with a modification of the material due to the removal of chlorine and to the condensation of titanium oxide hydrates to form crystalline titania. ***Bottom panel:*** Pictures of systems containing the solid from the desiccation of the $TiCl_4$ hydrolysis solution, as prepared and after heat treatments at different temperatures, dispersed in glycerol and irradiated with UV light for 15 min with a 200W Hg lamp (see sect. 2.5.9 for details).

oxide hydrates [27, 33]. The chlorine content decreased with increasing heat treatment. Nonetheless, we like to emphasise that considerable amount of Cl was still found in such heat-treated solids even after annealing at temperatures above 150 °C (Table 2.1), in accord with literature [32]. This observation indicates that the chlorine was not simply trapped as HCl within the solid, but more likely bonded to the Ti-species, as suggested above. This hypothesis is supported by the distinct mass loss (about 45% weight loss) that the solid obtained from the desiccation of the $TiCl_4$ hydrolysis exhibit at temperatures between 100 and 400 °C, as evident in the thermogravimetric data presented in Figure 2.9. In agreement with this observation elemental analysis carried on powders heat-treated at 850 °C for 24 hrs, detected chlorine only in traces amounts.

The intensity of the blue colouration of heat-treated solids suspended in glycerol and irradiated in the same conditions, strongly depended on the time and temperature of the annealing (Fig. 2.9- bottom panel). Indeed, the photochromic response of heat-treated solids was relatively weak for all heat-treated materials and significantly decreased with increasing crystallinity, *i.e.* conversion. When fully converting the latter at 850 °C for 24 hrs, no photochromism was observed. However, the progressive decrease of the photochromic activity in such samples annealed at increasing temperatures cannot be simply addressed to the decreasing surface to volume ratio of the particles as a consequence of the thermal treatment. More likely the suppression of the photochromic response in powders heated at 850 °C rather seems to suggest a correlation with the degree of conversion of the titanium oxide hydrates in crystalline TiO_2 and the increased crystalline fraction in the particles.

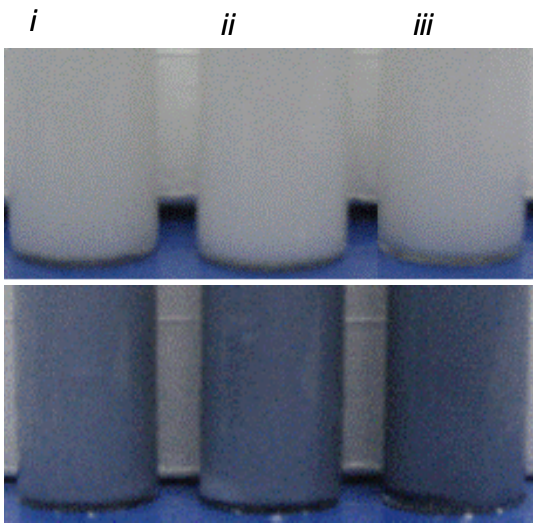

Figure 2.10: Glycerol dispersions of titanium oxide hydrates precipitated with bases, for instance: *i)* with KOH *ii)* with NaOH and *iii)* with NH3, before (top panel) and after 5 min irradiation with UV light with a 200W (bottom panel).

Indeed, also commercial "crystalline" TiO_2 based nanopowders containing anatase (P25-Degussa) or rutile (Aldrich) as the prevalent polymorph, when dispersed in glycerol, displayed – if any (in case of Aldrich nanopowders) – a chromic effect that was drastically lower than that observed in fresh solids isolated from our hydrolysis solutions (Fig. 2.1, bottom panel/right pictures). Furthermore, the photocromic effect was completely lost after treating the nanopowders at 850°C for 24 hrs.

2.3.9. Solid titanium oxide hydrates from precipitation with bases

Similar blue photochromic behaviour was observed for solids that had been precipitated from fresh hydrolysis solutions by addition of KOH, NaOH or NH_3 (see sect. 2.5.7), when these were re-dispersed in glycerol and irradiated with UV light for 5 min (Fig. 2.10) (see sect. 2.5.9).

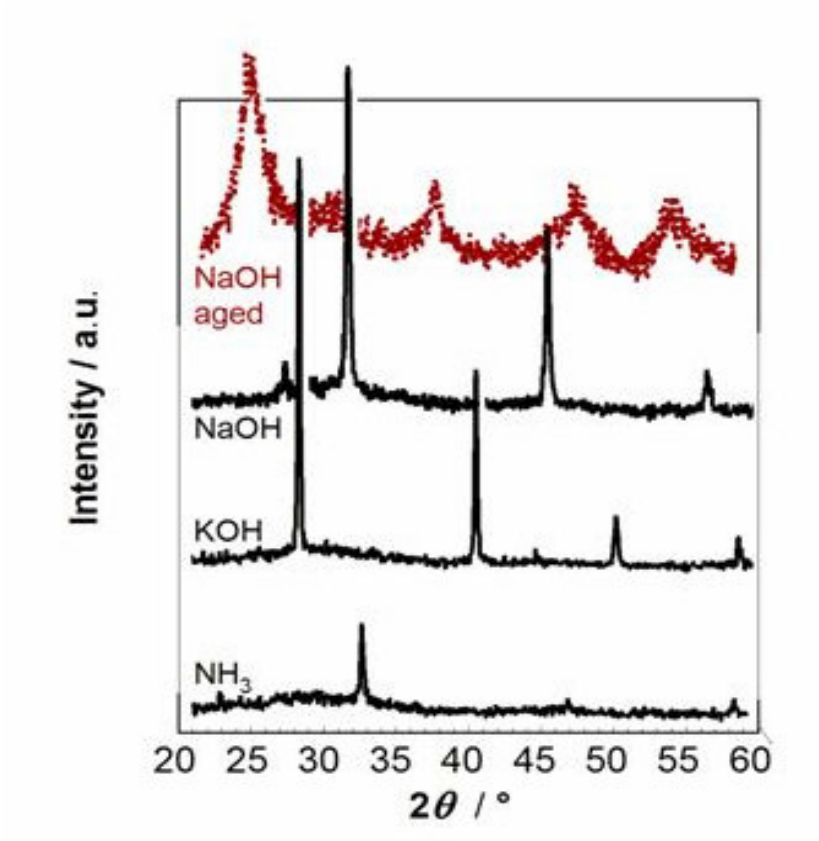

Figure 2.11: Wide-angle X-ray scattering diffractogram of titanium oxide hydrates precipitated from the freshly prepared hydrolysis solution of $TiCl_4$ with NaOH, KOH or NH_3 and dried in air for 12 h. The intense peaks visible in the three corresponding patterns (in black) are not related to any titanium dioxide polymorph and disappear over ageing at room temperature (in red) while the pattern of anatase becomes discernible.

Freshly precipitated solids were completely soluble in water acidified with HCl at very low pH (< 0.5), over ageing instead the solubility progressively decreased. Interestingly, freshly precipitated solids were predominantly of amorphous nature, similar to the materials obtained by desiccation while solid aged for less than 7 days at room temperature exhibited the diffraction features of the anatase polymorph (Fig 2.11). It is worth to note that some X-ray reflections were detected for all of these solids, which, however, could not be assigned to any known titania polymorph; *cf.* Figure 2.11. Such pronounced diffraction features obtained, in particular, with KOH

and NaOH, might stem from layered sodium or potassium titanium oxide hydrates [34, 35]. It is possible that such compounds decomposed during the condensation reactions that occurred relatively fast at room temperature. In fact over ageing those intense reflections completely disappeared while the diffraction features of anatase became visible (Fig. 2.11).

2.3.10. Mechanistic aspects of the photochromism

Although the detailed mechanism of the photochromic effect is not entirely clear, some aspects should be discussed. In the initial stages of $TiCl_4$ hydrolysis where mononuclear species appear to dominate, the generation of $[Ti(H_2O)_6]^{3+}$ under the synergetic action of glycerol and light, which is evident from UV-vis and EPR spectroscopy, must be due to a redox process involving a transfer of an electron to a Ti^{IV} species. In principle, the reduction of transition metal centres with alcohols is well established and used for a variety of synthetic procedures. It has also been proposed that glycerol can act as a reducing agent upon irradiation in the case of TiO_2 under formation of CO_2 as an oxidation product which manifests in the formation of small "bubbles" [36]. We did not observe the latter in any of our photochromic systems but we cannot exclude the generation of CO_2 since we did not yet dispose of a reliable method for its detection.

If glycerol acted as the primary reducing agent, the electron transfer would require a contact between Ti^{IV} and glycerol. The UV-vis spectra revealed that glycerol, in spite of its potential to act as a multidentate ligand, virtually did not coordinate at least to mononuclear Ti^{III}. Therefore, the possibility of outer-sphere complexes of hydrated titanium species with glycerol should also be considered. In this case, the glycerol might act as a photochromic sensitizing agent for the inner-

sphere ligands water or hydroxide. For example, glycerol might interact with Ti^{IV}-OH groups via hydrogen bonds thus favouring a light-induced homolytic scission of the Ti-O bond resulting in a Ti^{III} species and an $OH^{\cdot}$ radical, which could *e.g.* react with glycerol or recombine to hydrogen peroxide. If hydrogen peroxide was formed, glycerol would not be consumed but act as a catalyst unless the hydrogen peroxide would react in the following with glycerol (as an alternative, the hydrogen peroxide might decompose to H_2O and O_2). In fact, an indirect support of the presence of organic species in Ti^{IV} reduction under the influence of light is in agreement with earlier observations with poly(vinyl pyrrolidone) [37]. The above considerations can also be adapted to polymeric titanium oxide hydrates, where a reduction to Ti^{III} is evident from EPR spectra.

Finally, we emphasize that the electronic band structure model of semiconductors, which has been used as a suitable simplification in many processes and has also been employed in the (often conflicting) reports on photochromism and other photo-induced phenomena observed for TiO_2 [38], cannot be applied for the explanation of the photochromism of mononuclear or oligonuclear titanium species. The reason is that this model is based on the cooperative interaction of a large number atoms that this would require [39], which clearly can not be the case for mononuclear systems.

2.4. Conclusions

Summarising, our data illustrate that products from the low-temperature hydrolysis of $TiCl_4$ and TTIP can display a pronounced photochromism from turning from transparent to pink when most likely predominantly mononuclear titanium species are present, or transparent-to-blue in case of polynuclear species (*i.e.*

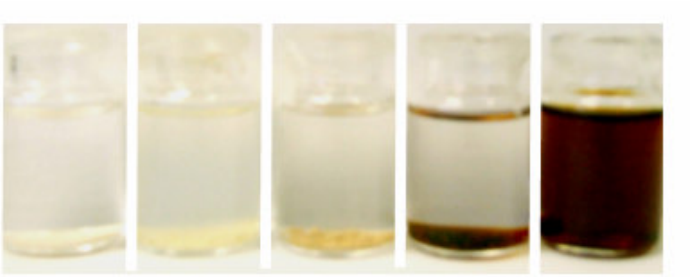

Figure 2.9: Effect of conversion of titanium species into TiO_2 on the development of the red colouration resulting from the interactions with dihydroxyarenes. From right to left: $TiCl_4$ hydrolysis solution (freshly prepared), solid titanium oxide hydrates, as obtained by the vacuum assisted desiccation of $TiCl_4$ hydrolysis solution heat treated at 200 ^oC; P25 nanopowder; Aldrich nanopowder; solid obtained from the desiccation of $TiCl_4$ hydrolysis solution, heat treated at 850 °C, for 24 hrs. A solution of *1,2*-dihydroxybenzene in isopropanol was added to all systems.

titanium oxide hydrates). These species are often present as impurities in titanium dioxide, stemming from the TiO_2 synthesis as a result from an incomplete conversion to TiO_2. Thereby, the synthetic procedure selected for the production of crystalline TiO_2 considerably influences the ratio of TiO_2 / titanium oxide hydrates produced. Our findings seem, therefore, to explain the previously reported photochromism of "TiO_2", but according to our data most likely resulted from the incomplete conversion of the titania precursors rather than from any crystalline titania polymorphs. Indeed, in all our systems, the presence of polynuclear titanium oxide hydrates rather than crystalline TiO_2 particles was confirmed with the widely forgotten colour reactions of the former with certain aromatic alcohols. To this end, we utilized *1,2*-benzenediol (pyrochatechol) and *2,3*-dihydroxynaphthalene and introduced them to our systems (see sect. 2.5.8 for details). The freshly prepared hydrolysis $TiCl_4$ solution turned from colourless to deep red, in agreement with Hauser *et al.* [40, 41] who observed that the reaction of titanium oxide hydrates with dihydroxyphenols and dihydroxynaphthols gives rise to a red colouration (Fig. 2.9). More converted species, however, only gave rise to a very pale red colour and fully converted TiO_2

remained entirely colourless during such treatment (Fig. 2.9). Note that the presence of glycerol did not interfere with or affect this chromic behaviour. Clearly, whilst our study did not lead to a quantitative and predictive understanding of the complex formation of the crystalline TiO_2, identification of and demonstrating certain beneficial characteristics of titanium oxide hydrates may shed some light on the reported, often conflicting results obtained with the use of "TiO_2" in other applications than photochromic products, including photocatalysis, photovoltaics and/or O_2-production.

We also conclude that the presence of certain suitable medium, such as glycerol, is critical to promote the colour change observed in titanium oxide hydrates systems upon UV-light irradiation. However, the origin of this desirable effect of glycerol on the photochromic response of these systems is still not to entirely clear.

Finally, our data implies moreover that the photochromic response of titanium oxide hydrates (in the presence of glycerol and maybe also of other polyalcohols such as sugars, starch and cellulose) may be exploited as a semi-quantitative indication for the extent of conversion of TiO_2 precursors to crystalline titania.

2.5. Materials and Methods

2.5.1. Materials

$TiCl_4$ (purity > 99%), titanium tetraisopropoxide (TTIP) and acetic acid were purchased from Sigma-Aldrich, isopropanol (IP) (HPLC grade), glycerol from Fisher Scientific, and KOH and metallic Zn (both in pellets) from AnalaR-BDH.

2.5.2. Mononuclear Ti-species from the hydrolysis of $TiCl_4$

10 ml of $TiCl_4$, without further purification, were hydrolysed by slow drop-wise addition to 250 ml of distilled water cooled in an ice bath under continuous

stirring. As a result a completely clear and colourless solution with a pH value of 0.1 was obtained. *Addition of glycerol*: Mixtures with a range of concentration between 1 and 390 mmol glycerol/mmol Ti were produced, adding a given aliquot (generally 5 ml of the freshly prepared solutions of hydrolysis of $TiCl_4$) to different amounts of glycerol. The resulting systems were clear and colourless at all concentrations. When a concentration of 1 mmol glycerol/mmol Ti or more was used, the resulting systems were stable at room temperature for more than 48 hours.

2.5.3. Polynuclear titanium oxide hydrates from $TiCl_4$

Systems with higher pH values (up to pH = 12) were obtained by adding, under cooling with an ice bath, to the hydrolysis solutions of $TiCl_4$ (with and without glycerol) a basic solution of KOH previously dissolved in a small amount of distilled water.

2.5.4. Polynuclear titanium oxide hydrates from TTIP

10 ml of TTIP were mixed to 300 ml of isopropanol and stirred under cooling in an ice bath. Thereafter 90 ml acetic acid were slowly added. About 0.5 ml of water was subsequently added drop wise to the stirred mixture. The resulting solution was clear and slightly yellowish with a pH value of about 3.5. *Addition of glycerol*: 5 ml of hydrolysis solution of TTIP were added to different amounts of glycerol in order to produce mixtures with a concentration of glycerol between 1 and 400 mmol glycerol/mmol Ti.

2.5.5. Solid titanium oxide hydrates by desiccation

An aliquot of 250 ml of the above solutions of hydrolysis of $TiCl_4$ were

desiccated in vacuum (ca. 10^{-1} bar) at 35 - 40 ^{o}C. Under vacuum, the water was removed within few hours, however the system was at this stage still liquid, but

denser and with a yellowish oily appearance. The liquid took about 24 hours to dry. The remaining solid was continued to be desiccated for about 4 more days or until no significant variation of the mass in the solid was detected anymore. This process resulted in pale yellowish glass-like solids which were highly hygroscopic. In fact, the mere exposure to humidity of the surrounding environment turned them into rubber-like materials. At the same time HCl was released. When left in open vessels in air at room temperature the solids kept evaporating acid and a fine white dust slowly covered the surroundings. Over time the solubility of the solids slowly decreased, however a large presence of chlorine (molar ratio Ti:Cl =1:1.6) was detected in elemental analyses even after 2 months; and acid was found to be released from the solids exposed to humid air even two years after its production. The slow release of HCl when the material came in contact with the air seems to indicate that the evaporation of HCl could not simply be due to adsorbed HCl which would probably desorb more rapidly, but rather to a modification of the material which consists of chlorinated compounds. Indeed small chlorinated titanates, which can be volatile, can evaporate from the solid, hydrolyse with the humidity in the surrounding air and condense, therefore the release of acid and the formation of the white dust.

*Addition of glycerol: S*olids were first dispersed in a small amount of water (at RT) as it was difficult to grind them to prepare uniform dispersions. They dissolved almost completely allowing the production of uniform dispersions with glycerol.

2.5.6. Heat treatment

The solids obtained by desiccation of $TiCl_4$ hydrolysis solutions were split in fractions. Each fraction was then thermally treated in air at, respectively, 100 or

200 °C for 2.5 h, at 750 °C for 12 h, or at 850 °C first for 12 h then for additional 12 h, and finally at 950 °C for 24 h.

2.5.7. Solid titanium oxide hydrates precipitated with bases

Samples of the hydrolysis solution of $TiCl_4$ were neutralised with, respectively, KOH, NaOH or NH_3, by adding a stoichiometric amount of the bases necessary to neutralise the quantity of HCl which would have formed upon complete hydrolysis. A copious precipitation occurred as soon as the pH was increased above 3. The precipitate, appearing as gelatinous slurry, was separated via centrifugation from the mother liquor and desiccated in air at room temperature for at least 10 hours. Samples of the precipitated materials were still completely soluble in water at very low pH < 0.5 (by reacidification with HCl) even when left for 2 days in air.

2.5.8. Treatment with *1,2*-dihydroxybenzene and 2,3-dihydroxynaphthalene

This investigation was meant to be purely qualitative. To this aim few drops of Pasteur pipette of freshly prepared $TiCl_4$ hydrolysis solution, a tip of a small spatula of the solid from the desiccated hydrolysis solution treated at 200 °C for 2.5 h and 850 °C for 24h, and the tip of a small spatula of commercial anatase and rutile based nanopowders, respectively P25-Degussa and Aldrich, were added solutions 0.18 M of *1,2*-dihydroxybenzene in isopropanol and $1.25 \cdot 10^{-3}$ M of *2,3*- dihydroxynaphthalene in isopropanol.

In other cases the dihydroxyarenes were directly added to the hydrolysis solutions or to the dispersions in water (or water / isopropanol) comprising the powders described above, resulting from the thermal treatments or precipitated by means of addition of bases to the hydrolysis solutions.

2.5.9. UV irradiation

UV irradiation of the hydrolysis solutions, glycerol mixtures and dispersions comprising solid titanium oxide hydrates was performed using a 100 W/200 W mercury lamp (Ely Chemicals, main emission wavelength at 254 nm) in the central spot of the light cone and at a distance of around 10 cm from the free surface of the samples, corresponding to an intensity of radiation of respectively of 225 mW / cm^2 and 424 mW / cm^2. The duration of irradiation varied in different experiments.

2.5.10. UV-vis spectroscopy

UV-Vis spectroscopy was performed with a Perkin Elmer Lambda 950 spectrometer.

2.5.11. Particle size analysis

A Zetasizer Nano-ZS, Malvern Instruments, was used to investigate the presence of particles and to determine their dimensions. The scale limit range of the instrument is between 3 nm and 6 μm.

2.5.12. X-Ray diffraction

X-ray diffraction patterns were recorded with an X'Pert Pro Panalytical instrument equipped with an X-ray copper source (Cu K_α radiation, wavelength 1.5406 Å) and operating in the θ-θ geometry. Powders were applied as acetone slurry on silicon stabs. Furthermore, a Siemens Diffractometer D5000 instrument with a copper X-Ray source and operating in θ–2θ coupling mode was also used. Powder samples were mounted on a PMMA holder.

2.5.13. Electron Paramagnetic Resonance (EPR)

EPR spectra were retrieved at X-band (9.3 GHz) using a CW Bruker ELEXSYS E500 spectrometer, equipped with a liquid helium cryostat ESR900 Oxford Instruments. The hydrolysis solutions of $TiCl_4$ were reduced with metallic Zn at room temperature and then loaded in quartz glass tubes while the pH neutral samples of the mixtures as well as the glycerol dispersions of the powders were irradiated for 5 min with UV light. All samples were stored in liquid nitrogen prior to analysis. The EPR measurements were carried on at 22 K with microwave power 0.2 milliwatts, modulation amplitude 0.1 milliteslas. The measurement range was between 1500 G and 3800 G.

2.5.14. Elemental analyses

Analyses of carbon, hydrogen, oxygen and chlorine were performed by the service of the Laboratory of Organic Chemistry at ETH Zürich, and titanium analyses by Peter Link AG, Ebnat-Kappel, Switzerland

2.5.15. Thermal analysis

Thermogravimetric analyses were conducted with a TGA Q500 (TA Instruments) in air using a scanning rate of 10 ^{o}C / min.

2.6. References

1. W. Reinders and H. L. Kies, *The equilibrium of the system TiO_2-SO_3-H_2O at 25 °C.* Rec. Trav. Chim. Pays-Bas 1940. **59**: p. 785.
2. R. J. Nussbaumer, P. Smith, and W. Caseri, *Transparent, anatase-free TiO_2 nanoparticle dispersions.* J. Nanosci. Nanotechnol., 2007. **7**: p. 2422.
3. H. Brintzinger and W. Brintzinger, *Zur Kenntnis der molekulardispers gelösten Kieselsäuren und Titansäuren.* Z. anorg. allg. Chem., 1931. **196**: p. 44.
4. T. Graham and J. Otto, *Lehrbuch der Chemie.* 2. Band, 2. Hälfte, 2. Abtheilung, Vieweg und Sohn, Braunschweig, 1849.
5. D.-S. Lee and T.-K. Liu, *Preparation of TiO_2 sol using $TiCl_4$ as a precursor* J. Sol-Gel Sci. Technol., 2002. **25**: p. 121.
6. H. Rose, *Ueber das Titan und seine Verbindungen mit Sauerstoff und Schwefel.* Gilb. Ann. (Ann. Chem. Phys.), 1823. **73**: p. 67.
7. R. Weber, *Ueber die iosmeren Modifikationen der Titansäure und einiger Titanverbindungen.* Pogg. Ann. (Ann. Chem. Phys. 196), 1863. **120**: p. 287.
8. H. R. Weiser and W. O. Milligan, *X-ray studies on the hydrous oxides. IV Titanium dioxide.* J. Phys. Chem., 1934. **38**: p. 513.
9. T. Graham, *Liquid diffusion applied to analysis.* Phil. Trans., 1861. **151**: p. 183.
10. Y. Inoue and H. Yamazaki, *Studies of the hydrous titanium oxide ion exchanger. V. The stability of the hydrogen form in air.* Bull. Chem. Soc. Jpn., 1980. **53**: p. 811.
11. M. P. Baura-Peña, M. J. Martínez-Lope, and M. E. García-Clavel, *Synthesis and characterization of a hydrated titanium(IV) oxide.* Thermochim. Acta, 1991. **179**: p. 89.

12. B. Wawrzyniak, B. Tryba, and A. W. Morawski, *TiO_2-nitrogen modified for water decolourisation under VIS radiation.* J. Adv. Oxid. Technol., 2007. **10**: p. 17.

13. W. Zhou, S. Tang, L. Wan, K. Wei, and D. Li, *Preparation of nano-TiO_2 photocatalyst by hydrolyzation-precipitation method with metatitanic acid as the precursor.* J. Mater. Sci., 2004. **39**: p. 1139.

14. R. Schwarz and E. Menner, *Zur Kenntnis der Kieselsäuren (I.).* Ber. deutsch. chem. Ges. , 1924. **57**: p. 1477.

15. G. Tammann, *Über die Wirkung von Silicium auf Metatitansäurehydrat.* Z. Anorg. Chem., 1905. **43**: p. 370.

16. R. Schwarz and H. Richter, *Zur Kenntnis der Kieselsäuren (V. Mitteilung).* Ber. deutsch. chem. Ges., 1929. **62**: p. 31.

17. C. B. Hurd, W. J. Jacobe, and D. W. Godfrey, *Studies on the hydrogel of titania. I. The effect of temperature on time of set.* J. Am. Chem. Soc., 1941. **63**: p. 723.

18. A. Gutbier, B. Ottenstein, E. Leutheusser, K. Lossen, and F. Allam, *Kolloidsynthesen mit Hilfe von Titan(III)-chlorid.* Z. anorg. allg. Chem., 1927. **162**: p. 87

19. F. Allam, *Zur Kenntnis des Systems Titan (IV) - Oxyd/Wasser*, PhD thesis 1927, Universität Jena: Jena.

20. U. Gesenhues, *Calcination of metatitanic acid to titanium dioxide white pigments.* Chem. Eng. Technol., 2001. **24** (7): p. 685.

21. C. F. Rammelsberg, Monatsber. königl. preuss. Akad. Wiss. *Physik.-math. Klasse.*, 1874. p. 490.

22. J. Otto and R. Otto, *Ausführliches Lehrbuch der anorganischen Chemie,* 2. Band, 2. Abtheilung, Vieweg und Sohn, Braunschweig, 1863. p. 187.

23. M. H. Klaproth, *Beiträge zur chemischen Kenntniss der Mineralkörper.* Decker & Co., Posen 1795. **1**.

24. M. B. Robin and P. Day, *Mixed valence chemistry - a survey and classification.* Adv. Inorg. Chem. Radiochem., 1968. **10**: p. 247.

25. S. Cassaignon, M. Koelsch, and J.-P. Jolivet, *From $TiCl_3$ to TiO_2 nanoparticles (anatase, brookite and rutile): thermohydrolysis and oxidation in aqueous medium.* J. Phys. Chem. Solid, 2007. **68**: p. 695.

26. H. Hartmann, H. L. Schläfer, and K. H. Hansen, *Zur Lichtabsorption komplexer Ionen des dreiwertigen Titans.* Z. Anorg. Allg. Chem., 1956. **284**: p. 153.

27. H. R. Weiser, W. O. Milligan, and W. C. Simpson, *The elimination of sorption–desorption hysteresis in hydrous oxide gels. II. Tantalum pentoxide, stannic oxide, and titanium dioxide.* J. Phys. Chem., 1942. **46**: p. 1051.

28. H. Rose, *Ueber die Titansäure.* Pogg. Ann. (Ann. Chem. Phys. 137), 1844. **61**: p. 507.

29. J. Huheey, E. Keiter, and R. Keiter, eds. *Anorganische Chemie*. De Gruyter, Berlin 2003.

30. D. M. D'Alessandro and F. R. Keene, *Intervalence charge transfer (IVCT) in trinuclear and tetranuclear complexes of iron, ruthenium, and osmium.* Chem. Rev., 2006. **106**: p. 2270.

31. S. Fujii, Y. Sugie, and C. Sakamoto, *Adsorption of phosphorous oxoacid on hydrous titatnium(IV) oxide in an aqueous solution.* Bull. Chem. Soc. Jpn., 1986. **59**: p. 2611.

32. T. Koenig and O. van der Pfordten, *Untersuchungen über das Titan.* Ber. deutsch. chem. Ges., 1888. **21**.

33. K. E. Zimens and J. A. Hedvall, *Orientierende Messungen über die Beeinflussung der magnetischen Suzeptibilität durch Struktur- und Gefügeänderungen.* Chalmers tekn. Högskolas Handl., 1942. **9**: p. 3.

34. W. Chen, X. Sun, and D. Weng, *Morphology control of titanium oxides by tetramethylammonium cations in hydrothermal conditions.* Mater. Lett., 2006. **60**: p. 3477.

35. T. Sasaki, Y. Komatsu, and Y. Fujiki, *A new layered hydrous titanium dioxide* $H_xTi_{2-x/4}O_4 \cdot H_2O$. J. Chem. Soc., Chem. Commun., 1991. p. 817.

36. C. Rentz, *Lichtreaktionen der Oxide der Titans, cers und der Erdasauren.* Helv. Chim. Acta, 1921, **4**: p. 961.

37. R. J. Nussbaumer, W. R. Caseri, and P. Smith, *Reversible photochromic properties of* TiO_2*-polymer nanocomposites.* J. Nanosci. Nanotechnol., 2006. **6** (2): p. 459.

38. R. P. Muller, J. Steinle, and H. P. Boehm, *Characterization of photochemically or electrochemically reduced blue titanium dioxide.* Z. Naturforsch., 1990. **45b**: p. 864.

39. U. Kreibig and M. Vollmer, eds. *Optical Properties of Metal Clusters*. 1995, Springer: Berlin.

40. O. Hauser and A. Lewite, *Über das Verhalten von Phenolen, Naphtholen und Phenol-carbonsäuren gegen vierwertiges Titan.* Ber. deutsch. chem. Ges., 1912. **45**: p. 2480.

41. O. Hauser and A. Lewite, *Über das Verhalten von Phenolen, Naphtholen und deren Carbonsäuren gegen vierwertiges Titan.* Ber. deutsch. chem. Ges., 1915. **48**: p. 213.

Chapter 3

Solution-processable photochromic titanium oxide hydrate / poly(vinyl alcohol) hybrid systems

3.1. Introduction

In Chapter 2 we have shown that titanium oxide hydrates display a pronounced, reversible photochromic response if irradiated with UV light, when in presence of suitable chemical substances such as glycerol, in agreement with the literature [1-4]. This can be of interest for a wide range of applications such as in the manufacturing of photochromic parts for UV sensors, security features, smart coatings for windows and the like.

Glycerol was found to be particularly suitable to induce the desired photochromism in titanium oxide hydrates and, in addition, to effectively stabilise the titanium species preventing their extensive condensation and/or aggregation. Indeed completely transparent dispersions – even of high content of titanium oxide hydrates – were produced in glycerol and water/glycerol mixtures, which were stable in ordinary laboratory conditions for as long as two months. We thereby attributed the remarkable stability of such dispersions to the strong interactions that established between the titanium species and the surrounding

OH-groups of the glycerol which may act as chelating ligands, which prevented homo-interactions between the inorganic molecules themselves that would lead to precipitation of larger molecules or clusters.

In this chapter, in order to further explore the potential of titanium oxide hydrates, hybrid systems were prepared using a polymer matrix as the high molecular weight of the molecules and, then, the high level of entanglements could allow obtaining solid and coherent hybrid systems – following strategies that have proven successful for other functional hybrids [5-7]. For this purpose we employed a high molecular weight poly(vinyl alcohol) (PVAl), M_w = 130.000 g ⁄mol, in view of the fact that this polymer is transparent and colourless and bears a chemical structure very similar to that of the glycerol therefore

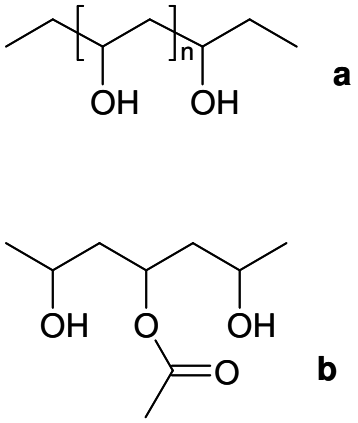

Figure 3.1: a-Chemical structure of poly (vinyl alcohol). As PVAl is obtained from the hydrolysis of poly(vinyl acetate), **b**-some residual acetate (CH3COO-) group can still be present on the chain in place of OH groups.

we expected to observe, for the resulting hybrid systems, a photochromic behaviour similar to that observed for the mixtures containing of titanium oxide hydrates and glycerol. In particular we used a PVAl which contained about the 10 – 11.6 % of residual acetate

groups (resulting from the incomplete hydrolysis of the precursor polymer *i.e.* poly (vinyl acetate)) because such relatively high content of acetate groups allow to readily dissolve the polymer in water at low temperature (below 90 ^{o}C).

3.2. Preparation and characterization of titanium oxide hydrates / poly(vinyl alcohol) hybrids

Mixtures of hybrid material were prepared by adding freshly prepared hydrolysis solution of $TiCl_4$ (see Chapter 2) to PVAl 4%wt. aqueous solutions at room temperature. Concentrations of titanium species (expressed as mol Ti / g PVAl) ranging from $3.5 \cdot 10^{-10}$ to $1.00 \cdot 10^{-2}$ mol Ti / g PVAl were thereby used. In order to induce the formation of titanium oxide hydrates [8-11] we attempted to increase the pH value by addition of bases, such as KOH. However, such procedures lead to the rapid precipitation of the inorganic species. This could be a consequence of the decreased stabilization effect of the alcohol groups of the matrix towards the forming titanium oxide hydrate due to the high amount of water in the mixtures provided by polymer solution, compared to when alcohols were added in pure form (see Chapter 2).

Therefore, although freshly prepared (and still very acidic) mixtures obviously contained predominantly mononuclear titanium species, we selected to cast them in petri dishes and let them dry in ambient conditions. In particular mixtures were poured in polystyrene (PS) petri-dishes because the poor interactions of PS with PVAl, would allow an easy removal of the films, when fully desiccated, by pealing.

Once completely dried, the mixtures resulted in fully colourless and transparent self-supporting films with thicknesses in the range of 0.3 - 0.7 mm. However, a large amount of acid kept being released from the films even several months after their manufacturing.

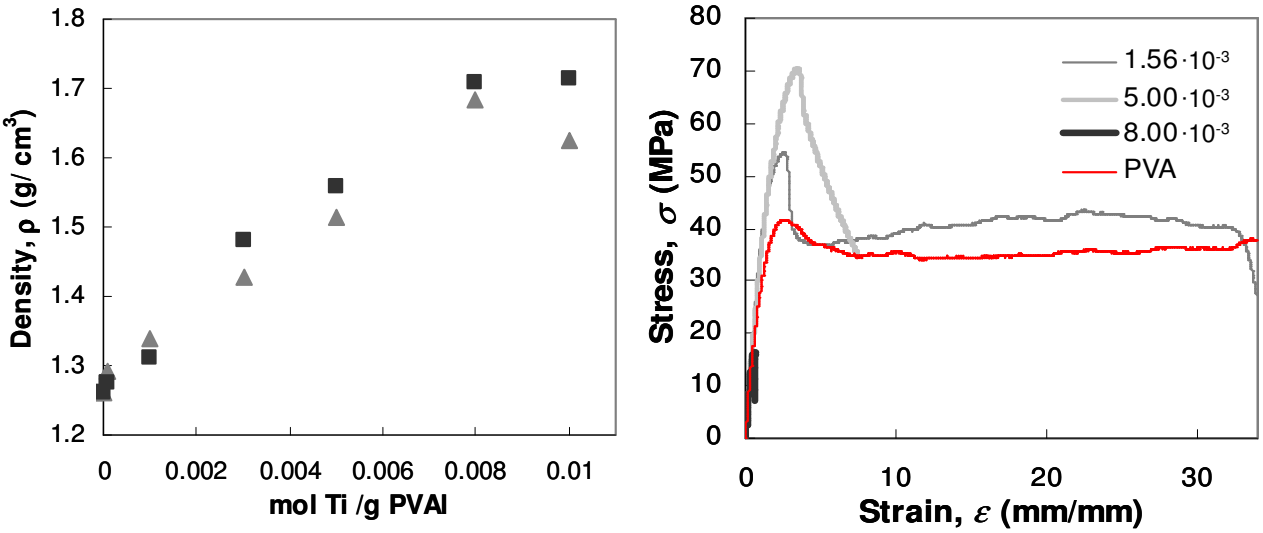

Figure 3.2: ***Left panel***: Density of hybrid structures of increasing titanium oxide hydrates content, before (grey triangles) and after (black squares) annealing at 200 °C for 20 min. ***Right panel***: Typical stress-strain ($\sigma - \varepsilon$) curves of hybrid films of different concentrations of titanium species (mol Ti / g PVAl), as indicated in the graph. Data for the neat PVAl (in red) is also shown for comparison. The Young's modulus E is comparable for the different films while the elongation at break ε decreases dramatically for increasing content of titanium oxide hydrates.

Nevertheless, beneficially, dried hybrid films with a content of Ti species > $3.5 \cdot 10^{-10}$ mol Ti / g PVAl of were found to be insoluble in water. This allowed removing the excess acid from the films through a simple washing procedure in distilled water at room temperature (see sect 3.7.3 for details).

Washed films, once dried, appeared shrunk and stiffened – an effect that was more pronounced for higher concentrations of titanium species. Indeed, in agreement with these observations the density of the washed hybrid material increased with titanium oxide hydrates content from 1.26 g / cm^3 to 1.68 g / cm^3 in the range of concentrations considered (Fig 3.2, left panel). The mechanical properties were characterised by simple tensile tests. The hybrid materials were more brittle, as is evident from Figure 3.2 (right panel). In fact, the strain at break, ε, was found to be 34 % (with respect to the starting length) for systems

with concentration of $1.56 \cdot 10^{-4}$ mol Ti / g PVAl and was reduced to only 0.6 % in hybrid materials containing $8 \cdot 10^{-3}$ mol Ti / g PVAl .

The Young's modulus, on the other hand, appeared not to be particularly sensitive to the addition of titanium species, varying from 3.7 GPa, for hybrids containing 1.56 10^{-4} mol Ti / g PVAl to 4.19 GPa for materials with $8 \cdot 10^{-3}$ mol Ti / g PVAl. For comparison PVAl used for the mixtures displayed a Young's modulus around 3.5 GPa.

From the above observations it is clear that titanium species significantly interacted with the polymer matrix. This is most prominently illustrated by the fact that the hybrid becomes insoluble at very low concentrations of inorganic component. The origin is not entirely clear yet; in addition to the formation of hydrogen bonds, chemical cross-linking cannot be excluded.

3.3. Estimation of the molecular weight and density of titanium oxide hydrates

The insolubility of the PVAl / titanium oxide hydrate films allowed to roughly estimate the molecular weight and then the density of titanium oxide hydrates after removal of chlorine.

3.3.1. Estimation of molecular weight of titanium oxide hydrates.

Three hybrid mixtures respectively with concentrations of, $1.0 \cdot 10^{-3}$, $2.5 \cdot 10^{-3}$ and $3.0 \cdot 10^{-3}$ mol Ti / g PVAl were produced mixing in polystyrene beakers the corresponding amounts of $TiCl_4$ hydrolysis solution (0.35 mol Ti / dm^3) (see sec. 2.5.2) to 12.5 g of PVAl 4%wt. aqueous solution containing exactly 0.5 g of the polymer. Mixtures were allowed to dry completely directly in the beaker in order to avoid possible mass losses during the casting in petri-dishes. The resulting solid films were carefully pealed and washed in distilled water to remove the acidic content. To this aim films were soaked in water and the

bath was regularly changed with fresh water until no more release of acid was detected, *i.e* until the pH of the washing bath was stable at the value of 6 (same as the pH of the distilled water used for the washing).

Neutralised films were dried in vacuum at room temperature for about four days and then weighed. The weight of the titanium species was calculated from the difference between the weights of the desiccated films and that of the PVAl (0.5 g). The masses obtained allowed calculating the molecular weight of the titanium species, as the moles of titanium added to each mixture were known. On average the molecular weight resulted to be ≈ 90 g / mol.

3.3.2. Estimation of the density of titanium oxide hydrates.

The density of the three hybrid d_{hf} samples was measured with a pycnometer (see sect. 3.7.4). From these data it was possible to retrieve the volume of each hybrid sample V_{hf} as follows:

$$V_{hf} = \frac{m_{hf}}{d_{hf}} \qquad \text{Eq.3.1}$$

(where m_{hf} is the total mass of hybrid film). Considering that the total volume of the hybrid film is given by the sum of the volumes of the titanium species and of the polymer

$$V_{hf} = V_{Ti\ species} + V_{PVAl} \qquad \text{Eq. 3.2}$$

and being the volume of PVAl for known each sample and given by the ratio of the mass on the density :

$$V_{PVAl} = \frac{m_{PVAl}}{d_{PVAl}} = \frac{0.50g}{1.26g \cdot cm^{-3}} \qquad \text{Eq. 3.3}$$

we could retrieve the volume of the titanium species by the difference:

$$V_{Ti\ species} = V_{hf} - V_{PVAl}\,. \qquad \text{Eq. 3.4}$$

Because the moles of titanium species present in each film are also known and so is the their molecular weight, $MW_{Ti\ species}$ ~ 90 g/mol (see sect.3.3.1), we could calculate the mass of titanium oxide hydrates in each film (Equation 3.5) .

$$m_{Ti\ species} = mol_{Ti\ species} \cdot MW_{Ti\ species} \qquad \text{Eq. 3.5}$$

Thereby, the density of titanium oxide hydrates was calculated as:

$$d_{Ti\ species} = \frac{m_{Ti\ species}}{V_{Ti\ species}} \qquad \text{Eq. 3.6}$$

where $V_{Ti\ species}$ had been earlier retrieved by Equation 3.4. The average value of the density of titanium oxide hydrates resulted to be ≈1.95 g /cm^3.

The estimate values of the molecular weight and of the density of the titanium oxide hydrates, obtained as described above, enabled us also to estimate the volume fraction of the hybrid we prepared. For instance, the hybrids that we report about contain a volume fraction of titanium species between $2.0 \cdot 10^{-6}$ %vol. ($3.5 \cdot 10^{-10}$ mol Ti / g PVAl) and 36.8 %vol ($1.0 \cdot 10^{-2}$ mol Ti / g PVAl).

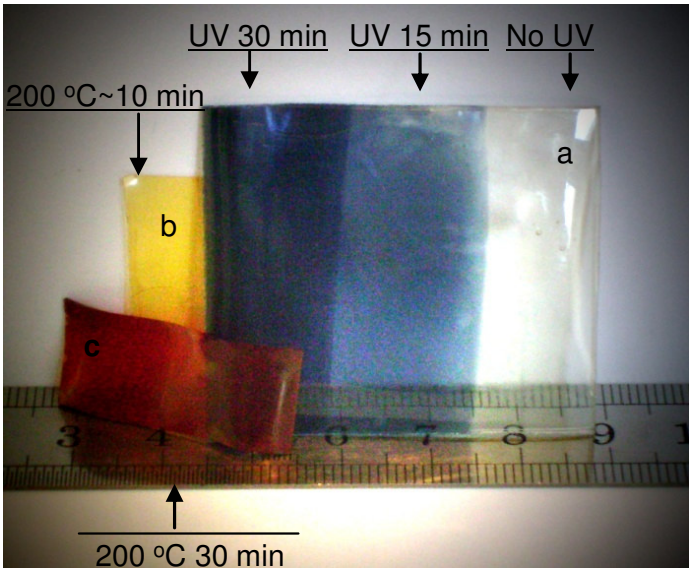

Figure 3.3: ***a-***Hybrid film with concentration of $2{,}0 \cdot 10^{-3}$ mol Ti / g PVAl, UV-irradiated for different time. Before exposition to UV light the film is colourless (area on the right), after 15 min UV irradiation film turn bright blue (area in the middle) and the colour deepens for longer exposition (area on the left) ***b-*** samples of the same hybrid film heated at 200 ºC for ~10 min (yellow) and ***c-*** for 30 min (red film). The material remains transparent after both irradiation and thermal treatments.

3.4. Photochromism

In order to evaluate if the removal of the acid from the *solid* hybrid films was successful to induce the formation of titanium oxide hydrates, films thoroughly washed, after drying in vacuum, were irradiated with UV light for 30 min with a 100 W Hg lamp (main wavelength 254nm). Reassuringly films displayed an intense photochromism turning from colourless to deep blue (Fig 3.3 - a) characteristic for polynuclear titanium oxide hydrates, as described in the previous chapter. Indeed, in agreement with this observation, the UV-vis spectra of the hybrid ($2.0 \cdot 10^{-3}$ mol Ti / g PVAl) irradiated, showed a broad absorption band with a maximum around 700 nm, which are features compatible with the presence of polynuclear species such as titanium oxide hydrates (Fig 3.4, left panel). Similarly, electronic paramagnetic resonance (EPR) measurements carried out at

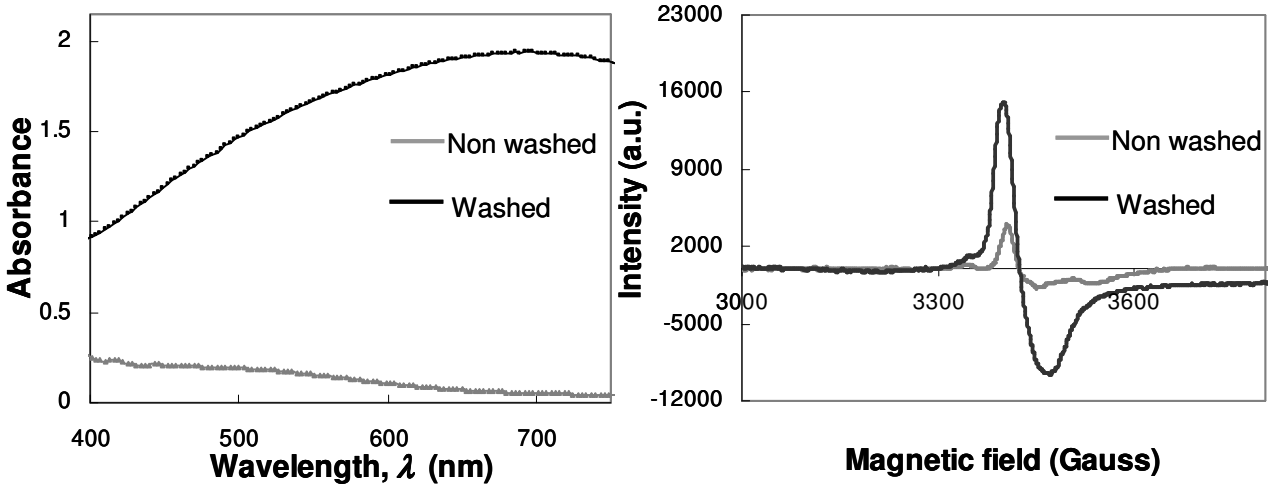

Figure 3.4: ***Left panel*****:** UV-vis absorption spectra and ***Right panel*****:** X-band EPR spectra of titanium oxide hydrates / PVAl hybrids ($2.0 \cdot 10^{-3}$ mol Ti / g PVAl) irradiated with UV light 15 min with a 100 W Hg lamp (see sect. 3.7.6 for details), before (grey) and after (black) removal of the acidic content by immersion in water. This washing procedure results in a notable enhancement and visible blue shift of the UV absorption band and in an increase of the EPR Ti^{III} signal intensity. From both spectroscopic analyses one can deduce that titanium species are already present as *poly*-nuclear entities even before extraction of the acid.

room temperature exhibited signals at $g \approx 2$ (flexus at 3420 Gauss; Fig 3.4, right panel), as already observed in Chapter 2 for the glycerol-containing systems. For comparison, unwashed films were irradiated with UV-light under the same conditions as for the "neutral" ones. Interestingly, these hybrids only turned to a very pale violet brownish colouration and the corresponding UV-vis spectra (Fig 3.4, left panel) showed an absorption band of significantly lower intensity compared to that of the washed materials. Similarly, EPR response of such acidic hybrids was distinctly lower compared to the neutral ones, however, its characteristic features, such as field position and line shape, were still very similar to those observed for neutralised samples (Fig 3.4, right panel).

This implies that even in films not neutralised through the washing step, at least some polynuclear titanium oxide hydrates were present, which very likely formed during the drying stage. Therefore, the condensation of titanium species in such systems could occur

also without increasing the pH value (see Chapter 2).

However, differences in the spectroscopic analyses, between the as-cast and washed films, especially with respect to spectral intensities suggest that the chemical state and/or composition of such species undergoes some transformation during the rinsing in water resulting in a notably enhanced photoactivity. Such transformation, mainly manifested through the extraction of HCl from the hybrid film could be compatible with the hydrolysis and condensation of *chlorinated* titanium oxide hydrates.

These chlorinated species very likely formed already while the liquid hybrid mixtures were drying as the environment became progressively poorer in water and richer in HCl (Chapter 2). The formation of chlorotitanates was supported by the observation of a white fine dust that covered the surfaces in the immediate surrounding of the drying mixtures. Being such compounds rather volatile and reactive species they are expected to evaporate from the hybrid mixtures before their full solidification hydrolyse in contact with humid air and condense on the surrounding surfaces. Chlorinated titanium oxide hydrates seem therefore to be scarcely photochromic species or at least very unstable ones. However, the low pH value of the final architectures may also play a critical role in the spectral characteristics observed for the non washed films (see Chapter 2).

The intensity of the photochromic response of solid titanium oxide hydrates / PVAl hybrids, from colourless to blue, increased with the concentration of inorganic species (Fig. 3.5 - top left panel) as well as with time of exposure to the UV radiation (Fig. 3.5 - bottom left panel) and in a linear fashion (Fig. 3.5 – top and bottom right panels). Only prolonged irradiation caused degradation of the hybrid resulting in a progressive irreversible (unwanted) colour change of the material to yellow. Concomitantly the material photochromic response decreased (Fig. 3.6). However, as visible in Figure 3.6, for a 0.7 mm thick hybrids film comprising $3.0 \cdot 10^{-3}$ mol Ti / g PVAl (or 14.8 %vol inorganic species) the absorption band in

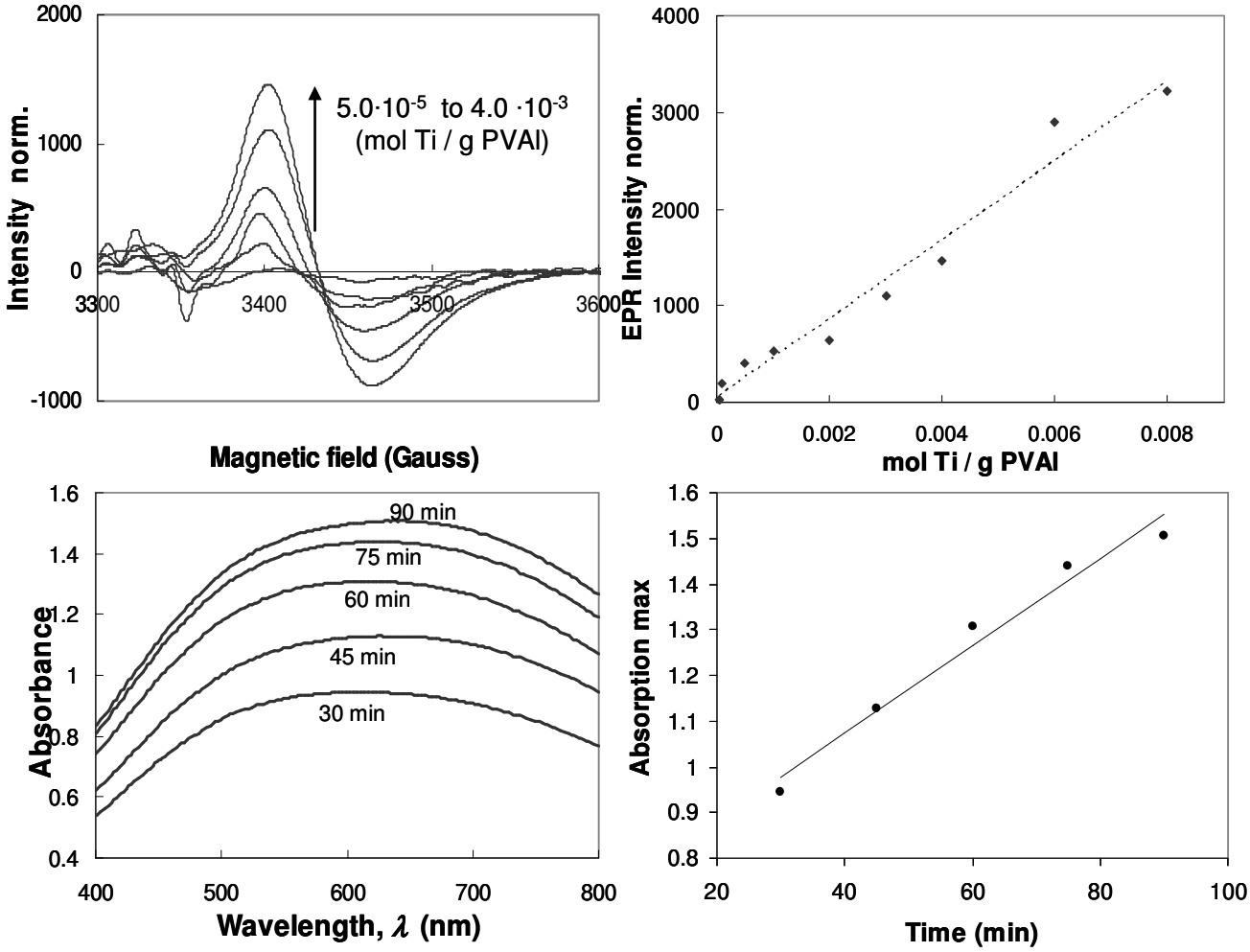

Figure 3.5: ***Top left panel*****:** X-band EPR spectra (recorded at 298 K) of titanium oxide hydrates / PVAl hybrid films of different content of the inorganic species ($5.0{\cdot}10^{-5}$, $1.0{\cdot}10^{-4}$, $5.0{\cdot}10^{-4}$, $2.0{\cdot}10^{-3}$, $3.0{\cdot}10^{-3}$ and $4.0{\cdot}10^{-3}$ mol Ti / g PVAl), which were photoreduced by irradiation with UV light for 30 min (see for detail sect. 3.7.6. ***Top right panel*****:** Intensity of the EPR Ti^{III} signal (calculated from the flexus to the maximum) normalised to the sample weight as a unction of the concentration of titanium species in the hybrid material. The intensity of the signal increases linearly with the content of the inorganic species. ***Bottom left panel*****:** UV-vis absorption spectra for a film comprising 5.0 10^{-3} mol Ti / g PVAl (0.5 mm thick), irradiated at consecutive intervals of 15 min. ***Bottom left panel*****:** Absorption max of the UV-vis spectra vs. irradiation time.

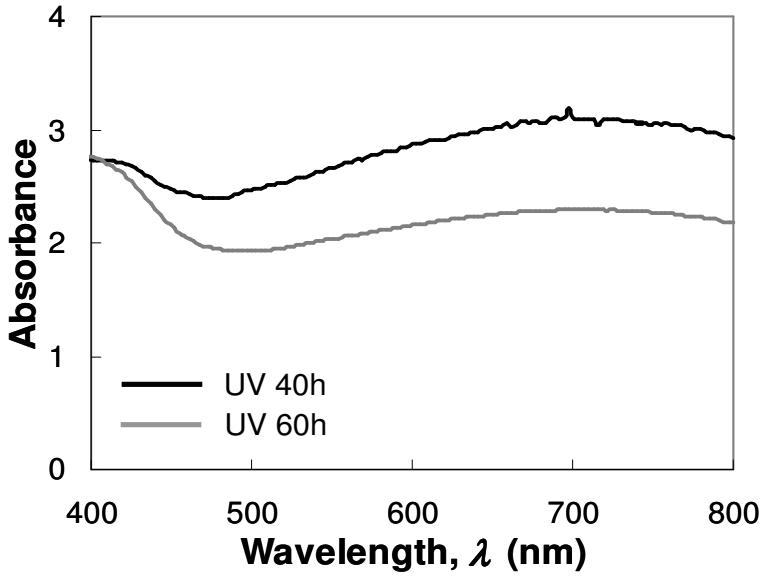

Figure 3.6: UV-vis absorption bands of a sample of hybrid films ($3.00 \cdot 10^{-3}$ mol Ti / g PVAl, 0.7mm thick) continuously irradiated with UV light for 40 h (black) and 60 h (grey). The prolonged exposure to UV irradiation induces a reduction of the intensity of the band and development of a new band below 500 nm, absent in the spectra of films irradiated for less time (see Fig. 3.3- bottom left panel).

the region 400-500 nm as measured in UV-vis spectroscopy, only decreased significantly after 60 hrs of exposure to UV-light. Films irradiated for 40 hrs displayed a very similar photochromic response as found for the structures irradiated for a shorter period of time. The degradation process seemed to be accelerated in hybrids with higher content of the titanium species. Indeed, similar irradiation conditions applied to samples of neat PVAl did not induce any visible colour modifications.

Without doubt, from the above it is evident that titanium oxide hydrates /PVAl hybrids are attractive candidates for use in a broad range of applications: from the production of photochromic coatings for fabric (fibers can readily be spun) and different materials surfaces to the manufacture of large area free-standing films for applications as UV shields or filters or more complex structures. Indeed, also fibres were readily spun. We like to emphasise in addition that

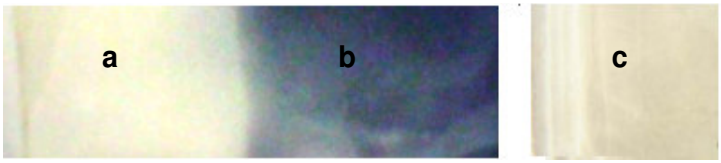

Figure 3.7: ***a-*** Sample of hybrid film ($2{,}0 \cdot 10^{-3}$ mol Ti / g PVAl) before exposition to UV light, **b-** after 15 min exposition to UV light and **c-** decoloured through immersion in water for 40 min. Increasing the content of the titanium species in the hybrid material results in more compact architectures, which are less prone to swelling by water. This decreases the rate of decolouration (from few minutes of low concentrations to few hours for higher content of titanium species). The time necessary to completely bleach the reduced hybrid material also depends on the intensity of the colour and therefore the time of exposition to UV light.

hybrids also showed a pronounced photochromic response when exposed sun light.

Finally, it is worthwhile to note that the photochromic effect can be reversed by simply immersing the coloured material in water at room temperature. The swelling, which occurs during the soaking, very likely facilitates the diffusion of the oxygen (which is naturally present in the water) into the material and reverse the oxidation state of titanium from Ti^{III} to Ti^{IV} with a consequent bleaching of the blue colouration (Fig. 3.7). Indeed samples of photoreduced hybrid material soaked in thoroughly degassed water in a closed vial, remained coloured as long as the vial was kept sealed.

Of course the higher is the concentration of titanium species in the hybrid material, the more compact less prone to swell will be the resulting structure, therefore the rate of decolouration decreases with the content of titanium species. In particular full bleaching of films in our investigation was found to last from 15 min to more than 2 hour for respectively the lowest and the highest concentrated films.

The reversibility of the photochromic effect opens up the possibility to perform cycles of colouration-decolouration switching between a blue and colourless appearance.

3.5. Thermochromism

Another interesting property of the titanium oxide hydrates / PVAl hybrid materials is the possibility to induce a colour change not only after exposure to UV light but also by selected heat-treatments at temperature above 150 ^{o}C in air. In fact, the hybrids progressively turned from colourless to bright yellow (Fig. 3.3 - b), and then over time to intense ruby red (Fig. 3.3 - c) whilst remaining transparent.

The rate at which the colour change occurred was significantly affected by the specific temperature selected for the heat treatment. As an example, bright red coloured materials were obtained in only 25 to 30 min at 200 ^{o}C while samples of hybrids remained almost unaltered when exposed to 160 ^{o}C for the same period of time. In contrast to the *photo*-chromism described above the colouration induced by such thermal treatments was permanent and therefore related to some irreversible chemical modification in the structure of the hybrid.

It is well known that PVAl if heated in air at temperatures above 200 ^{o}C changes colour to red [12]. This colouration has been associated with the oxidative thermal degradation of the polymer, which occurs through removal of H_2O molecules and consequent formation of carbonyl groups and double-bonds [12-14]. The increase in the number of unsaturated bonds results in the conjugation of the backbone and, in turn, in the development of a colouration.

Therefore, it seems that this thermochromism is effectively enhanced by the presence of the titanium species. In fact, the rate of colouration of our hybrid was significantly higher and occurred at drastically lower temperatures compared to the neat polymer, especially at high content of Ti species. Indeed the observed thermochromism may be attributed to the the thermally-induced reduction of the OH content in the hybrid through:

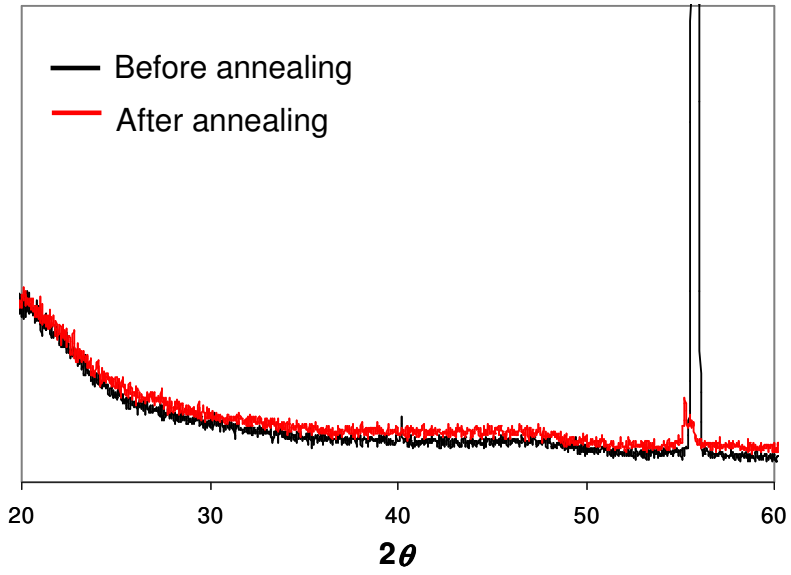

Figure 3.8: X-ray diffractograms retrieved for samples of PVAl / titanium oxide hydrates hybrid film with concentration of $1{,}0 \cdot 10^{-2}$ mol Ti / g PVAl before (blak) and after (red) annelainh at 200 ^{o}C for 2 h. The only peaks visible are addressable to the silicon stabs used to mount the films.

i) the dehydroxilation of the polymer similar to neat PVAl [12-14] *ii)* further condensation of the titanium oxide hydrates (see Chapter 2) and *iii)* condensation between hydroxyl groups of the titanium species and of the polymer. These mechanisms are in agreement with the reduction of the swelling in water and with increased density (Fig. 3.2 left panel) observed in annealed hybrids.

Furthermore, we found that the photochromic response was lost in such materials. Clearly, the reduction of the amount of OH-groups in the polymer, during annealing at elevated temperatures, would decrease the "stabilising" effect of the polymer for the formation of Ti^{III}. In addition, the condensation between the titanium species and the polymer through the formation of chemical bonds between the two components may require higher energy for Ti-O bonds to be cleaved than UV light. No evidence of the formation of inactive crystalline phases was obtained was obtained from X-ray diffraction pattern analysis (Fig. 3.8). In addition, we like to note that the reduction in the photochromic response of

the heat-treated samples cannot be attributed to the development of crystalline TiO_2 forms. Indeed the annealed films remained completely amorphous (Fig. 3.8).

3.6. Conclusions

In this chapter we presented a hybrid material based on titanium oxide hydrates and PVAl. Our approach was motivated by the idea that the combination of the titanium species with a polymer bearing a structure similar to that of the small molecules previously used (Chapter 5) would allow obtaining solid systems that display a desirable combination of properties such as transparency and photochromism. Indeed this material was found to be fully transparent, even at high loads of inorganic species, and exhibited *reversible* photochromism and *irreversible* thermochromism.

One of the most outstanding properties of this hybrid material, however, is its insolubility, that permits to induce the formation of titanium oxide hydrates by neutralising the hybrids in their solid state. Thereby, the water seems to induce the hydrolysis of chlorotitanates. An interesting consequence of this is the acidic hydrolysis of the residual acetate groups in the PVAl, as deduced by the characteristic vinegary smell of acetic acid which became perceptible as soon as the acidic hybrid material become swollen with water. This observation was substantially confirmed by the analysis of transmission IR spectra retrieved for the films before and after washing reported in Figure 3.9 (only showing the spectra portion of our interest). Here the evident ester carbonyl peak at 1740 cm^{-1} and the C-O-C peak at 1250 cm^{-1} of the acetate, present in both the spectra of the plain PVA and unwashed hybrid film, decreases in the spectrum of the film after washing concomitantly a weak peak at 1660 cm^{-1} of a carboxylic carbonyl that could be associated to the formation of acetic acid, and possibly trapped in the film structure over drying, become visible.

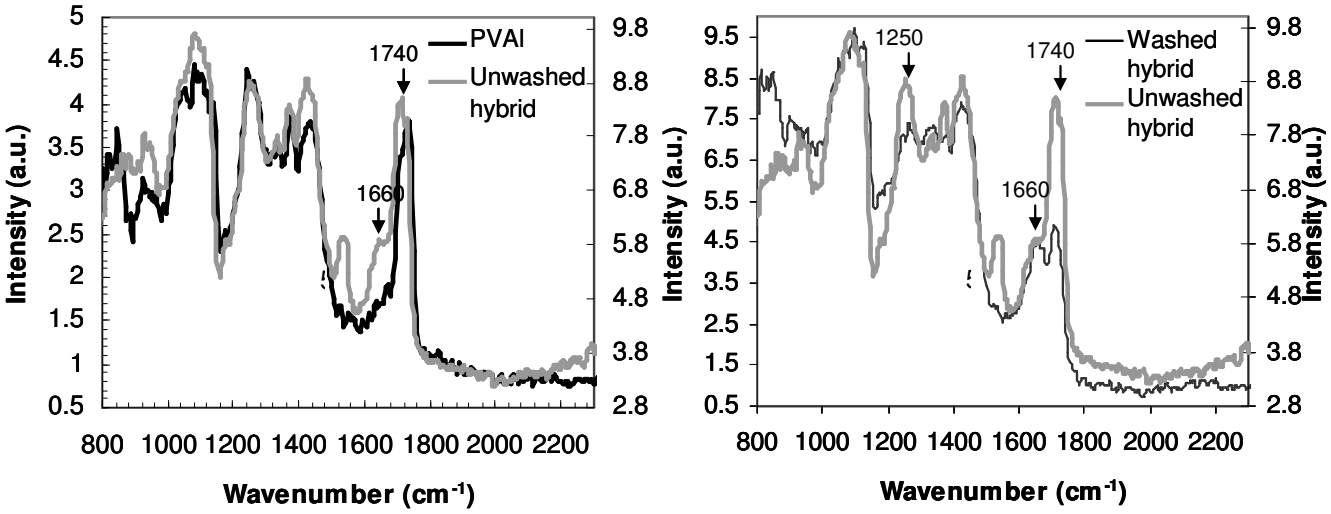

Figure 3.9: Left panel: FTIR spectra for the neat PVAl (in black) and the hybrid before the removal of the acidic content through washing in distilled water (in grey). In both the spectra peaks at 1740 cm-1 and 1250 cm-1 addressable to the acetate ester carbonyl and C-O-C respectively are visible. **Left panel:** The spectrum of the washed hybrid film (in black) presents a marked decrease of both peaks which is in agreement with the hydrolysis of the acetate groups.

Interestingly, no hydrolysis of acetate groups was observed for the plain PVAl even in very concentrated acidic solutions at room temperature.

The increased number of anchoring OH-groups for the titanium species possibly allowed for a further physical or even chemical crosslinking to occur between the two components, in agreement with the observed shrinking and stiffening of the material upon washing.

Clearly, further knowledge to, e.g., understand the effect of the polymer chemical structure on the chromic responses as well as on the other physical properties of the resulting hybrid materials needs to be gained to elucidate the full potential of this highly versatile hybrids.

3.7. Materials and methods

3.7.1 Materials

$TiCl_4$ (purity > 99%) and polyvinyl alcohol (PVAl) ($M_w \approx 130.000$ g / mol, residual content of acetyl= 10.0 - 11.6 %) were purchased from Sigma-Aldrich.

3.7.2. Films preparation

Mixtures with concentration of titanium species the range from $3.5 \cdot 10^{-10}$ to $1.0 \cdot 10^{-2}$ mol Ti / g PVAl were prepared by rapidly adding corresponding amounts of $TiCl_4$ hydrolysis solution (0.35 mol Ti / dm^3. See sec. 2.5.2) to a 4 wt.% aqueous solution of PVAl over stirring at room temperature. These as-prepared mixtures were cast in polystyrene petri-dishes and allowed to dry in air at room temperature.

The concentration of the PVAl employed for the preparation of the mixtures was selected to obtain stable mixtures that resulted in fully transparent films, at least in the range of concentration of titanium species investigated here. Indeed, at polymer concentrations >4%, sudden gelation often occurred in some systems preventing their casting. Lower polymer concentrations, on the other hand, resulted in films comprising white opaque aggregates.

After drying in air at room temperature, transparent colourless and self-supporting films with thicknesses in the range between 0.3 and 0.5 mm were obtained. Reference films of neat PVAl were produced by casting a 4 wt.% PVAl solution in petri-dishes and letting dry in ambient conditions. All films were afterward stored in vacuum (10^{-3} atm) until required for analyses.

3.7.3. Neutralization of solid hybrids

In order to remove the HCl content, as-cast solid hybrid films were soaked in distilled water. The hybrid films were still strongly hydrophilic, therefore shortly after the immersion in water they started to swell (to a higher extent the lower was the concentration of the titanium species) concomitantly, the acid contained in the material was released in the washing bath. The water was refreshed several times until no more acid was detected, for instance, until the pH of stabilised at 6. The procedure could last between 30 min and 1 hour depending on the concentration of the hybrid material.

3.7.4. Density measurements

Densities of hybrid films at different concentrations were characterized by helium gas pycnometry at ambient temperature with a Quantachrome Micro-Ultrapycnometer-1000 equipped with a Nanocell. Amounts of ~100 mg of each hybrid sample were employed and Pulse Mode was applied for purging the cell prior to the measurements. The instrument was operated in the Multi Run Mode and density values were determined by averaging over 10 runs.

Density data from these measurements were, then, used to retrieve the density of titanium oxide hydrates, which was estimated to be ≈ 1.95 g / cm^3 (see sec. 3.3.2). Calculations were made considering a molecular weight for the oxide hydrates of around 90 g / mol (from an average carried on hybrid films with different concentrations of titanium species. See sec. 3.3.1) and PVAl density of 1.26 g / cm^3.

3.7.5. Mechanical properties determination

Mechanical testing was performed at room temperature with an Instron TensileTester (Model 5864) at a cross-head speed of 5 mm / min. Strips of a width of 1.5 mm and gauge

length 15 mm were cut from neutralised hybrid films and a PVAl film desiccated in vacuum for 5 days.

3.7.6. UV irradiation

UV irradiation of the architectures was performed in air at room temperature with a 100 W mercury lamp (Ely Chemicals, main emission wavelength at 254 nm). Samples were individually placed at a distance of around 15 cm in the central spot of the light cone and therefore exposed to UV radiation with intensity of 191 mW / cm^2.

3.7.7. UV-visible spectroscopy

UV-Vis spectroscopy was performed with a Perkin Elmer Lambda 950 spectrometer, equipped with an integrating sphere in air. Absorption spectra of each film sample were normalised with respect to corresponding film thickness.

3.7.8. X ray diffraction

X-ray diffraction patterns were recorded with X'Pert Pro Panalytical equipped with X-ray copper source (Cu Ka = 1.5406 Å) and working in the θ - 2θ geometry. Films were mounted onto silicon stabs.

3.7.9. Electron Paramagnetic Resonance (EPR)

Thin strips of films were put in quartz tubes filled with argon and sealed with Parafilm and irradiated for 15 min at room temperature and then frozen in liquid nitrogen. X-band EPR spectra were obtained using a Bruker ELEXSYS E500 spectrometer, mounting a liquid helium cryostat ESR900, Oxford Instruments. The EPR spectra were recorded for each sample at 22 K and at 298 K. The measurement range was between 1500 and 3800 G.

3.8 References

1. T. Graham, *Liquid diffusion applied to analysis.* Phil. Trans., 1861. **151**: p. 183.
2. C. F. Rammelsberg, Monatsber. königl. preuss. Akad. Wiss., *Fysi.-math. Klasse.* 1874. p. 490.
3. M. H. Klaproth, *Beiträge zur chemischen Kenntniss der Mineralkörper.* Decker & Co., Posen 1795. **1**.
4. J. Otto and R. Otto, *Ausführliches Lehrbuch der anorganischen Chemie,* 2. Band, 2. Abtheilung, Vieweg und Sohn, Braunschweig, 1863. p. 187.
5. C. Lü, Z. Cui, C. Guan, J. Guan, B. Yang, and J. Shen, *Research on preparation, structure and properties of TiO_2/polythiourethane hybrid optical films with high refractive index.* Macromol. Mater. Eng., 2003. **288**: p. 717.
6. R. J. Nussbaumer, W. R. Caseri, P. Smith, and T. Tervoort, *Polymer-TiO_2 nanocomposites: a route towards visually transparent broadband UV filters and high refractive index materials.* Macromol. Mater. Eng., 2003. **288**: p. 44.
7. L. Zimmermann, M. Weibel, W. Caseri, and U. W. Suter, *High refractive index films of polymer nanocomposites.* J. Mater. Res., 1993. **8** (7): p. 1742.
8. D.-S. Lee and T.-K. Liu, *Preparation of TiO_2 sol using $TiCl_4$ as a precursor.* J. Sol-Gel Sci. Technol., 2002. **25**: p. 121.
9. H. Rose, *Ueber das Titan und seine Verbindungen mit Sauerstoff und Schwefe.* Gilb. Ann. (Ann. Chem. Phys.), 1823. **73**: p. 67.
10. R. Weber, *Ueber die iosmeren Modificationen der Titansäure und einiger Titanverbindungen.* Pogg. Ann. (Ann. Chem. Phys. 196), 1863. **120**: p. 287.
11. H. R. Weiser and W. O. Milligan, *X-ray studies on the hydrous oxides. IV Titanium dioxide.* J. Phys. Chem., 1934. **38**: p. 513.

12. T. Nishino, S.C. Kani, K. Gotoh, and K. Nakamae, *Melt processing of poly(vinyl alcohol) through blending with sugar pendant polymer.* Polymer 2002. **43**: p. 2869.

13. B.J. Holland and J.N. Hay, *The thermal degradation of poly(vinyl alcohol).* Polymer, 2001. **42**: p. 6775.

14. P. S. Thomas, J.-P. Guerbois, G. F. Russell, and B. J. Briscoe, *FTIR study of the thermal degradation of poly(vinyl alcohol).* J. Therm. Anal. Calorim., 2001. **64**: p. 501.

Chapter 4

Tuneable refractive index of titanium oxide hydrates/ poly(vinyl alcohol) hybrid systems

4.1. Introduction

In the last decades, communication and information systems for data transfer or storage increasingly relied on light in view of the major advantages that photons offer on electrons as information carriers. In *dielectric* materials, for instance, light travels at significantly higher speed and larger bandwidth thereby only weakly interacting with materials compared to conventional electronic transmissions [1]. Modulated light pulses can, thus, propagate over long distances with minimum losses through confinement within a structure of controlled spatial refractive index distribution, as in optical fibres and waveguides [2]. Indeed, the realization of such structures underpinned the telecommunications revolution experienced during the late twentieth century.

Architectures with characteristic periodic modulation of refractive index – so called photonic crystals – are accordingly highly interesting objects because they allow controlling and manipulating light propagation [3] provided that the periodic dimensions are on the scale of the wavelength of light. Photonic crystals, therefore, offer a broad range of exciting optical possibilities in the production of integrated optical circuits for ultrafast telecommunications or photonic computers.

It is, therefore, evident that there is a great demand for materials which display suitable optical functionalities to be employed in photonic structures and, at the same time, can be processed in a straight-forward fashion. Such systems would allow for new strategies for designing structures that permit the control and manipulations of photons.

However, at present, the realization of well-defined and highly ordered architectures at the nanometer scale suitable for photonic applications has proven to be challenging. One of the impediments to fully reach and technologically exploit the potential of photonic structures effectively is presented by their manufacturing, which in most cases strongly relies on tedious and cost-intensive fabrication methods that often are limited to small areas only. The use of such complex technologies is compelled by the fact that inorganic systems, so far, are the preferred choice for the fabrication of most types of optical and photonic components and devices, principally due to the broad range of refractive indices accessible with these materials. Indeed, for the deposition of layers of inorganic material with controlled thickness below 100 nm, processing techniques such as plasma deposition [4, 5], assisted ion-beam sputtering [6] and electron-beam deposition and lithography [7, 8] are usually required.

Organic systems may offer a solution to overcome the technological limitations related to the use of inorganic materials in advanced optical and photonic applications, as they would be easy-to-process into large areas by solution-based methodologies, and can be nanostructured using relatively simple techniques such as embossing [9, 10] or soft lithographic methodologies [11]. However, in general, organic materials cannot provide a refractive index window comparable to that of inorganic materials which is required for such kind of applications.

Interestingly organic-inorganic systems such as the titanium oxide hydrates/PVAl hybrids described earlier (Chapter 3) can be regarded as an interesting alternative for straightforward, large-scale production of photonic structures as they would combine the desired optical properties of the inorganic species with the good processability of organic systems. In this chapter therefore, we report on the investigations about the optical properties of titanium oxide hydrates/PVAl hybrid systems and elucidate the potential of such material for the fabrication of photonic structures.

4.2. Optical properties of titanium oxide hydrates-PVAl

The complex refractive index $N = n + i\,\kappa$ is probably the most important parameter property to take into consideration in order to properly choose a specific material for optical and photonic applications. N, in fact, constitutes a quantification of the light-matter interaction. The term n determines how the light propagates and κ how it is absorbed or amplified within a medium [12]. The refractive index is directly linked to the material's density and dipole moment [12]. Of course such parameters are quite difficult to change within the same

material therefore probably the most common approach to obtain a desired refractive index consists of fabricating a "composite" of two distinct materials with very different individual refractive indices, n_1 and n_2. According to the effective medium theory [13] this method is expected to lead to an effective refractive index lying between n_1 and n_2 depending on the relative volume fractions of the two components x_1 and x_2 .

Indeed Lu and coworkers recently reported the fabrication of hybrid films comprising TiO_2 and triethoxysilane-capped polythiourethane via a sol-gel method resulting in refractive indices between 1.632 to 1.879 (at 632.8 nm) as the titania content was varied from 0 to 80 wt. % [14]. We, thus, expect the titanium oxide hydrates/PVAl hybrids are expected to possess optical properties resulting from the composition of those of the polymer and of the titanium species.

In order to analyse this effect, the content of titanium oxide hydrates of the hybrid material was varied. To this end mixtures containing 0 to 2.2 mol Ti / g PVAl were produced, and deposited on glass supports by dipcoating using the same withdrawal speed for all solutions. The resulting dried films contained an estimated volume fraction of titanium oxide hydrates between 0 and 99 %vol (considering a density for the titanium species of 1.95 g / cm^3 and a molecular weight of 80 g / mol. See sec. 3.3) and displayed thicknesses in the range between 70 and 200 nm — the solution more concentrated in titanium species produced the thinner films. Dry supported films were then immersed in distilled water to remove residual HCl (see Chapter 3) and let dry in air at room temperature for three days. However, both before and after the washing procedure, films appeared smooth, optically homogeneous and uniformly transparent in the visible and NIR region (up 1100 nm), even at very high concentration of titanium species.

As expected the refractive index of the hybrids, as deduced by spectroscopic ellipsometry performed on such films (see sec. 4.5.5), depended on the relative compositions of the material (Fig. 4.1 top panel left) with *n* increasing with the concentration of titanium oxide hydrates, from the 1.52 (at 550 nm) of the neat polymer to up to n_{550} = 1.9 for the films containing 2.2 mol Ti /g PVAl (about 99 %vol. of titanium oxide hydrates). Interestingly, a nearly linear dependence of the refractive index of the hybrids on the content of the inorganic species — which would be in agreement with a Bruggemann behaviour [13] (Eq. 4.1) — was found almost up to about 50 %vol. (Fig. 4.1, bottom panel left). Deviations for higher content of titanium species can be attributed to percolation phenomena. However, as it is visible in Figure 4.1 (bottom panel left), experimental data in the linear region did not entirely fit with the modelled prediction based on Bruggeman's effective medium theory formula expressed by Equation (4.1) [13]:

$$x_{PVAl}\left(\frac{\varepsilon_{PVAl}-\varepsilon}{\varepsilon_{PVAl}+2\varepsilon}\right)+x_{Ti\ species}\left(\frac{\varepsilon_{Ti\text{-}species}-\varepsilon}{\varepsilon_{Ti\text{-}species}+2\varepsilon}\right)=0 \qquad \text{Eq. 4.1}$$

where x_{PVAl} and $x_{Ti\text{-}species\ the}$ indicate the volume fractions of the polymer and the titanium oxide hydrates respectively and ε_{PVAl} and $\varepsilon_{Ti\text{-}species}$ their relative permittivities (considering that $n^2 = \varepsilon$). This could be probably due to the fact that the interaction between the polymer and the titanium species are too strong to be neglected.

Clearly, the refractive index of the hybrid materials compared well with some inorganic systems such as SiO_2 and TiO_2 [4], but is notably different to other polymer-based hybrid systems especially when considering the transparency of our

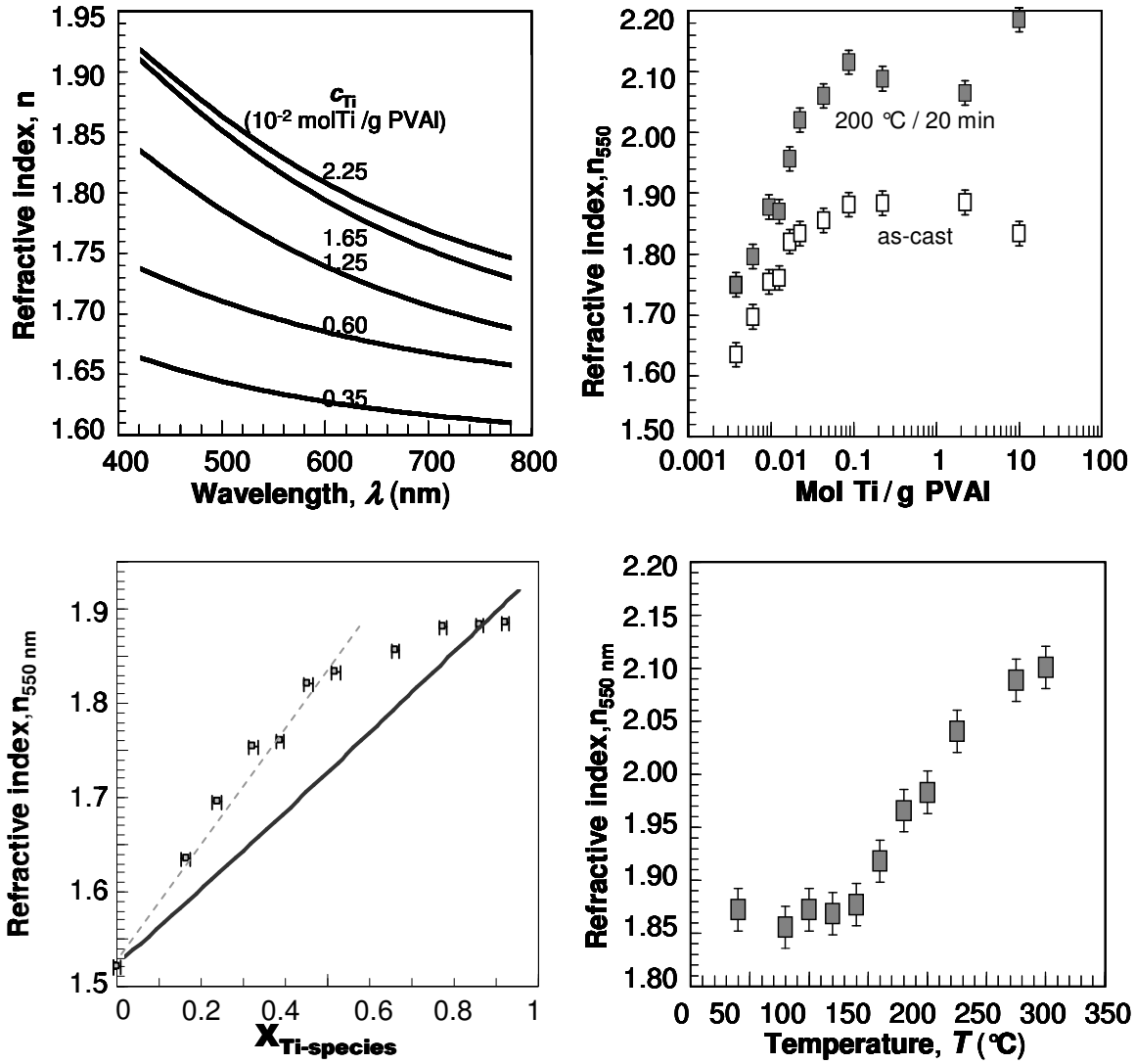

Figure 4.1: ***Top panel let:*** Refractive index dispersion curves for thin films of titanium oxide hydrates / PVAl at different concentration of titanium species, deduced from variable angle spectroscopic ellipsometry and, ***top panel right:*** values of *n* extrapolated at 550 nm for the same set of films before and after thermal annealing at 200 °C for 20 min. The refractive index visibly increases with the concentration of titanium oxide hydrates in the system. ***Bottom panel left:*** Refractive index (at 550 nm) of hybrids as a function of volume fraction of the titanium species (grey symbols), retrieved using an estimated density for the titanium species of 1.95 g /cm^{-3}. *n* varies linearly with the concentration of titanium species up to about 50 % in volume (trend in grey, dashed line). The solid black line shows the prediction of the behaviour of *n* with the volume fraction of the titanium species according to the Bruggemann model [13]. ***Bottom panel right:*** The refractive index (at 550 nm) of thin films of our hybrid material with concentration of $2.2 \cdot 10^{-2}$ mol Ti/g PVAl (about 99 % by volume) annealed for 20 min at temperatures indicated. Clearly n increases rapidly above 150 °C and seems to reach a plateaux for temperatures approaching 300 °C. Such an increase may be associated to the condensation and densification of the titanium oxide hydrates.

structures [14]. Remarkably, the refractive index of the hybrid films could be further enhanced to more than 2.1 8 (at 550nm) by thermal annealing. This effect was more pronounced for higher contents of the titanium species (Fig. 4.1, top panel right)and occurred more rapidly at higher temperature as evident from Figure 4.1 (bottom panel right). Indeed, short annealing times produced appreciable variation in *n* only for temperatures above 150 ^{o}C while higher temperature treatments induced more significant changes saturating at temperatures around 300 ^{o}C. [N.B. It is remarkable that the titanium oxide hydrates / PVAl hybrids did not melt at temperatures up to 300 °C, well above the melting temperature of the neat polymer (230 °C). This illustrates the strength of the interactions between the inorganic titanium species and PVAl as already described in Chapter 3. Of course degradation of the organic matrix at such high temperature cannot be excluded]. The increase in *n* occurred with a concomitant reduction in film thickness, as measured by variable angle spectroscopic ellipsometry and supported by surface profilometry data. From previous investigations (see Chapter 2 and 3) such densification should mainly be attributed to condensation of titanium oxide hydrates molecules and possibly condensation reactions between titanium species and the surrounding polymer. The condensation of the titanium oxide hydrates towards crystalline TiO_2 forms during annealing procedures (see Chapter 1) might, on the other hand, be the main origin of the increase in the refractivity of the hybrid material, as anatase and rutile have a higher refractive index (2.55 anatase and 2.7 rutile respectively [15]) compared to titanium oxide hydrates ($n_{550nm} \approx$ 1.88). This is also in agreement with the density of the titanium oxide hydrates being smaller than that of titania respectively (3.89 g / cm^3 for anatase and 4.27 g / cm^3 for rutile [15]). However, it is worth to mention that no evidence of the formation of any crystalline

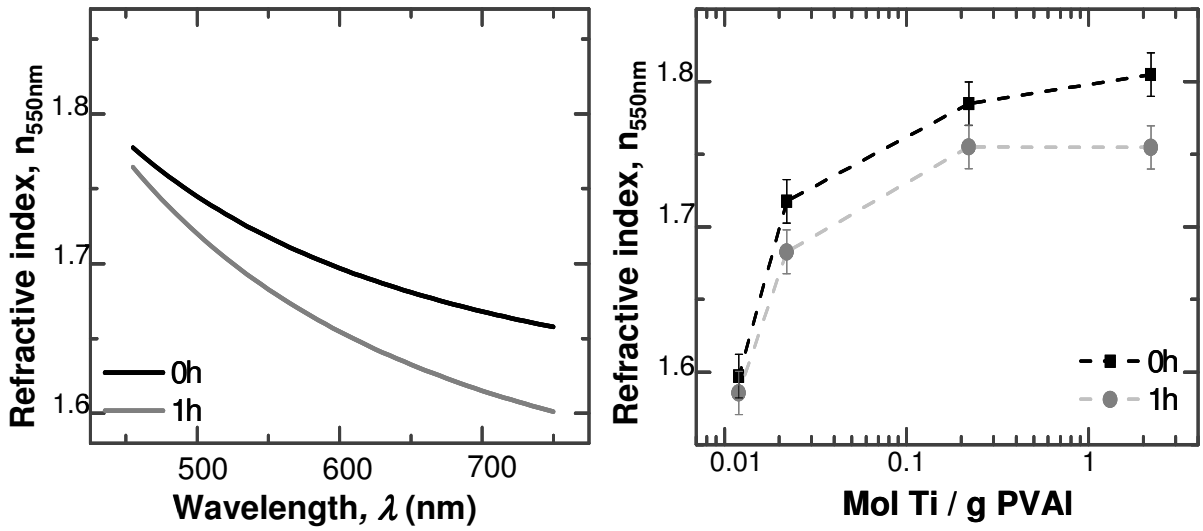

Figure 4.2: ***Left panel*****:** Reduction of the refractive index through UV irradiation. ***Right panel*****:** The refractive index at 550 nm before (black squares) and after (grey circles) one hour UV exposure as a function of concentration of titanium oxide hydrates in the hybrid material. Clearly, the reduction of n is more pronounced for hybrids with higher content of inorganic species. The phenomenon can be related to the photoreduction of titanium species in the hybrid which modify the dielectric characteristic of the hybrid material.

titania was obtained both from X-ray diffraction analysis and transmission electron microscopy.

Interestingly, it was possible to modulate the refractive index of the hybrids also by irradiation with UV light (see for detail sec. 4.5.4). Indeed *n* decreased linearly with time of exposure to UV light (Fig. 4.2) – an effect that was more pronounced in hybrids with higher content of titanium species (Fig. 4.2 right panel). It is important to note that such a phenomenon was not observed for neat PVAl or titanium oxide hydrates films, which would suggest that the effect may be related to the photochromism of titanium oxide hydrates / PVAl hybrid materials (Chapter 3). In fact, over irradiation with UV light the titanium in the hybrid materials reduced from diamagnetic Ti^{IV} to Ti^{III}, which is paramagnetic species. The new electronic configuration of the metal is expected to result in different interactions with light.

It is possible, as an example, that the magnetic dipoles in the hybrid material may align with the magnetic field of the electromagnetic wave, counterbalancing the effect of the electric dipoles on the electric field. Therefore, the photo-reduced hybrids that contain Ti^{III} would display a lower refractive index in comparison with to the non irradiated materials. Clearly one cannot exclude that the irradiation causes degradation of the polymer matrix.

4.3. *1*-dimensional photonic crystals.

From the above it is evident that titanium oxide hydrates / PVAl hybrid systems seem to fulfil the necessary requirements for the manufacturing of photonic structures, *i.e.* transparency over a wide range of wavelengths (from 400 to 1100 nm), solution processability and high refractive index that is tuneable a priori via controlling the composition of the hybrid material and a posteriori by applying selected thermal and UV treatments to the already deposited and dried layers.

In order to explore the potential and test versatility of the hybrid material for optical and photonic applications in the visisible near IR regime, we, therefore, fabricated dielectric mirrors- *i.e.* distributed Bragg reflectors (DBRs). Such structures, also known as one-dimensional photonic crystals, are of great technological interest because they offer the advantage of being selective in terms of the reflected wavelengths. They are also considerably less absorptive than their metallic counterparts and can be employed in the fabrication of many optical devices. As a consequence, DBR applications include optical filters and mirrors [16], dielectric omnidirectional reflectors [17], hollow fibers [18], microcavities for light emitting diodes [19-22] and sensors [23, 24].

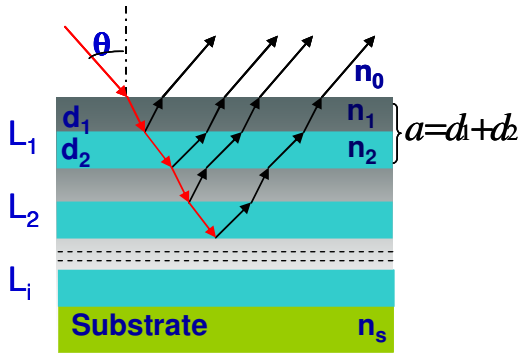

Figure 4.3: Schematic of a distributed Bragg reflector (DBR) showing the relevant system parameters. *n* and *d* refer to the refractive index and the thickness of the dielectric layers; *L* represent the period of the DBR. θ is the angle of incidence of light defined between the line of propagation of light and the normal to the surface of the multilayer. The working principle of such structures is based on the interference between light that is partially reflected or transmitted at each layer. The coherence between reflected light can be achieved only for specific values of the thickness and refractive index of the two dielectrics layers.

4.3.1. Dielectric distributed Bragg reflectors: a brief overview

Dielectric Bragg reflectors are structures that present a periodic variation of the refractive index in one direction, obtained by alternating layers of materials with respectively low and high refractive indices (Fig. 4.3). The periodic modulation of the refractive index can actually alter the dispersion of light through the structure resulting in a photonic band gap, implying that, if the dimensions of the periods are those of the incident wavelength, the propagation of light through the multilayer is forbidden along some directions (incomplete band gap) [3]. The key characteristics of the reflected light, suchas the peak wavelength of the main reflection and its intensity as well as the range of wavelengths reflected, critically depend on the refractive indices, n_1 and n_2, and the thicknesses, d_1 and d_2 of the alternating high / low refractive index layers [12, 25].

At normal incidence ($\theta = 0$ in Fig. 4. 3) the peak wavelength of the main Bragg reflection is given by Equation 4.2 [26]:

$$\lambda_0 = \frac{2a\bar{n}}{m} \qquad \text{Eq. 4.2}$$

where $\bar{n}$ is the average refractive index along the structure and $a = d_1 + d_2$ the thickness of the period of the DBR (as indicated in Fig. 4.3) and m is an integer. The bandwidth of the reflection ($\Delta\omega/\omega_0$ - Eq. 4.3) and its intensity (R - Eq. 4.4) are strongly controlled by the mismatch of the refractive indices, $\Delta n = n_1 - n_2$ [12, 25].

$$\frac{\Delta\omega}{\omega_0} = \frac{4}{\pi}\arcsin\left(\frac{n_1 - n_2}{n_1 + n_2}\right) \qquad \text{Eq. 4.3}$$

$$R = \left[\frac{n_0(n_1)^{2L} - n_s(n_2)^{2L}}{n_0(n_1)^{2L} + n_s(n_2)^{2L}}\right] \qquad \text{Eq. 4.4}$$

Therefore, the increase in Δn results in a wider band gap and an increased reflectivity R. In addition R can be enhanced by increasing the number of periods, L, in the multilayer structure.

Another interesting property of such structures is that the reflected light strongly depends on the angle of incidence θ of the impinging light. This can be explained on the basis of thin film interference effects. Light is partially transmitted and reflected at each interface (Fig. 4.3) and the reflected beams will undergo

constructive interference only if the Bragg condition $2nd\cos\theta = m\lambda$ (where m is an integer and λ is the wavelength of impinging light) is satisfied. As a consequence, when the angle of incidence of light varies, also the phase relation between different reflected light rays changes leading to constructive interference for different wavelengths. The dependence of the peak wavelength of the main Bragg reflection on the angle of incidence of light is expressed by the Equation 4.5.

$$\lambda\theta = \frac{2a\sqrt{n^{-2} - \sin^2\theta}}{m} \qquad \text{Eq. 4.5}$$

4.3.2 All-polymer DBRs based on titanium oxide hydrates/ PVAl hybrids

Double-sided symmetric DBRs with a wide stop-band in the visible were produced by alternating layers of the high refractive titanium oxide hydrates/ PVAl hybrid (n_{550} = 1.77, containing of 1.25 $\cdot 10^{-2}$ mol Ti / g PVAl, with the low refractive index material, poly[4,5-difluoro-2,2-bis(trifluoromethyl)-1,3dioxole-co-etrafluoroethylene] (PFP) (n_{PFP} ~1.29 at 550 nm) (Fig. 4.4). Layers of the two materials were deposited on glass substrates via dip-coating from solution of the two materials (see for details sec. 4.5.2). The material diffusion between layers (Fig. 4.5, top panel) was limited by ensuring that each layer dried fully before applying the next one. In this manner, large area (cm^2) DBRs could be produced (Fig. 4.5, bottom panel). Layers of different thicknesses could be readily realised by simply adjusting the withdrawal speed used for the dip-coating deposition with higher speeds producing thicker films (see section 4.5.3 for details).

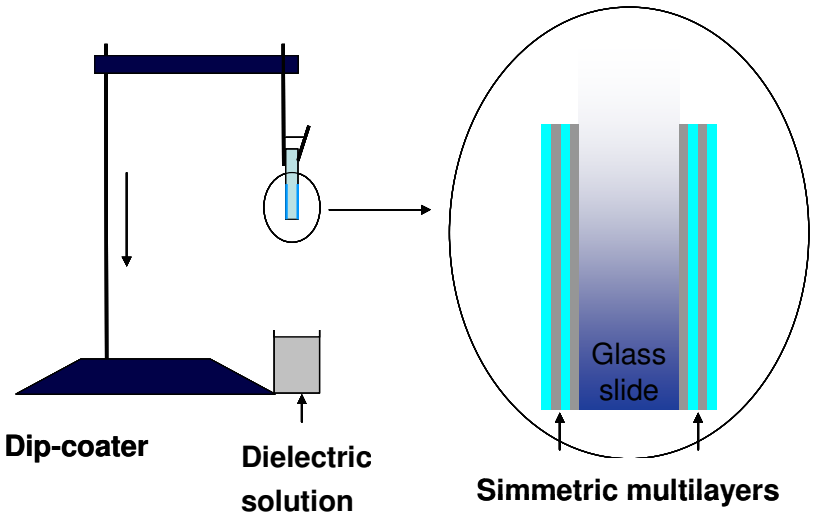

Figure 4.5: Alternate dipcoating of the two dielectric solutions on a glass support allow producing double sided and simmetric multilayers. The thickness of the deposited layers is directly proportional to the speed of withdrawal from the solution. The technique has virtually no restriction on the dimensions or the nature of the substrate to coat and can be operated in air at ambient conditions. In the circle on the right side is a schematic of the section of a glass slide covered by symmetric multilayers produced by dip coating.

Accordingly 8 period DBRs were fabricated with lattice parameters controlled by the deposition conditions. Indeed, the titanium oxide hydrates / PVAl and PFP layers thicknesses were varied from 105 to 125 nm and 50 to 80 nm, respectively, when changing the dip-coating speed. This resulted in a shift of about 0.6 eV (almost 150 nm) in the central position of the stop band, which was clearly detectable by eye (Fig. 4.6), so as the reflectivity dependence on the light incidence angle resulting in a pronounced change of the reflected colour as function of viewing angle (Fig. 4.6 - bottom panel on the side).

For technological applications DBR structures with reflectivities above 99 % are usually required. This may be realised by increasing the number of periods in such

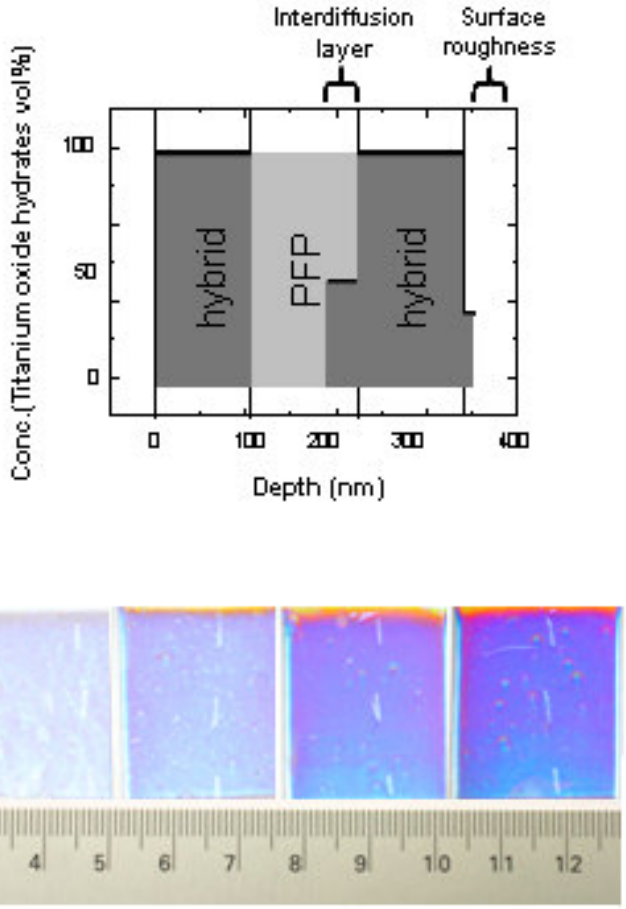

Figure 4.5: ***Top panel:*** Schematic of a tri-layer structure, alternating titanium oxide hydrates / PVAl hybrid and perfluorinated polymer (PFP), used to analyse eventual interdiffusion of the two components at the interfaces. Interestingly the different types of modelling (see sec. 4.5.5 for detail) suggest that when the perfluorinated polymer is deposited on the hybrid, the interface between the two materials is well defined. Differently, some interface diffusion may occur when the hybrid is deposited on top of the perfluorinated polymer. However, reassuringly, this effect can be minimised if the PFP layer is allowed to dry thoroughly before depositing the hybrid. ***Bottom panel:*** Sequence of pictures taken during fabrication of a 4 period DBR structure by dip-coating our hybrids and the perfluorinated polymer on a glass support of 2 x 2.7 cm^2. From left to right, respectively, are one, two, three and four double layers. The intensity visibly increases with the number of periods.

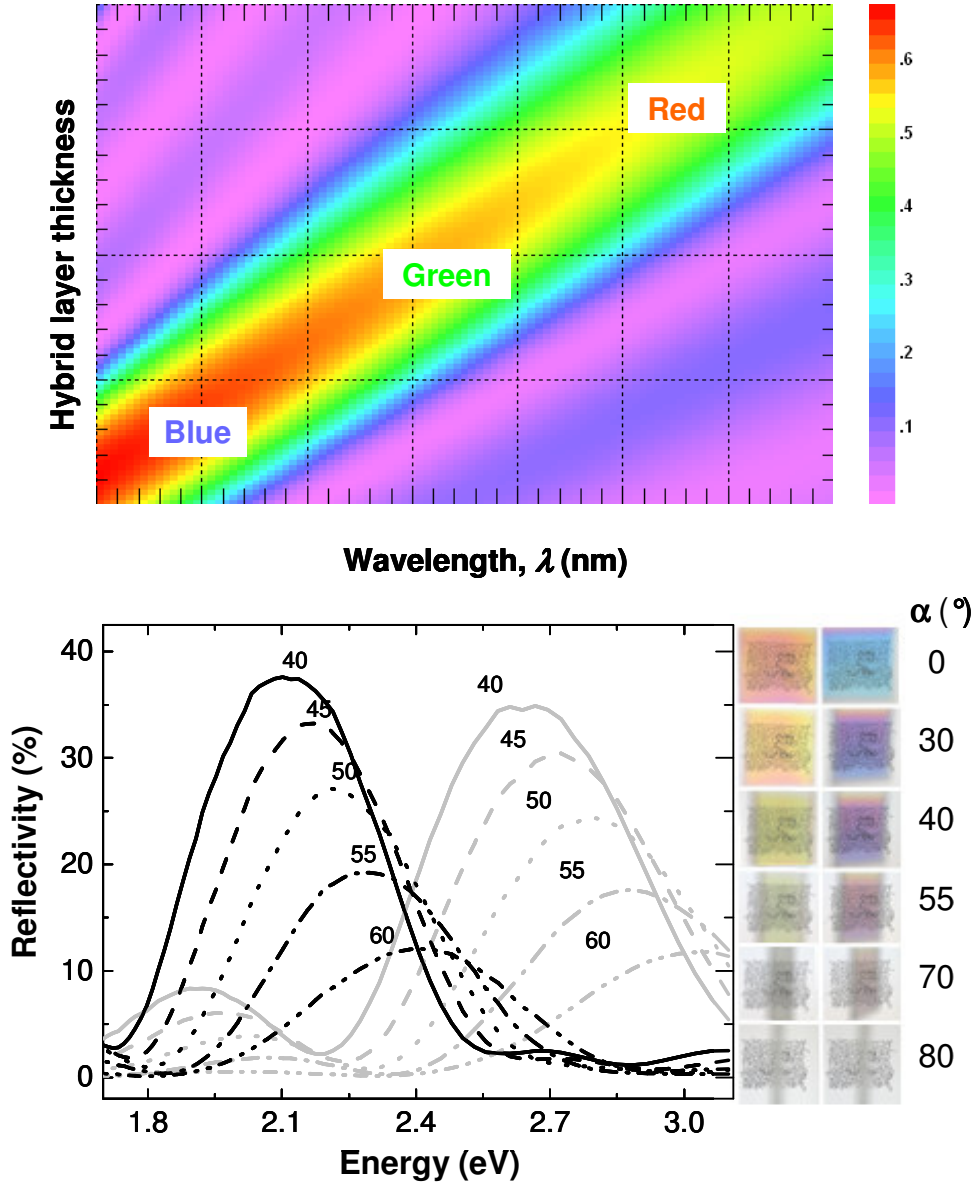

Figure 4.6: ***Top panel***: Change in the main reflection wavelength, at normal incidence, for a model 5 period DBR, when the thickness of the hybrid film vary from 50 nm to 150 nm while assuming that the other three parameters, n_{hybrid} (1.7 at 550 nm), n_{PFP} (1.3 at 550 nm) and d_{PFP} (80 nm) remain constant. The simple variation of one DBR parameter leads to a drastic change in the reflected colour from blue to red. ***Bottom panel:*** Reflectivity of two 8 bilayers dielectric mirrors based on of titanium oxide hydrates / PVAl and PFP measured at different angles of incidence of light. The two structures were made with different lattice parameters and therefore display different stop-bands. In particular in black are the reflectivity curves for a DBR with period thickness ($a = d_1 + d_2$) of around 150 nm while the in grey are reported the reflectivity curves for a 200 nm period DBR. In both cases, however, as the incident angle increases the band gaps shift to lower wavelengths. *On the side:* Sequences of photographs reporting the two DBR pictured at different viewing angles.

multilayer structures (Eq. 4.4). This should lead, in addition, to the narrowing of the stop-band. In accord with this, we found that 16 period DBRs, displayed a normal incidence reflectivity close to 100 % (T = 2.5 %) at the maximum of the stop band (Fig. 4.7) within the experimental uncertainty of the equipment used to evaluate *R* (< 2 %). Deviations of *R* from the ideal behaviour, *i.e.* non-zero minima, most likely are associated with small inhomogeneities throughout the DBR structures. However, it is worth mentioning that from optical models made using the transfer matrix formalism the estimated inhomogeneity in film thickness and /or refractive index of the 32 layer structures seem to be less than 8 % (Fig. 4.8 **a**) (see sec. 4.5.11 for details). This is in good agreement with the total thickness variations measured using three dimensional profilometry that was found to be around 5 % throughout the structure (Fig. 4.8 **b** and **c**). This is surprisingly small considering the complexity of the structure, the simplicity of the fabrication method and the fact that neither processing conditions nor the structure have been optimised – so far. Results of the optical modelling also supported the values of the refractive indices as experimentally determined using ellipsometry. In fact, even small discrepancies between the actual values of refractive index and thickness of the single layers and those used for the model would result in very large spectral differences between the measured and modelled reflectivities as DBRs systems operate entirely via highly sensitive interference mechanisms.

Finally it is important to note that, differently from the single layers of titanium oxide hydrates /PVAl hybrids used to determine the refractive index via ellipsometry, the layers of hybrid material deposited during the manufacture of the DBR have not been washed according to the procedure described in Chapter 3. This precaution was taken in order to prevent eventual damages to the multilayer during the washing step

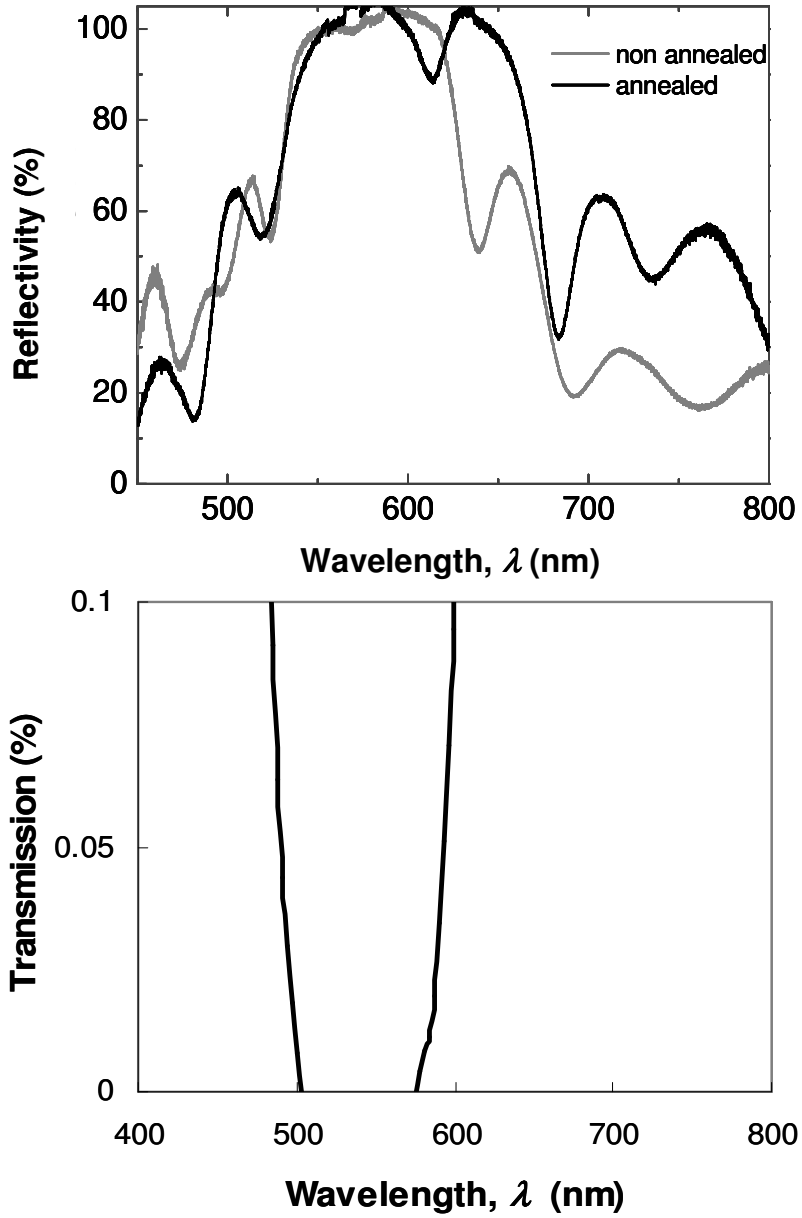

Figue 4.7: ***Top panel:*** Normal incidence reflectivity of dielectric mirrors based on 16 bilayers of titanium oxide hydrates / PVA and PFP, before (grey line) and after (black line) annealing at 200 ^{o}C for 20 min. Before annealing the DBR displayed reflectivity of ~ 100% in the region between 500 and 610 nm. After annealing the width of the band gap visibly increased as well as the region of 100% reflectivity and the reflectivity increases. ***Bottom panlel:*** Detail of transmission measurements performed with a UV-vis spectrophotometer on the annealed 16 bilayer DBR. The multilayer area of probed in the measurement was much larger (1.5 x 0.5 mm) than the area analysed with normal incidence reflectivity (around 100 μm ^{2}) therefore it accounts for the transmission of a more inhomogeneus portion of the DBR.

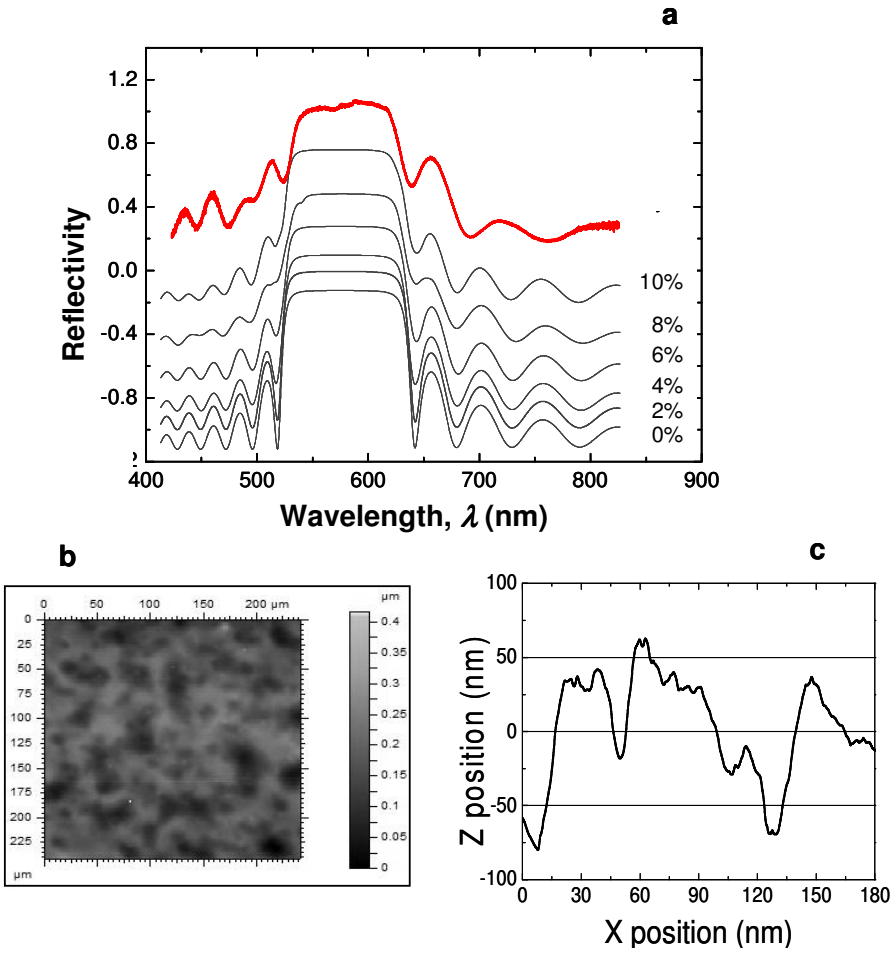

Figure 4.8: a- Optical modelling of the DBR mirrors using the transfer matrix formalism (see sec. 45.11). The various reflectivity curves (here offset one from the other to improve clarity) represent different degrees of disorder on the multilayer stack (e.g. small thickness difference between layers) starting from 0 % (ideal case) up to 10 % disorder. Comparison with the experimental data (red curve) indicates a degree of disorder smaller than 8 %. **b-** Two-dimensional profilometry map of the surface of the 16 bilayer non-annealed DBR; and **c-** linear profile of the surface which shows that the surface roughness is < 5 % of the total thickness of the multilayered stack.

Nevertheless, the good agreement of the modelled reflectivity and the experimentally determined ones, suggests that washing did not induce appreciable modifications of the refractive index, *n*, of the hybrids.

4.3.3 Post-deposition tailoring of DBR response

Finally we explored the option to tune the DBR properties by suitable thermal treatment or by irradiation with UV light as such procedures clearly influence *n* and *d*

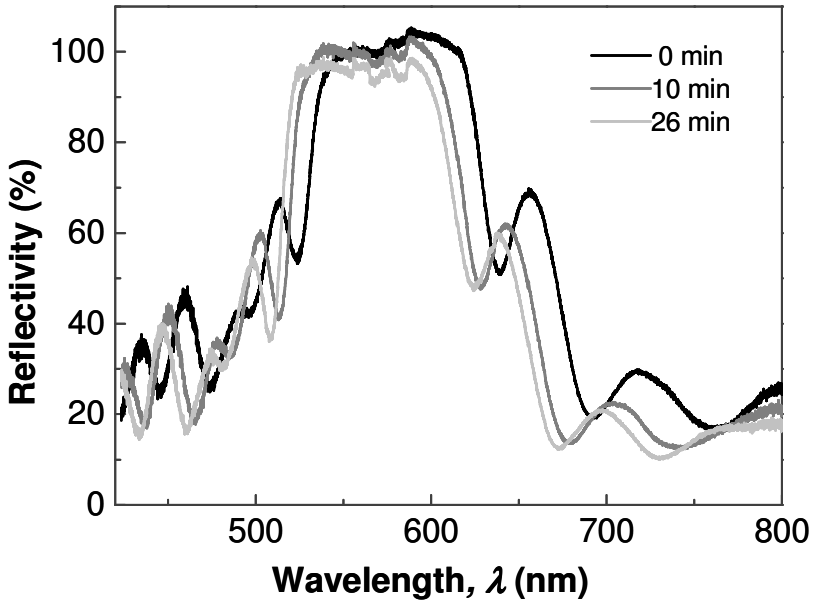

Figure 4.9: Effect of UV irradiation on the stop band (collected at normal incidence) of a 16 period DBR. The reduction of the refractive index of the hybrid material induces significant modifications of the band gap of the structure already after 20 min of UV exposure. The most visible effect of the reduced refractive index contrast between titanium oxide hydrates / PVAL and PFP layers is the blue shift and the reduction of *R*.

Therefore, this should provide an effective tool for post-deposition tuning of the optical response of such dielectric mirrors.

Indeed, as a consequence of the increase Δn after annealing at 200 ^{o}C for 20 min, the band-gap of the16 bilayer DBR at normal incidence resulted visibly widened (Fig. 4.7- top panel) and the reflectivity enhanced as visible in the fig 4.7. In contrast, upon UV irradiation, the reduction of the refractive index mismatch induced a decrease of the reflectivity and a pronounced blue shift of the stop-band as evident from data presented in Figure 4.9 reporting *R* for increasing irradiation time.

4.4. Conclusions

Thin titanium oxide hydrates / PVAl hybrid films transparent in the visible and NIR, with thicknesses in the order of tens of nanometre can be readily

produced using common solution processing techniques. The refractive index of the hybrids increased with the content of the titanium oxide hydrates to more than 1.9 8 (at 550 nm). Annealing the hybrids yielded to refractive indices as high as 2.1 (at 550 nm) while the films remained transparent. Exposure to UV light induced, on the other hand, a reduction of the refractivity of the hybrid material. This high versatility of the hybrid systems allowed fabrication of all-solution processed dielectric mirrors that can exhibit reflectivity at normal incidence close to 100%. We also demonstrated the possibility to modify the characteristics of the DBR stop band using suitable heat treatments or UV radiation. The possibility to tailor the optical properties of such hybrid material by post-deposition treatments offers clearly a higher freedom in the design of DBR structures, compared to existing system, thus and may open up novel routes for fabricating photonic structures such as three dimensional photonic crystals through the patterning of multilayered architectures in the sub-micrometer range. Indeed, hybrid materials based on titanium oxide hydrates / PVAl may have a strong potential also for the manufacture of other complex photonic structures and devices with promising optical properties such as Fresnel lenses and gratings [12], integrated optical devices [2], and a plethora of optical components which can be produced by employing lithographic techniques.

4.5. Materials and methods

4.5.1. Materials

$TiCl_4$ (purity > 99 %), poly(vinyl alcohol) (PVAl) ($M_w \approx 130.000$ g / mol, residual content of acetate=10-11.6%),(poly[4,5-difluoro-2,2-bis(trifluoromethyl)-1,3-dioxole-co-tetrafluoroethylene] (PFP) and perfluorodecaline (99 %) were purchased from Sigma-Aldrich.

4.5.2. Materials preparation

Hybrid mixtures with a range of concentration of titanium species ranging from 3.8 10^{-3} to 2.22 mol Ti/g PVAl were prepared by adding corresponding amounts of $TiCl_4$ hydrolysis solution (0.35 mol Ti /dm^3 – according to the procedure reported in section 2.5.2) to 2 wt. % aqueous solution of PVAl. The resulting clear and colourless mixtures were used soon after to deposit layers of the hybrid material on glass substrates by dip-coating.

For the manufacture of the DBR samples, we used a titanium oxide hydrates/ PVAL hybrid mixtures with a concentration of titanium species of $1.25 \cdot 10^{-2}$ mol Ti/g PVAl. Once dried, such concentrations would provide layers with a refractive index of $n_{550} = 1.77$.

PFP was used as low refractive material ($n_{550} = 1.30$). The polymer was deposited from a 1 mg / ml solution in perflourodecaline.

Both materials were transparent in the range of wavelengths from 400 - 1000 nm.

4.5.3. DBR Fabrication

Layers of PVAl / titanium oxide hydrates hybrid and PFP were alternately deposited on glass supports by dip-coating from the respective solutions (see sec.

4.5.2) in ambient conditions. Each layer was allowed to dry for about 30 to 40 min before starting the deposition of the next layer in order to minimise interdiffusion of the dielectrics at the reciprocal interface.

Each DBR sample was fabricated using a selected speed of withdrawal, v, for both the dielectrics. For instance v_1 = 5.4 cm / min was used for the fabrication of one set of 8 period DBRs while v_2 = 8.2 cm / min, was employed to produce the other 8 and 16 period DBRs. Using these withdrawal speeds we could produce layers with thicknesses of about 100 and 120 nm for the hybrid material films and about 50 and 90 nm for the PFP, the higher speeds producing the thicker films.

Film thicknesses were determined using surface profilometry and ellipsometry measurements (see sec. 4.5.10 and 4.5.5)

4.5.4. Heat and UV treatments

Hybrids containing $2.2 \cdot 10^{-2}$ mol Ti / g PVAl were annealed for 20 min at temperatures in the range between 40 and 300 ^{o}C. All the other single layer hybrids and the two DBR structures were annealed at 200 ^{o}C for 20 min.

UV exposure of the hybrid single layers and multilayer structures was carried out using a L9610-011 UV diode by Hamamatsu Photonics with central wavelength at 365 nm and output intensity of 4.6 W/cm^2.

Both treatments were performed in air and at atmospheric pressure with no special precautions to control humidity.

4.5.5. Ellipsometry

Refractive indices and film thicknesses were measured using a SOPRA GES-5 rotating polariser variable angle spectroscopic ellipsometer (VASE). Three

incident angles close to the effective Brewster angle of each sample were used, and the wavelength was scanned between 400 and 800 nm at 5 nm intervals. Additional ellipsometric measurements were also performed using a SOPRA ES4G spectroscopic ellipsometer. Excellent agreement was found between the data collected using the two equipments. All data were modelled using Cauchy dispersion laws. Once the refractive indices were obtained, ellipsometry was also applied to 8 bilayer DBR structures in order to evaluate the periodic thicknesses of the layers. The material diffusion between PFP and titanium oxide hydrates / PVAl hybrid layers was assessed on simple three layer structures using ellipsometry. In particular being the n and k known for the hybrid film and the PFP film it is possible to predict the values of $\tan\psi$ and $\cos\Delta$ that a perfect bilayer of our material would exhibit. The matching of the calculated optical constants and the experimental ones is then refined allowing interdiffusion between the layers — i.e. considering a thin layer where the optical constant of the two dielectrics mix — with slightly different geometries.

4.5.6. Variable angle reflectomety

The SOPRA Ges-5 piece of equipment was also used to measure the reflectivity of the multilayer structures as a function of the incident angle. The latter could be varied using a calibrated automatic goniometer which allowed to access incident angles from 40 to 90 degrees with respect to the sample normal. Normal incidence transmission experiments were performed by placing the sample vertically and the goniometer arms at 90 degrees. The reference for both, reflection and transmission experiments was collected in this configuration by interchanging the sample by the bare substrate. The measured data was also modelled using the

WinElli piece of software by SOPRA in order to double check the periodic film thicknesses of the DBR structures deduced using ellipsometry.

4.5.7. Normal incidence reflectometry

Normal incidence reflectivity was measured using a confocal LabRam HR 800 instrument (Jobin-Yvon / Horiba), with light coming from a halogen lamp being focused into a small area of the sample using an Olympus BX41 microscope (fitted with a long distance, small aperture 10x objective). The reflected light was detected using a Peltier cooled charge coupled device (CCD). As reference, a Therlabs B1EO2 mirror with more than 99 % reflectivity over the measured spectral range was employed. The system was tested using silicon wafers; the reported reflectivities have less than 3 % uncertainty. Measurements were taken at several spots throughout the samples to check film homogeneity.

4.5.8. Transmission spectroscopy experiments

Additional transmission data were collected using a Perkin Elmer Lambda 950 spectrometer UV-NIR spectrophotometer, equipped with integrating spheres in air. These data are in good agreement (after appropriate corrections are made) with the corresponding reflectivity measurements.

4.5.9. Transmission electron microscopy

Transmission electron microscopy measurements were carried out on samples of titanium oxide hydrates / PVAl with increasing concentrations of titanium species which were deposited on gold grids via dip-coating from solution of the liquid hybrid

material. Samples were analysed before and after annealing for one hour at 200^{o}C. Measurements were performed on a JEOL-JEM-2010 Electron Microscope with acceleration voltage of 200 KV.

4.5.10. Surface profilometry

A Dektak 3 surface profilometer was employed to double check the ellipsometry deduced film thicknesses. Good agreement was found in all cases. Moreover, the surface of the 16-bilayer DBR structures was characterised using a 3-D Nanopic 2100 from KLA Tencor atomic force profilometer.

4.5.11. Optical Modelling of the DBRs

A home made program based on the transfer matrix formalism was employed to model the reflectivity of the fabricated DBRs. To simulate the effect of structural inhomogeneities on the reflectivity values, a series of calculations of the possible reflectivity that could be obtained if the structural structural parameters (thickness and refractive index of the two layers) were made slightly vary respect to a mean value. The results from such calculations were then averaged to obtain an effective reference response. The variation percentage of the parameters with respect to the mean value defined the degree of inhomogeneity (in %). We found that variations on refractive index or film thickness are equivalent in terms of accounting for DBR inhomogeneity.

4.6. References

1. J. D. Joannopoulos, P. R. Villeneuve, and S. Fan, *Photonic crystals: putting a new twist on light* Nature, 1997. **386**: p. 143.
2. T. Tamir, ed. *Integrated optics*. Topics in applied physics Vol. 7. 1975, Springer-Verlag: Berlin-New York.
3. J. D. Joannopoulos, S. T. Johnson, J. N. Winn, and R. D. Meade, eds. *Photonic crystals-Molding the flow of light*. 2nd ed. 2008, Princeton University Press: Princeton and Oxford.
4. F. Gracia, F. Yubero, J. P. Holgado, J. P. Espinos, A. R. Gonzalez-Elipe, and T. Girardeau, *SiO_2/TiO_2 thin films with variable refractive index prepared by ion beam induced and plasma enhanced chemical vapor deposition.* Thin Solid Films, 2006. **500** (1-2): p. 19.
5. J.-Q. Xi, M. Ojha, J. L. Plawsky, W. N. Gill, J. K. Kim, and E. F. Schubert, *Internal high-reflectivity omni-directional reflectors.* Appl. Phys. Lett., 2005. **87**: p. 031111.
6. T.-H. Chang, S.-H. Chen, C.-C. Lee, and H.-L. Chen, *Fabrication of autocloned photonic crystals using electron-beam guns with ion-assisted deposition.* Thin Solid Films, 2008. **516**: p. 1051.
7. H. W. P. Koops, O. E. Hoinkis, M. E. W. Honsberg, R. Schmidt, R. Blumb, G. Böttger, A. Kuligk, C. Liguda, and M. Eich, *Two-dimensional photonic crystals produced by additive nanolithography with electron beam-induced deposition act as filters in the infrared.* Microelectron. Eng., 2001. **57-58**: p. 995.
8. T. F. Krauss, R. M. De la Rue, and S. Brand, *Two-dimensional photonic-band gap structures operating at near infrared.* Nature, 1996. **383**: p. 699.

9. N. Stutzmann, T. A. Tervoort, C. W. M. Bastiaansen, K. Feldman, and P. Smith, *Solid-state replication of relief structures in semi-crystalline polymers.* Adv. Mater., 2000. **12** (8): p. 557.

10. N. Stutzmann, T. A. Tervoort, C. W. M. Bastiaansen, and P. Smith, *Patterning of polymer-supported metal films by microcutting.* Nature, 2000. **407**: p. 613.

11. A. Seki, M. Ichicawa, N. Suganuma, Y. Tanaka, T. Koyama, and Y. Taniguchi, *Organic polymer DBR laser by soft lithography II: optimization of distributed Bragg reflector.* J. Photopolym. Sci. Technol., 2003. **16** (2): p. 329.

12. E. Hecht and A. Zajac, eds. *Optics*. 3rd ed. 1997, Addison Wesley Publishing Company.

13. T. C. Choy, ed. *Effective Medium Theory: Principles and Applications*. 1999, Oxford University Press: Oxford.

14. C. Lü, Z. Cui, C. Guan, J. Guan, B. Yang, and J. Shen, *Research on preparation, structure and properties of TiO_2/polythiourethane hybrid optical films with high refractive index* Macromol. Mater. Eng., 2003. **288**: p. 717.

15. U. Diebold, *The surface science of TiO_2.* Surf. Sci. Rep., 2003. **48**: p. 53.

16. T. Alfrey, E. F. Gurnee, and W. J. Schrenk, *Physical optics of iridescent multilayered plastic films.* Polym. Eng. Sci., 1969. **9**: p. 400.

17. Y. Fink, J. N. Winn, S. Fan, C. Chen, J. Michel, J. D. Joannopoulos, and E. L. Thomas, *A Dielectric omnidirectional reflector.* Science, 1998. **282**: p. 1679.

18. M. Skorobogatiy and A. Dupuis, *Ferroelectric all-polymer hollow Bragg fibers for terahertz guidance.* Appl. Phys. Lett., 2007. **90**: p. 113514.

19. P. K. H. Ho, D. S. Thomas, R. H. Friend, and N. Tessler, *All-polymer optoelectronic devices.* Science, 1999. **285** (9): p. 233.

20. L. Hou, Q. Hou, Y. Mo, J. Peng, and Y. Cao, *All-organic flexible polymer microcavity light-emitting diodes using 3M reflective multilayer polymer mirrors.* Appl. Phys. Lett., 2005. **87**: p. 243504.

21. L. Persano, A. Camposeo, P. D. Carro, E. Mele, R. Cingolani, and D. Pisignano, *Very high-quality distributed Bragg reflectors for organic lasing applications by reactive electron-beam deposition.* Opt. Express, 2006. **14** (5): p. 1951.

22. E. F. Schubert, Y.-H. Wang, A. Y. Cho, L.-W. Tu, and G. J. Zydzik, *Resonant cavity light-emitting diode.* Appl. Phys. Lett., 1992. **60** (8): p. 921.

23. A. Convertino, A. Capobianchi, A. Valentini, and E. N. M. Cirillo, *A new approach to organic solvent detection: high-reflectivity Bragg reflectors based on a gold nanoparticle/teflon-like composite material.* 2003. **15** (13): p. 1103.

24. M. Lee and P. M. Fauchet, *Two-dimensional silicon photonic crystal based biosensing platform for protein detection.* Opt. Express, 2007. **15** (8): p. 4530.

25. R. Tilley, ed. *Colour and optical properties of materials*. 2000. Wiley & sons: New York.

26. O. Deparis, C. Vandenbem, M. Rassart, V. L. Welch, and J.-P. Vigneron, *Color-selecting reflectors inspired from biological periodic multilayer structures.* Opt. Express, 2006. **14** (8): p. 3547.

Chapter 5

Future applications of titanium oxide hydrates and their hybrids

5.1. Introduction

Within the work presented in this thesis, it emerged that titanium oxide hydrates exhibit remarkable optical properties: they show a reversible photochromic behaviour in a suitable chemical environment, high UV absorbance, transparency in the visible wavelength region and a high refractive index. More importantly, structures of hybrid systems with polymers like PVAl, readily produced by solution processing, displayed refractive indices up to over 2, tunable with the concentration of titanium oxide hydrate in the systems, as well as by selecting suitable temperature treatments and/or irradiation with UV light.

In light of these results further use and applications can be envisaged. For instance, the photoactivity of such materials may be further enhanced and the hybrid formulations adjusted in order to widen the spectrum of their functionalities. Hereafter, we therefore report some of the possible pathways we envision to broaden

the optical properties of titanium oxide hydrates and their hybrids, with focus on possible attractive applications from the production of photochromic parts for optical devices and gadgets, to photonics products, photocatalysis or energy harvesting.

5.2. Photochromism

The origin of the photochromic behaviour in titanium oxide hydrates upon irradiation with UV light in a suitable chemical environment (see Chapter 2) is still not fully understood. According to our data (see Chapter 2), the phenomenon seems to result from a redox reaction – that very likely proceeds via a radicalic mechanism – between the titanium oxides hydrates and the chemical compounds in the surrounding; i.e. the metal in the titanium oxide hydrates is reduced resulting in the typical blue colouration, while the surrounding chemical compounds are oxidised. The presence of oxidising species such as oxygen (O_2) can reverse the state of oxidation of the metal and, as a consequence, lead to the bleaching of the colouration, rendering the metal again available for reduction. In hybrid systems with low permeability to atmospheric O_2 or strong coordination ability, such as those with PVAl presented in Chapter 3, these processes can be slowed down if not entirely prevented, therefore the photoinduced colouration can persist over years.

Given the stability and reversibility of the photochromism of hybrid systems comprising titanium oxide hydrates we can envisage their employment for the production of versatile re-usable UV indicators, but also the production of coloured patterns for fashion apparels. The latter may be fabricated with high resolution, simply by using a patterned mask that would allow the impregnation of textiles with invisible patterns that would turn blue when worn in the sun. The coloration should persist also

after the exposition the light exposure, yet could be erased, if required, by immersion in water.

5.2.1. Colour fastness

One of the major limiting factors for the effective employment of our hybrid materials in products that depend on the reversibility of the photochromic response, for instance in applications such as UV sensors, smart labels or prints, is the change in colour that occurs when they are subjected to several cycles of exposition to light / water. This colour change is likely the consequence of the progressive oxidation of the organic component. In fact, UV light exposure may trigger radicalic reactions that can induce modifications of the structure of the organic molecules in the matrix. In case of PVAl-based hybrids, reactions would proceed with elimination of water and formation of double bonds [1, 2], and as the conjugation of these double bonds increases, the material will yellowish and may eventually darken to red. At the same time, the intensity and the quality of the photochromic response of the material will decrease (see Chapter 3).

Therefore in order to effectively employ such hybrid materials further work must be devoted to investigate suitable hybrid formulae of prolonged operational life, in particular, with respect to the unwanted colour change due to the oxidation of the polymer matrix. In future work colourless antioxidants may thus be introduced to the system. Antioxidants are molecules that are oxidized very easily therefore preventing or slowing down the oxidation of other molecules in the surroundings. The addition of antioxidants to the titanium oxide hydrates / PVAl hybrid systems, described in this thesis, may thus prevent the propagation of radicalic reactions that lead to the formation of double bonds in the polymer, as the additives would be oxidized first

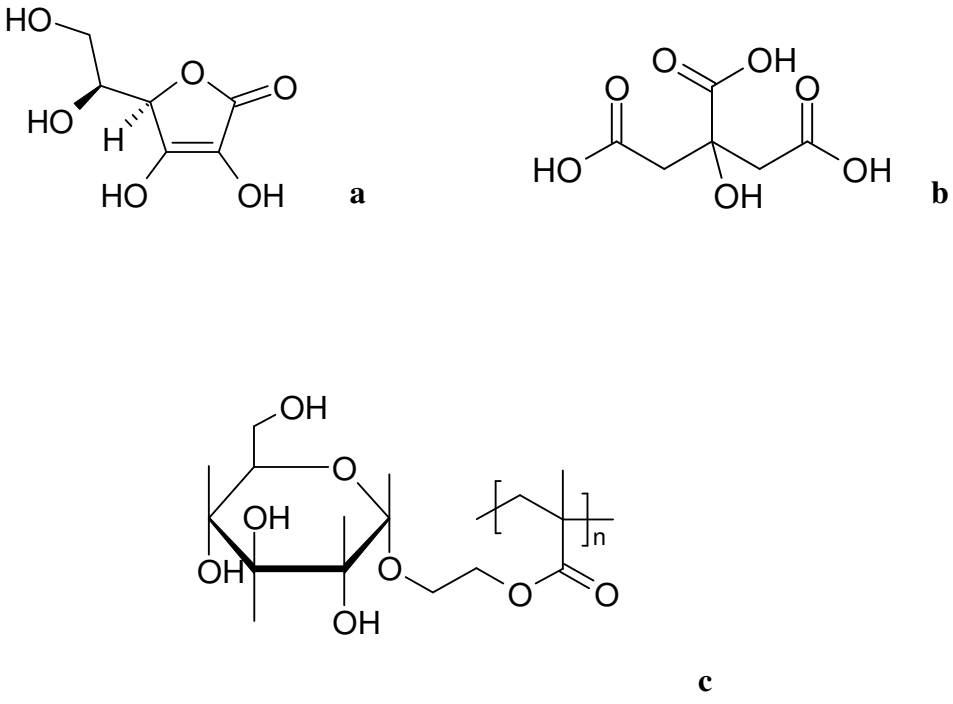

Figure 5.1 Molecular structures of **a-** ascorbic acid, **b-** citric acid and **c-** polyGEMA [3]. Because these colourless compounds are very easily oxidised if added to the formulation of the titanium oxide hydrate / PVAl hybrids they may help preventing the photo-oxidative degradation of the polymer during the irradiation with UV light or at least delay it, without compromising the optical characteristics of the hybrid material.

terminating these reactions.

Non-colored antioxidants of interest may include ascorbic acid, citric acid or similarly structured molecules. Colorless compounds are preferred in order to avoid interference with the photochromic behaviour of the material and for straight-forward evaluation of their efficiency in preventing the oxidation of the polymer in the hybrids (Fig 5.1 **a** and **b**).

Clearly it will be necessary to ensure that these often small-moleculecular species are not extracted when the hybrid is immersed in water; which may occur when simply blending the antioxidant to the hybrid material. Alternatively,

macromolecular structures containing entities with a similar chemical structure of the above antioxidants, may be employed. Prime candidates here are polymers such as poly(glucosylethyl methacrylate) (polyGEMA) (Fig 5.1 **c**) which have been demonstrated to reduce the thermal degradation of PVAl [3]

5.2.2 Colour spectrum of photochromic response

Another aspect related to the photochromic properties of the titanium oxide hydrates is the colouration that can be induced over irradiation, which so far has been limited to blue, originating from the Ti^{III} species produced in this process. A possible way to achieve a broader colour range in the photochromic response of our hybrids may be through the incorporation of other metals atoms into such oxide hydrates. Indeed, since the blue photochromism of the titanium oxide hydrates is most likely a result of the cooperative effect of a large amount of interconnected titanate units [4, 5], it is expected that the incorporation of foreign atoms may lead to variation in colour, photosensitivity and reversibility upon exposure to water. Transition metals like manganese, zirconium, molybdenum, tungsten or vanadium may be successful for this purpose as their ions present electrons in the *d* orbital that can participate to charge transfer mechanisms.

The integration of such metals in the very structure of the titanium oxide hydrates could be carried out at two different stages of their synthesis, for instance, before or during the titanium oxide hydrates formation. To this end, we could follow the synthesis of titanium oxide hydrates by hydrolysis of e.g. titanium tetrachloride, carried out in cold (0 ^{o}C) acidic solutions, as described in Chapter 2, in which titanium oxide hydrates form slowly. The metals such as Mn, Mo, W and V, could then be incorporated in form of a solution of salts. In case of Zr the related chloride may be

preferred as its chemical structure is similar to that of titanium tetrachloride, used in this thesis, and therefore, a similar chemistry can be expected.

Preliminary investigations could be carried out on systems with concentration of foreign atoms between 0.2 and 5 atomic percent. For this purpose, in a first set of experiments the foreign metals may be added to a freshly prepared $TiCl_4$ hydrolysis solution. At this stage titanium oxide hydrates would not have been formed yet. Co-precipitation of titanium oxide hydrates with foreign metal atoms can then be induced by increasing the pH value of the mixture using a method which is already known to be suitable for the production of titanium oxide hydrates. As a result, the formation of the oxide hydrates would occur in an environment containing different metals, which may be trapped in the forming molecules.

Initial experiments may focus on the introduction of zirconium as zirconium tetrachloride can be expected to behave similarly to $TiCl_4$, as mentioned above. The experience gained from those experiments will be subsequently translated to the incorporation of molybdenum, tungsten and vanadium. Molybdates and tungstates will be used for this purpose rather than the respective chlorides.

In a second set of experiments, the addition of the metals would follow the formation of the titanium oxide hydrates, which are produced again through an increase in pH. We can expect that in this second route the foreign metal rather than being trapped within the molecules would bond at the surface of the titanium oxide hydrates if they are present as clusters or particles. Therefore, materials obtained following the two different method, most likely display different absorption of the electromagnetic spectrum with respect to the neat titanium oxide hydrates. This in turn could also affect the photochromic properties. In addition, the ageing of powders obtained from these systems (following procedures as described in Chapter 2) should

be studied in order to understand the effect of the presence of the foreign metals on the development of specific crystalline structures that may be different from those formed by the oxides of the single metals.

5.3. Photonic crystals

Photonic crystals (PhC), consist of periodic spatial arrangement of alternating dielectric materials of high and low refractive index (or dielectric constant, as described in Chapter 4). If the periodicity of these structures is in the range of wavelengths of the light, the dispersion of light travelling in the structure can be altered. In fact, the propagation of certain modes of the incident light may become forbidden along certain direction (incomplete photonic band gap) [6]. We, thus, can distinguish between one, two and three-dimensional PhC depending if the two materials are arranged in a periodical fashion in one, two or three dimensions (Fig. 5.2).

Photonic structures can have a wide range of applications worth to explore, from low-cost (flexible or rigid) dielectric distributed Bragg reflectors (DBR) for vertical cavity lasers or resonant cavity [7-13] devices for optical communication and information systems, to planar lenses and concentrators [14, 15], or from collector systems for organic and/or inorganic photovoltaics [16] to sensor applications [17]. Furthermore, multilayer coatings may be used in the production of large-scale window coatings to reflect the “hot” infrared part of the sun light.

A broad technological success of such structures, however, relies predominantly on the manufacture costs and, thus, in the choice of materials and processing techniques used for their production. Therefore, the materials selected for

their fabrication not only need to satisfy specific optical requirements but also have to be suitable to be deposited or patterned in a straight-forward fashion.

5.3.1. Use of titanium oxide hydrates / PVAl hybrids

As we reported in Chapter 4 of this thesis, hybrids made of PVAl and titanium oxide hydrates displayed a high transparency between 400 and 1000 nm with a refractive index that could be tuned by adjusting the content of the inorganic species or through thermal treatments and irradiation with UV light.

The incorporation of other heavy metals such as zirconium, molybdenum, tungsten or vanadium into titanium oxide hydrates is expected to affect also the refractive index of the resulting mixed metal oxides. This should open an additional path to manipulate the optical properties of the oxide hydrates as well as the corresponding hybrid materials thereof, by modifying the composition of the metal oxide hydrates.

In Chapter 4, we demonstrated that titanium oxide hydrates / PVAl can readily be deposited from solutions into thin layers on a wide range of substrates, allowing us to produce distributed Bragg reflectors (DBR) (also known as one-dimensional photonic crystals) comprised of alternating nanometric films of our hybrid material and a suitable solution-processable fluorinated polymer. Such structures could provide high reflectivity (close to 100%) already at small numbers of periods (N = 16). Therefore, the use of hybrids based on mixed metal oxide hydrates for the production of DBR may provide to be another powerful tool to allow broadening the design of possible photonic structures, both with wide and narrow band-gaps.

5.3.2. Two and three- dimensional photonic crystals

Clearly, the high refractive index of titanium oxide hydrates and the possibility to modulate the refractivity locally may also allow designing and fabricating other optical devices consisting of two and three-dimensional photonic crystals (2-D and 3-D PhC) in which, again, the spectral characteristics of the band gap depends upon the refractive index contrast and on the periodic dimensions [6, 18, 19].

These kinds of architectures can confine the propagating light in two and three dimensions. For example, line-shaped defects in two-dimensional structures potentially allow integration with planar optical waveguide technology as wavelengths of light within the PhC bandgap would propagate loss-less in the structure also through tight bendings [20, 21]. This could represent a major advantage with respect to conventional waveguides such as optical fibers, which rely on total internal reflections and, thus, cannot be bended without loss of light (Fig. 5.2 **a**, **b**). Point defects, such as a punctual/local anomaly in the dimensions of one of the two dielectrics can also occur. These would act as a cavity, where a specific mode of light can be localised. If the frequency of the mode is within the bandgap of the crystal, in fact, the light cannot escape (Fig. 5.2 **c**, **d**).

Applications of such more dimensional photonic structures range from the production of filters to cavities for lasers [21]; and 2D-PhC may also be used to produce sensors for the detection of molecules. For instance, in case of hollow, tubular patterned crystals the absorption of chemical compounds in the cavities alters both the refractive index and the internal diameter of the crystals, which can be monitored as shift of the bandgap [22].

However, despite the broad range of applications that can be envisioned with photonic structures, progresses have been limited by their manufacturing. Indeed, the

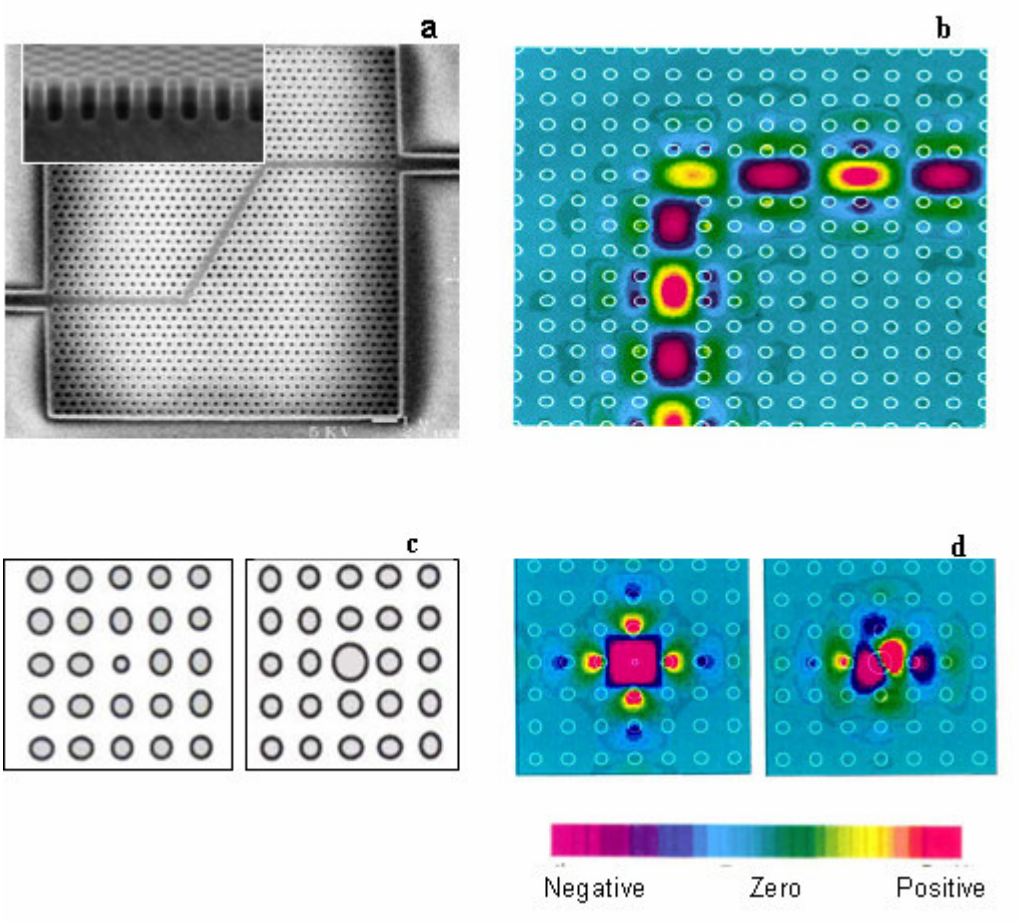

Figure 5.2: a- Scanning electron microscopy (SEM) images of a nanofabricated 2D photonic crystal slab containing a double-bend device with two 60° bends (**inset-**a side-view of the etched pattern that gives rise to the photonic properties) (images from [23, 24]). **b-** An example of the projected photon bands in a similar structure that show guidance effect of the band gap structure through a sharp bending (90^{o} bend). The guided light is red, while in green are the propagating modes and the yellow represent the band gap (after [21]). **c- Photonic structure containing punctual defects which** can consist in the widening or compression of only one feature of an otherwise perfectly uniform structure such as a uniform arrays of holes or pillar of constant radius. **d-** These kind of defects can actually pin modes with wavelength in bandgap in specific positions as it is visible in the band projections [21].

current method of choice [25] for the production of 2-D PhC are lithography[26], electrochemistry, sol-gel techniques, self-assembly [27] and the likes. These procedures are complex, lengthy and expensive. Titanium oxide hydrate / PVAl materials (and possibly hybrids of the mixed metal oxide hydrates) thus, are promising alternatives in terms of processability and tuneability of the optical properties. We envisage their use for the manufacture of 2-D PhC with band gaps in the range of wavelengths of visible and near IR light, as outlined below.

5.3.2 2D photonic structures based on titanium oxide hydrates / PVAl hybrid materials.

Patterning polymeric materials by micro/nanoembossing (Fig. 5.3 **c)** [28] is a well established technique to realise high quality replicas of a given master pattern (Fig. 5.3 **a**, **b** and **d**). Due to the simplicity of this process it is expected that it can be readily adopted for producing suitable micro- and, possibly nanostructures, similar to those in Figure. 5.3 **a** and **b**, in hybrid films. Both inorganic moulds and structures based on thermoplastic polymers such as polypropylene, poly (ethylene terephthalate) or polystyrene may be employed for these purposes. The hybrids may be embossed in the solid state. Alternatively, liquid mixtures of titanium oxide hydrates and PVAl can be cast on the mould and left to desiccate (Fig. 5.4 **a**). The mould may also be applied on top of the cast, still liquid film until they fully solidifiy (Fig. 5.4 **b**). Vacuum might be used to assist this process. In both cases, once the material is solidified, the mould may be simply peeled off or dissolved in a suitable apolar solvent (Fig. 5.4 **e** and **f**).

Another interesting tool that may allow obtaining photonic crystal devices could be by irradiation with UV light [13] which was shown in this thesis (Chapter 4)

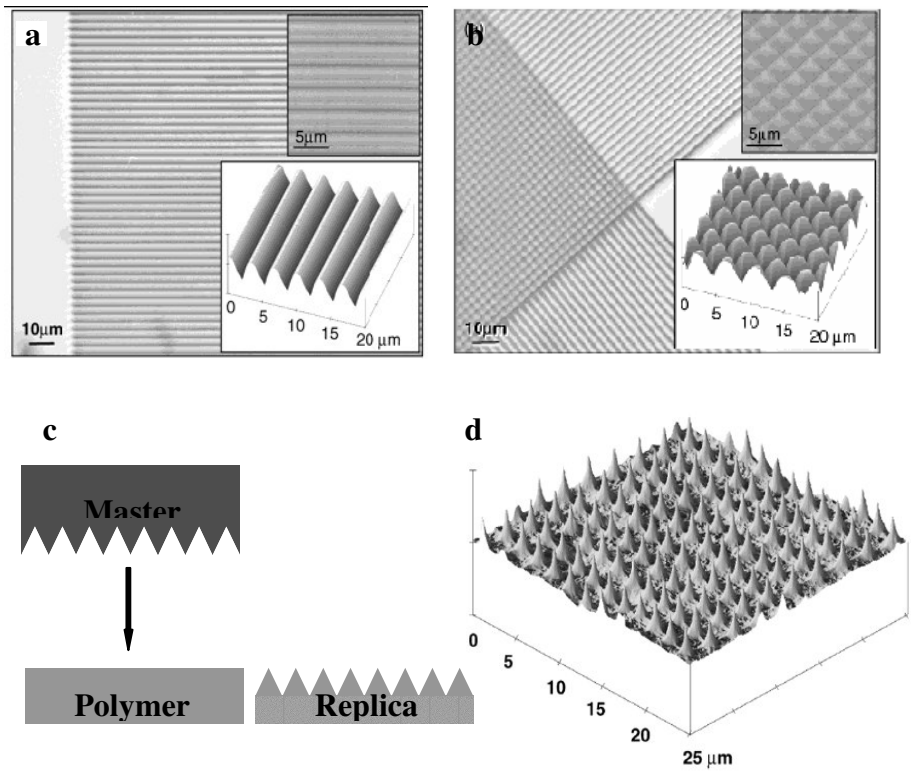

Figure 5.3: a-b Optical, scanning electron and scanning probe micrographs of polymer relief structures obtained through embossing (after [29]). **c-** Schematic of the embossing process. **d-** Scanning probe micrograph of an example of an epoxy replica of the melt embossed film of picture **b** [29]. The images illustrate the technique accuracy and definition in transferring the feature of the master pattern, which can be exploited to produce suitable relief structures in titanium oxide hydrates / PVAl architectures.

to effectively alter the refractive index of titanium oxide hydrates / PVAl hybrid materials. A periodical and controlled modulation of the refractive index could therefore be introduced in pre-fabricated structures by irradiating the material through a mask (Fig. 5.5 **a** and **b**). We believe that this technique could, for instance, be worthwhile to be explored for the fabrication of planar lenses and gratings essentially when using architectures of thickness of 1 to 5 µm. Irradiation may also be applied to pre-formed layered structures as those described in Chapter 4 (Fig. 5.5 **c** and **d**) to produce 3D photonic structures. Indeed we found that UV light modifies

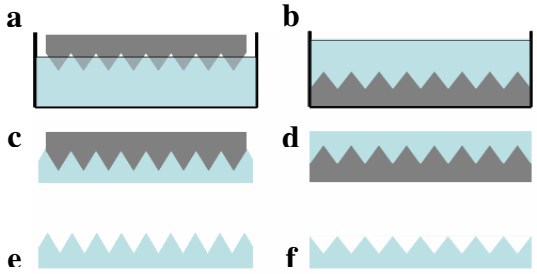

Figure 5.4: Examples of possible uses of polymeric structures for the production of patterned films of titanium oxide hydrates / PVAl hybrid films. **c-** The mould can be placed on top of the solution or **d-** immerged in the hybrid material solution. Once the hybrid is fully solidified, **e-f-** the mould can be released by dissolving the polymeric mould in a suitable apolar solvent or simply removed mechanically. **g-h-** The pattern of the mould should be transferred to the titanium oxide hydrate-PVAl hybrid film.

the refractive index of the hybrid material but does not affect that of the perfluorinated polymer for exposure time < 40 min.

5.3.3 Production of dichroic structures

An intriguing use of the PVAl / titanium oxide hydrate materials could be the production of dichroic films for applications in optical devices. As an example, dichroic films can allow the fabrication of color-polarizing filters which could be used as low cost components in bicolored liquid crystal displays.

Preliminary experiments showed that, for example, highly dichroic titanium oxide hydrate/polymer hybrids could be produced by mechanical deformation (draw ratios of < 20), followed by heat treatment. To this end, 1 to 5% wt (with respect to the PVAl content) of glycerol may be added to the hybrid material as preliminary investigations revealed that this softens the hybrids, yielding rubber-like films that can be stretched to higher draw ratios than without glycerol. The alcohol can

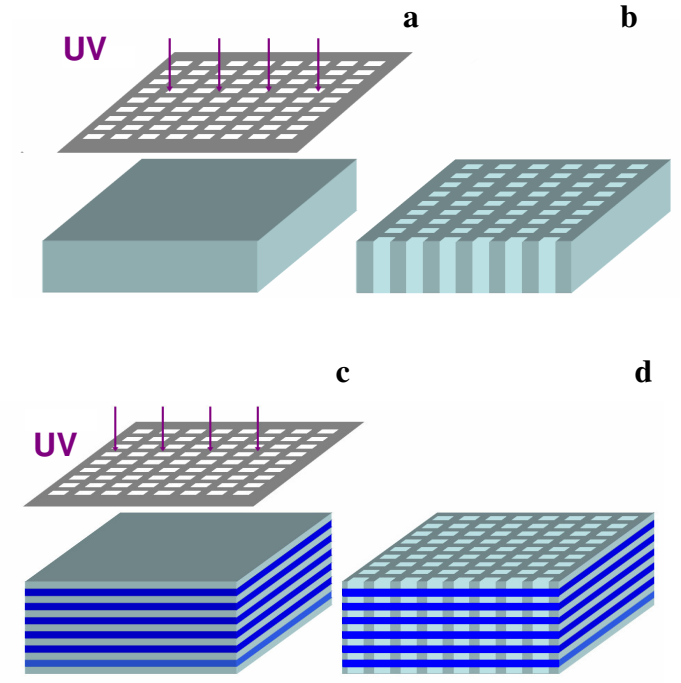

Figure 5.5: Shematic diagram of the process for the production of an ordered lattice in a titanium oxide hydrates / PVAl membrane by **a-b-** exposition to a pattern of intense UV light through a mask. The refractive index, *n*, of this hybrid material decreases upon irradiation with UV light and does not recover the pristine values after the light exposure. **c** Similarly, patterned irradiation of DBR structures consisting of layers of titanium oxide hydrates / PVAl hybrid material and a fluorinated polymer (PFP) might produce structures with a refractive index modulation in three dimensions.

subsequently be extracted in a washing procedure necessary to remove the excess acid contained in the hybrid (see Chapter 3).

The washing as well as the heat treatments (using temperatures > 180^{o}C) should be conducted with the stretched film still in tension to increase the birefringence of the specimen and prevent undesired deformations. Accordingly, the dichroism of the resulting films can be controlled both by selection of annealing temperature (affecting *n*) and drawing ratios (affecting the molecular orientation). Investigation of their effect on the final optical properties of the dichroic films is

therefore required. Polarised microscopy and UV-vis spectroscopy may be used for this purpose.

5.4 Use of titanium oxide hydrates in photocatalytic applications

In the literature several reports about the photocatalytic activity of colloidal and nanocrystalline titania have been published [30-34]. In most cases, the catalytic properties of the colloids were found to strongly depend on the method used for their production rather than on the presence or absence of a certain crystalline modification in the colloid [35, 36]. Indeed the nature of the precursor compound, the additives selected for the hydrolysis and the pH value at which the colloids were used for photocatalysis can affect the photoactivity of the resulting structures.

Based on the data provided in this thesis, it seems worthwhile to investigate if, possibly, titanium oxide hydrates may have been the origin of some of the photocatalytic functionalities of these colloidal systems reported in the literature. Indeed the reaction conditions described in these reports very likely were not effective enough to allow complete conversion of the initially formed titanium oxide hydrates into crystalline titanium dioxide.

In titanium oxide hydrates the metal atom may indeed act as a catalytic centre, especially when considering that in presence of reducing agents or suitable alcohol-rich environment Ti^{IV} centres are reduced to Ti^{III} upon irradiation with light. This is reversible, as we have shown in Chapter 2 and 3. As a consequence, one may imagine that the oxidation state, and possibly the chemistry of the Ti-species in such oxide hydrates, may remain unaltered in the overall reaction if a rapid electron transfer from Ti^{III} to another species (that will be reduced) is allowed – provided that an oxidising

species is added. Electrons would then be transferred to such species and the regeneration of the former oxidation state is obtained.

To gain a better understanding of the influence of the chemical surrounding on such processes, it could thus be interesting to investigate the oxidation potential of the titanium species towards a given chemical. As an example, irradiation of colloidal titania in presence of acetic acid is known to produce methane [36] or colloidal and nanocrystalline titania induced the decomposition of chlorinated pollutants [32, 37]. Comparison of the performance of titanium oxide hydrates to those reported for titania in analogous environments and reaction conditions may give indications on the true photocatalytic activity of these structures. Clearly, such photocatalysed reactions in our systems, due to their radicalic nature, are not completely controllable and predictable. As a consequence, the number of possible adducts may be broad, depending on several parameters including the type and number of the chemical species in the surrounding medium, the pH value or temperature.

Preliminary investigations were also performed with mononuclear species, from the hydrolysis of $TiCl_4$, which revealed that these materials have good potential to promote the photoreduction of metal ions. For instance, when UV irradiation was carried out on a hybrid system containing citric acid, mononuclear species from the hydrolysis of $TiCl_4$, and iron(III) chloride, such systems (pH<1), before irradiation showed the typical yellow coloration of the Fe^{III} became colourless upon irradiation suggesting that the ferric ion was reduced to Fe^{II}. The reduction of Ti^{IV} to TI^{III}, instead, occurred only after all the iron present was reduced to $Fe^{(II)}$ and only after continuous irradiation eventually the solution did turn blue.

When titanium oxide hydrates were used the reduction of iron from ferric to ferrous was also observed at higher pH (pH = 6). $K_3Fe(CN)_6$ was used as reducing agent, rather than iron trichloride, as iron hydroxides would precipitate at this pH value. Reassuringly, also in this system Fe^{III} was reduced to Fe^{II} as evident from a pronounced colour change to a dark bright, blue hue similar to the Prussian blue which is comprised of mixed valence iron cyanides of the approximate formula $Fe_7(CN)_{18}(H_2O)_x$ (or when soluble $KFe[Fe(CN)_6]$).

The above preliminary study on the possible photocatalytic activity of titanium oxide hydrate is merely based on a visual analysis of the photochromic response of systems containing specific reducing agents. To gain a better insight of the potential of titanium oxide hydrates for the reduction of such ions the analysis should be expanded with appropriate techniques and comparisons need to be made with the activity of others systems, in particular those based on titania nanoparticles. Nevertheless, initial results are intriguing and encouraging in planning an extension of the study also to other metals. The photocatalytic activity of titanium oxide hydrates is promising and still open to be explored in a broad range of applications such as in the production of aternative fuels (like H_2 from the splitting of water) or even for harvest solar energy.

5.5 References

1. H. Kaczmarek and A. Podg´orski, *The effect of UV-irradiation on poly(vinyl alcohol) composites with montmorillonite.* J. Photoch. Photobiol. A, 2007. **191**: p. 209.
2. J. F. Rabek, ed. *Polymer photodegradation. Mechanisms and experimental methods*. 1995, Chapman and Hall: London.
3. T. Nishino, S. C. Kani, K. Gotoh, and K. Nakamae, *Melt processing of poly(vinyl alcohol) through blending with sugar pendant polymer.* Polymer, 2002. **43**: p. 2869.
4. S. Cassaignon, M. Koelsch, and J.-P. Jolivet, *From $TiCl_3$ to TiO_2 nanoparticles (anatase, brookite and rutile): thermohydrolysis and oxidation in aqueous medium.* J. Phys. Chem. Solid, 2007. **68**: p. 695.
5. M. B. Robin and P. Day, *Mixed valence chemistry - a survey and classification.* Adv. Inorg. Chem. Radiochem., 1968. **10**: p. 247.
6. C. Paquet and E. Kumacheva, *Nanostructured polymers for photonics.* Mater. Today, 2008. **11** (4): p. 48.
7. T. Arakawa, M. Nishioka, Y. Nagamune, and Y. Arakawa, *Fabrication of vertical-microcavity quantum wire lasers.* Appl. Phys. Lett., 1994. **64**: p. 2200.
8. T. Granlund, M. Theander, M. Berggren, M. Andersson, A. Ruzeckas, V. Sundstro, and G. Bjo, *A polythiophene microcavity laser.* Chem. Phys. Lett., 1998. **288**: p. 879.
9. L. Hou, Q. Hou, Y. Mo, J. Peng, and Y. Cao, *All-organic flexible polymer microcavity light-emitting diodes using 3M reflective multilayer polymer mirrors.* Appl. Phys. Lett., 2005. **87**: p. 243504.

10. S. M. Jeong, Y. Takanishi, K. Ishikawa, and H. Takezoe, *Flexible microcavity organic light-emitting diodes with wide-band organic distributed Bragg reflector.* Jpn. J. Appl. Phys., 2006. **45** (28): p. L737.

11. L. Persano, A. Camposeo, P. D. Carro, E. Mele, R. Cingolani, and D. Pisignano, *Very high-quality distributed Bragg reflectors for organic lasing applications by reactive electron-beam deposition.* Opt. Express, 2006. **14** (5): p. 1951.

12. E. F. Schubert, Y.-H. Wang, A.Y. Cho, L.-W. Tu, and G.J. Zydzik, *Resonant cavity light-emitting diode.* Appl. Phys. Lett., 1992. **60** (8): p. 921.

13. S. Yokoyama, *Single-mode polymer DBR Lasers with two-dimensional microcavity structures.* IEICE Transaction Electronics, 2007. **E90-C** (1): p. 135.

14. E. Hecht and A. Zajac, eds. *Optics*. 3rd ed. 1997, Addison Wesley Publishing Company.

15. E. Reznikova, T. Weitkamp, V. Nazmov, A. Last, M. Simon, and V. Saile, *Investigation of phase contrast hard X-ray microscopy using planar sets of refractive crossed linear parabolic lenses made from SU-8 polymer.* Phys. Stat. Sol., 2007. **204** (8): p. 2811.

16. M. J. Currie, J. K. Mapel, T. D. Heidel, S. Goffri, and M. A. Baldo, *High-efficiency organic solar concentrators for photovoltaics.* Science, 2008. **321**: p. 226.

17. M. Karaman, S. E. Kooi, and K. K. Gleason, *Vapor deposition of hybrid organic-inorganic dielectric bragg mirrors having rapid and reversibly tunable optical reflectance.* Chem. Mater., 2008. **20**: p. 2262.

18. S. John, *Strong localization of photons in certain disordered dielectric superlattices.* Phys. Rev. Lett., 1987. **58** (23): p. 2486.

19. E. Yablonovitch, *Inhibited spontaneous emission in solid-state physics and electronics.* Phys. Rev. Lett., 1987. **58** (20): p. 2059.

20. T. F. Krauss, R. M. De La Rue, and S. Brand, *Two dimensional photonic-bandgap structures operating at near-infrared wavelengths.* Nature, 1996. **383**: p. 699.

21. J. D. Joannopoulos, P. R. Villeneuve, and S. Fan, *Photonic crystals: putting a new twist on light.* Nature, 1997. **386**: p. 143.

22. M. Lee and P. M. Fauchet, *Two-dimensional silicon photonic crystal based biosensing platform for protein detection.* Opt. Express, 2007. **15** (8): p. 4530.

23. E. Chow, S. Y. Lin, S.G. Johnson, P. R. Villeneuve, J. D. Joannopoulos, J. R. Wendt, G. A. Vawter, W. Zubrzycki, H. Hou, and M. Allemann, *Three-dimensional control of light in a two-dimensional photonic crystal slab.* Nature, 2000. **407**: p. 983.

24. J. S. Foresi, P. R. Villeneuve, J. Ferrera, E. R. Thoen, G. Steinmeyer, S. Fan, J. D. Joannopoulos, L. C. Kimerling, H. I. Smith, and E. P. Ippen, *Photonic-bandgap microcavities in optical waveguides.* Nature, 1997. **390**: p. 143.

25. V.V. Pokropivnyi, *Nanostructured materials two-dimensional nanocomposites: photonic crystals and nanomembranes (review). I. Types and preparation.* Powder Metal. Met. C., 2002. **41** (5-6): p. 264.

26. Z. Liu, P.-T. Lin, B.W. Wesselsa, F. Yi, and S.-T. Ho, *Nonlinear photonic crystal waveguide structures based on barium titanate thin films and their optical properties.* Appl. Phys. Lett., 2007. **90**: p. 201104.

27. J. D. Joannopoulos, *Self-assembly lights up.* Nature, 2001. **414**: p. 257.

28. N. Stutzmann, *Microstructuring of polymers and polymer-supported matter*. PhD thesis. 2001, ETH: Zurich.

29. N. Stutzmann, T. A. Tervoort, C. W. M. Bastiaansen, and K. F. Smith, *Solid-State replication of relief structures in semicrystalline polymers.* Adv. Mater., 2000. **12** (8): p. 557.

30. J. Moser and M. Grätzel, *Photoelectrochemistry with colloidal semiconductors; laser studies of halides oxidation in colloidal dispersions of TiO_2 and α-Fe_2O_3.* Helv. Chim. Acta, 1982. **65** (5): p. 1436.

31. I. A. Shkrob, M. C. S. Jr, and D. Gostzola, *Efficient, rapid photoxidation of chemisorbed polyhydroxyl alcohols and carbohydrates by TiO_2 nanoparticles in aqueous solution.* J. Phys. Chem. B, 2004. **108**: p. 12512.

32. N. Serpone, I. Texier, A.V. Emeline, P. Pichat, H. Hidaka, and J. Zhaoe, *Post-irradiation effect and reductive dechlorination of chlorophenols at oxygen-free TiO_2/water interfaces in the presence of prominent hole scavengers.* J. Photoch. Photobio. A, 2000. **136**: p. 145.

33. O.I. Micic, Y. Zhang, K. R. Cromack, A. D. Trifunac, and M. C. Thurnauer., *Photoinduced hole transfer from TiO_2 to methanol molecules in aqueous solution studied by electron paramagnetic resonance.* J. Phys. Chem., 1993. **97**: p. 13284.

34. R. Gao, J. Stark, D. W. Bahnemann, and J. Rabani, *Quantum yields of hydroxyl radicals in illuminated TiO_2 nanocrystallite layers.* J. Photochem. Photobiol. A, 2002. **148** (1-3): p. 387.

35. A. Sclafani, L. Palmisano, and M. Schiavello, *Influence of the preparation methods of titanium dioxide on the photocatalytic degradation of phenol in aqueous dispersion.* J. Phys. Chem., 1990. **94** (2): p. 829.

36. R. S. Davidson, C. L. Morrison, and J. Abraham, *A comparison of photochemical reactivity of polycrystalline (anatase), amorphous and colloidal form of titanium dioxide.* J. Photochem., 1984. **24**: p. 27.

37. J. Moser and M. Grätzel, *Photoelectrochemistry with Colloidal Semiconductors; Laser Studies of Halide Oxidation in Colloidal Dispersions of TiO_2 and a-FeO.* Helv. Chim. Acta, 1982. **65** (5): p. 1436.

Acknowledgements

Eventually I made it! And now, I would like to express my deep gratitude to all the beautiful people who gave me the possibility to start and, more importantly, successfully complete the work that was described in this thesis. Well, my first thought is for my supervisor Dr. Natalie Stingelin an incredible person that with care and generosity, guided me throughout these years of research and in writing this thesis. Surely, her love for knowledge, enthusiasm, mind openness and intellectual honesty are for me a reference to look at in my professional life. Thanks to her, I had the possibility meet excellent scientists that largely contributed to my work directly and indirectly and for this I will always be obliged.

I would also love to thank all my former collegues, now dear friends, that supported me in my research work and life through these years at Queen Mary. Among the many of them a particular thanks goes to the supercool rock and roll crew of Fianti, Raquel, Pilli, Jianmin, Antonio, Choothum, Moe, Emiliano, Paola, Nattakan, Bea, Chris, Dani, Monisha, Gianluca and Lyiang. I am very happy and feel very lucky

that I met them and grateful to them for filling my days with their presence, valuable opinions and discussions and, mostly, for the fun they brought in my life!

Of course, I cannot forget to thank the professors, doctors, technicians, administrative and all those that make the Materials Engineering department at Queen Mary such a cool place!

Finally I would like a special huggy thanks to Mamma and my whole family that with patient love (a lot!), trust, support and invaluable presence (and long telephone bills) cheered for me and helped me to achieve this goal.